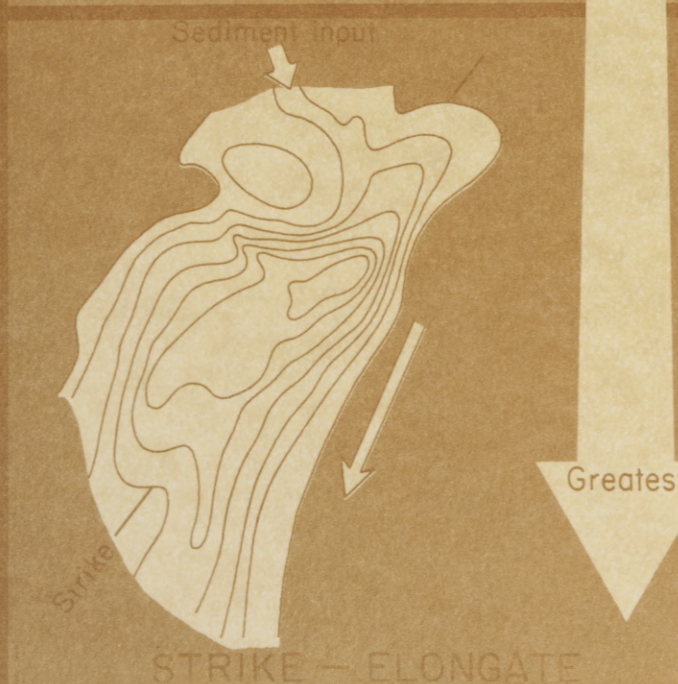
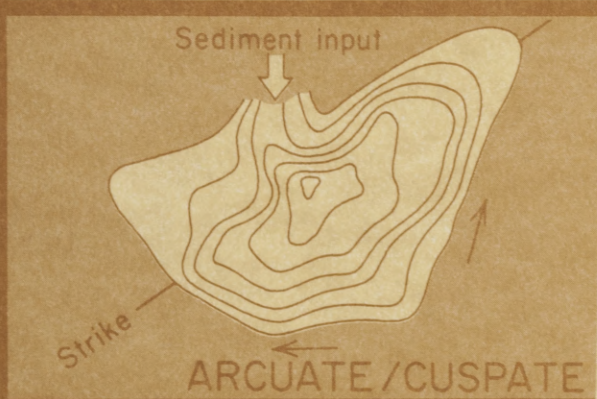
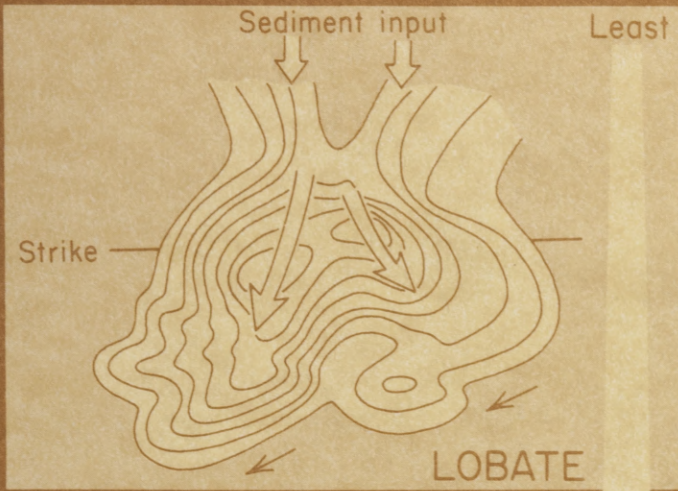


Wave-Dominated Delta Systems of the Upper Cretaceous San Miguel Formation, Maverick Basin, South Texas

Bonnie R. Weise



REWORKING BY MARINE PROCESSES

Greatest

Bureau of Economic Geology
W. L. Fisher, Director
The University of Texas at Austin
Austin, Texas 78712



1980



Wave-Dominated Delta Systems of the Upper Cretaceous San Miguel Formation, Maverick Basin, South Texas

Bonnie R. Weise

Bureau of Economic Geology
W. L. Fisher, Director
The University of Texas at Austin
Austin, Texas 78712



1980



CONTENTS

ABSTRACT	1
INTRODUCTION	1
DATA AND METHODOLOGY	2
GEOLOGIC SETTING OF THE MAVERICK BASIN	3
Basin history	3
Structural framework	3
Upper Cretaceous stratigraphy	4
SAN MIGUEL DEPOSITION	4
Sediment sources	4
Depositional systems and origin of sandstone geometry—general comments	5
Sandstone units of the western Maverick subbasin	8
<i>Transgressive-regressive cycles</i>	8
<i>Sandstones A and B</i>	9
<i>Sandstone C</i>	12
<i>Sandstone D</i>	12
<i>Sandstone E</i>	13
<i>Sandstone F</i>	13
<i>Sandstone G</i>	13
<i>Sandstone I</i>	14
Sandstone units of the eastern Maverick subbasin	15
Vertical sequences	15
<i>Textures</i>	15
<i>Sedimentary structures</i>	19
DEPOSITIONAL MODELS FOR THE SAN MIGUEL FORMATION	19
Wave-dominated delta model	19
<i>Facies</i>	20
<i>Incomplete strandplain-barrier sequences</i>	21
<i>Net-sandstone patterns</i>	22
Deltaic deposition during a major transgression	23
Modern and ancient depositional analogs	24
SANDSTONE PETROGRAPHY	27
Mineralogy	27
Diagenesis	29
SAN MIGUEL SANDSTONES AS PETROLEUM RESERVOIRS	30
History of production	30
Trapping mechanisms and types of fields	31
Role of diagenesis in reservoir development	31
CONCLUSIONS	31
ACKNOWLEDGMENTS	32
REFERENCES	32
APPENDIX	34

Figures

1. San Miguel study area showing well and outcrop locations	2
2. Structural framework of the Rio Grande Embayment	4
3. Structural configuration on top of the Olmos Formation	5
4. Location of Cretaceous volcanic plugs, Central and South Texas	5
5. Generalized dip section through the Maverick Basin showing Upper Cretaceous stratigraphy	6
6. Strike section Y-Y', simplified from plate V	6
7. Depocenters of San Miguel sandstone units and directions of sediment input	7
8. Strike section Z-Z', simplified from plate VI	7
9. Idealized net-sand pattern for a wave-dominated delta	8
10. Triangular process classification of deltaic depositional systems	9
11. Delta responses to variations in primary factors affecting geometry of deltaic sandstone bodies deposited during major transgressions	10
12. Dip section B-B', simplified from plate II	10
13. Two transgressive episodes of the San Miguel defined by the relative positions and order of deposition of sandstone units	11

14. Transgressive-regressive cycles shown by a schematic dip section through the axis of the western Maverick subbasin	11
15. Net sandstone, San Miguel unit A	12
16. Net sandstone, San Miguel unit B	12
17. Net sandstone, San Miguel unit C	13
18. Net sandstone, San Miguel unit D	14
19. Net sandstone, San Miguel unit E	15
20. Net sandstone, San Miguel unit F	16
21. Net sandstone, San Miguel unit G	16
22. Net sandstone, San Miguel unit I	17
23. Net sandstone, San Miguel unit P	17
24. Typical electric log patterns and vertical distribution of grain sizes and porosity in a core from San Miguel unit G in the Wood # 1 Weathers well, Zavala County	18
25. Distribution of various SP patterns in San Miguel unit G	18
26. Three-dimensional model of a wave-dominated delta system	20
27. Evolution of incomplete strandplain-barrier sequences of the San Miguel Formation	22
28. Spectrum of San Miguel deltas	23
29. Model of deltaic sedimentation in a basin in which rates of deposition and rates of subsidence varied	24
30. Effects of rising and stable relative sea level on delta formation	25
31. Delta abandonment, transgression, and development of sandy bars and shoals	26
32. Depositional environments and net-sand patterns of the Rhone delta system, France	27
33. Depositional environments of the São Francisco delta, Brazil	28
34. Depositional environments of the Nile delta system, Egypt	28
35. Oligocene wave-dominated delta systems	29
36. Generalized diagenetic sequence for Tertiary sandstones of the Texas Gulf Coast	30

Table

1. Stratigraphy and informal names of San Miguel sandstone units	3
--	---

Plates

I. Cross section A-A'	(in pocket)
II. Cross section B-B'	(in pocket)
III. Cross section C-C'	(in pocket)
IV. Cross section X-X'	(in pocket)
V. Cross section Y-Y'	(in pocket)
VI. Cross section Z-Z'	(in pocket)
VII. Photographs	
A. Horizontal <i>Ophiomorpha</i>	37
B. Vertical burrows, most of which are <i>Ophiomorpha</i>	37
C. Bed of horizontal laminations with few burrows	37
VIII. Photographs	
A. The San Miguel sandstone D exposed in a roadcut along U. S. Highway 277 north of Eagle Pass	38
B. Low-angle crossbeds	38
C. Hummocky cross-stratification	38
D. Deep, vertical <i>Ophiomorpha</i>	38
IX. Photographs	
A. Typical San Miguel sandstone with abundant feldspar	39
B. Leached feldspar grain partially replaced by calcite	39
C. Poikilotopic calcite cement	39
D. Quartz overgrowth and sparry calcite cement	39
E. Leached shell fragments	39
F. Authigenic kaolinite filling cavity rimmed with very coarse grained calcite, particularly poikilotopic calcite	39

ABSTRACT

Upward-coarsening sandstone units of the Upper Cretaceous San Miguel Formation in South Texas were deposited in wave-dominated deltas during minor regressive phases, periodically interrupting a major marine transgression. Sediments accumulated in the Maverick Basin within the Rio Grande Embayment. Cross sections and sandstone maps reveal that during deposition of the San Miguel, the Maverick Basin consisted of two subbasins that received sediments from the northwest and the north.

Net-sandstone patterns show that the thickest parts of San Miguel sandstone bodies are generally strike oriented. Where preserved, updip fluvial systems are indicated by dip-aligned sandstone trends. San Miguel deltas vary considerably in morphology and compose a spectrum of wave-dominated delta types. Modern analogs of San Miguel deltas include the Rhone, Nile, São Francisco, Brazos, Danube, Kelantan, Grijalva, and Senegal deltas. Sandstone geometry ultimately depended on three primary factors: (1) rate of sediment input, (2) wave energy, and (3) rate of relative sea-level change. Original delta morphology was determined by all three factors, but the degree of reworking of deltaic sediments after delta abandonment was determined by wave energy and rate of transgression.

The most common vertical sequences exhibited by the subsurface San Miguel coarsen upward from mudstone and siltstone to fine sandstone. Burrows are the dominant structures. Rare primary structures are small scale; large-scale crossbeds are observed only in outcrop. Strandplain or barrier-island facies sequences, which prevail in most wave-dominated delta deposits, are incomplete in the San Miguel. Typically, only the lower shoreface is preserved. Upper parts of the sequences, which normally contain large-scale primary structures, were destroyed by marine reworking during subsequent transgression. Intense burrowing obliterated primary structures in the upper parts of the truncated shoreface sequences.

Most of the San Miguel sandstones are arkoses, but the mineralogical composition of the sandstones changes vertically. Generally within each sandstone, quartz content increases upward with increasing mean grain size. Cements include sparry and poikilotopic calcite, quartz overgrowths, feldspar overgrowths, illite rims, and kaolinite. Porosity was eliminated principally by two types of calcite cement, which tend to cement completely the coarsest, best sorted, and originally most porous zones of the San Miguel sandstones. Zones of secondary porosity resulted

from leaching of shell material, calcite cement, and feldspars. Laterally, the distribution of high secondary porosity and calcite-cemented zones is unpredictable.

INTRODUCTION

Little has been published about the Upper Cretaceous terrigenous clastic formations of the Maverick Basin in South Texas. In the last few years, however, these formations have received greater attention because of oil and gas exploration and development. The San Miguel Formation, one of the clastic units, was first studied and named by Dumble (1892) for the San Miguel Ranch on the Rio Grande above Eagle Pass in Maverick County (fig. 1; Sellards and others, 1932). Dumble correlated the San Miguel with the Navarro Group of Central Texas, but Stephenson (1931) later confirmed, primarily on the basis of the molluscan fauna, that the San Miguel was part of the Taylor Group.

The San Miguel Formation crops out in a few small areas in Maverick County (fig. 1) and in the subsurface extends to the east, southeast, and south at least into Atascosa, La Salle, and Webb Counties, where sandstones of the formation pinch out. Total surface and subsurface area of the San Miguel Formation in Texas is at least 6,300 mi² (16,000 km²). In the subsurface, the formation extends an unknown distance into Mexico. On the basis of vertical sequences, formation thickness, and environmental relationships, the San Miguel Formation of this study in Texas does not appear to be equivalent to the San Miguel in Coahuila, Mexico, described by Caffey (1978). Detailed correlations of electric logs across the Rio Grande will be necessary to clarify the stratigraphic relationships of Upper Cretaceous units in Mexico and Texas.

Lewis (1977) presented a general model of San Miguel deposition, but his work (1962, 1977) concentrated on hydrocarbon traps and stratigraphy. The present study was conducted primarily to interpret sedimentary facies and delineate depositional systems within the San Miguel Formation. Principal objectives are to (1) describe the geometry of sandstone units, vertical sequences, and depositional systems of the San Miguel Formation using detailed cross sections and net-sandstone maps, (2) interpret the Maverick Basin geologic history during deposition of the San Miguel, including transgressive-regressive cycles and time relationships among individual sandstone units, (3) propose depositional models and modern and ancient analogs of San Miguel systems, and (4) discuss the influences of sediment characteristics and depositional patterns on porosity and, hence, oil and gas occurrence.

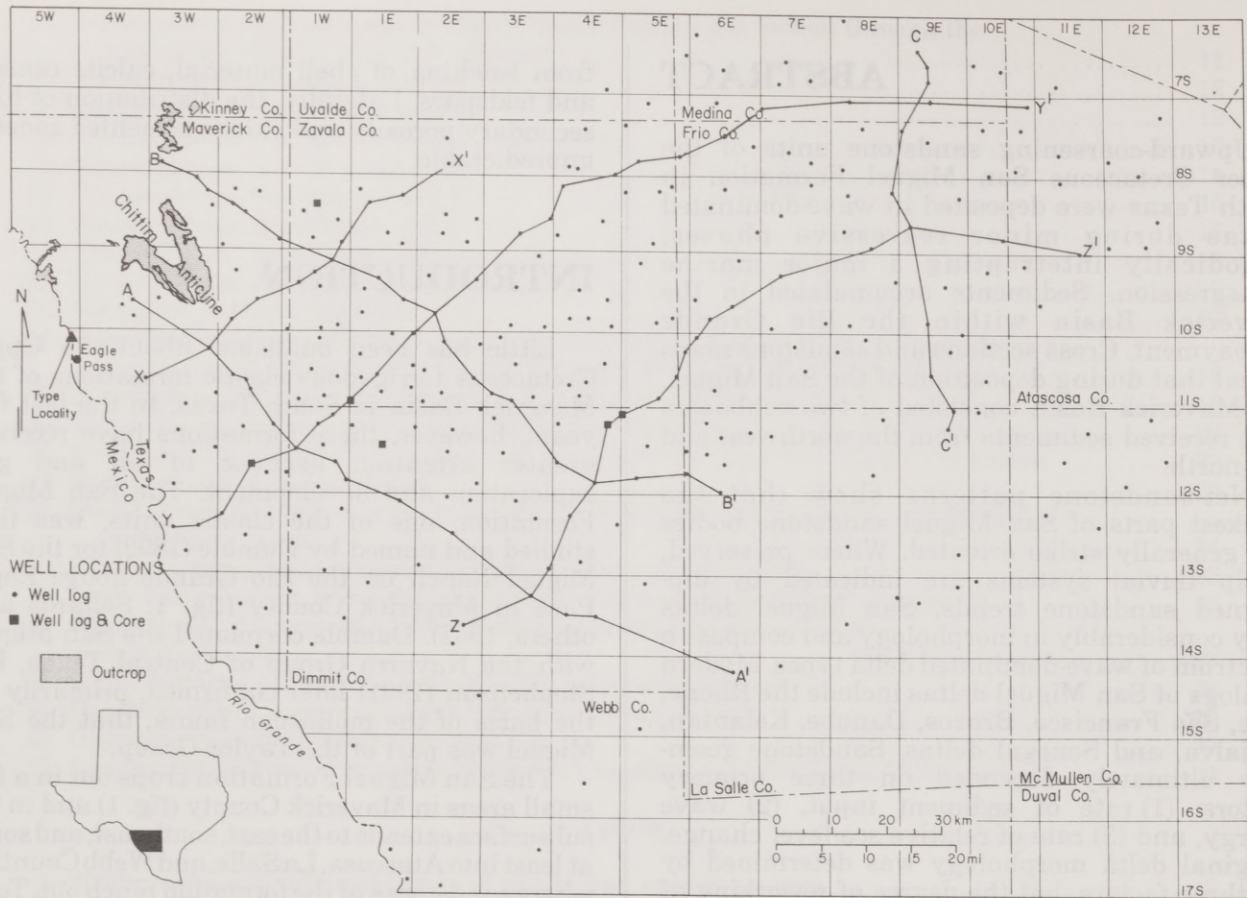


Figure 1. San Miguel study area showing well and outcrop locations. A-A', B-B', and C-C' are lines of dip cross sections. X-X', Y-Y', and Z-Z' are lines of strike cross sections. Location system is Tobin Grid system. Each grid equals one 7.5-minute quadrangle.

DATA AND METHODOLOGY

The San Miguel Formation was studied primarily using subsurface data, principally 375 electric logs. Well locations for 305 logs used to construct net-sandstone maps are plotted in figure 1; well names are listed in the Appendix. Subsurface investigation also included analyses of nine cores from the wells indicated on figure 1, plus four cores from additional wells (Appendix) not noted on the data base because of proximity to other wells. Most cores were examined with the binocular microscope, and textures, structures, and mineralogy were described. Mineral percentages, porosity, and grain sizes were estimated and diagenetic features described for 41 thin sections from selected core intervals.

Outcrop study was limited because of poor exposures; good exposures occur in only a small part of the outcrop belt (fig. 1). The best exposure of vertical sequences occurs in a roadcut along U. S. Highway 277 near its junction with Texas Highway 1665, approximately 14 mi (22 km) north

of Eagle Pass in Maverick County. Along the Rio Grande west of this roadcut, outcrops are numerous but are highly weathered. A few small outcrops on the Chittim Anticline (fig. 1) are also highly weathered.

Ten preliminary regional cross sections were constructed across the Maverick Basin to determine general sandstone distribution in the San Miguel Formation. Electric logs were correlated and individual sandstone units delineated. Some of the sandstone units have been given different informal names in various oil fields; in this study the units are designated A, B, C, D, E, F, G, H, I, and P (table 1).

After regional control was established, three dip and three strike stratigraphic cross sections (pls. I through VI; fig. 1) were constructed to show detailed correlations necessary to determine stratigraphic relationships and geometry of the various sandstone units. Net-sandstone values determined for the major sandstone units were used to construct net-sandstone maps. San Miguel depositional systems and basin history were interpreted on the basis of these maps, the cross sections, and the core data.

Table 1. Stratigraphy and informal names of San Miguel sandstone units.

WESTERN SUBBASIN			EASTERN SUBBASIN	
	This Study	Other Informal Names	This Study	Other Informal Names
RELATIVE AGE ↑ younger ↓ older	I	First San Miguel	P { younger lobe	
	H	Torch, King, Fitzsimmons, Second San Miguel		
	G			
	F	Big Wells	Olmos B	
	E			
	D	Basal San Miguel		
	C	Elaine, Atlas		
	B			
	A			

GEOLOGIC SETTING OF THE MAVERICK BASIN

Basin History

The San Miguel Formation was deposited in the Maverick Basin in the easternmost part of the Rio Grande Embayment of the Gulf Coast Basin (fig. 2). Walper (1977) inferred that the Rio Grande Embayment originated as an aulacogen resulting from the breakup of Pangaea, initiated during the Triassic. By Late Jurassic the embayment had become a distinct, structurally negative area receiving sediments from basin margins. During the Early Cretaceous, carbonate deposition began on a broad shelf and dominated sedimentation until the latest Cretaceous, when renewed tectonism in source areas to the west and northwest caused an influx of clastics into the Maverick Basin and other parts of the Rio Grande Embayment. By the late Eocene, the embayment was filled, and centers of deposition had begun to shift gradually southeastward into the Gulf Coast Basin (Spencer, 1965).

Structural Framework

The Maverick Basin is separated from the East Texas Embayment to the northeast by the San Marcos Arch, which trends southeastward from the Llano Uplift (fig. 2). During Cretaceous sedimentation, this arch acted as a mildly positive structure that subsided at a much slower rate than adjacent basins (Loucks, 1976). The Maverick Basin is bounded on the north by the Balcones Fault Zone and on the northwest by the Devil's River Uplift. On the west, the basin is separated from other basins of the Rio Grande Embayment by the southeastward-trending Salado Arch. Alignment of the arch is related to older trends

established by Paleozoic tectonic activity and modified by folding associated with uplift of the Sierra Madre Oriental during the Laramide orogeny (Murray, 1961).

Several smaller structural features lie within the Maverick Basin. The most prominent of these is the southeastward-plunging Chittim Anticline, which is clearly defined by the San Miguel outcrop pattern (fig. 3). Folding occurred during latest Cretaceous and Tertiary (Spencer, 1965) and thus did not affect San Miguel sedimentation.

The Pearsall Ridge trends northeastward through the eastern part of Zavala County and the western half of Frio County (fig. 3). This ridge was probably mobile during Early Cretaceous (Rose, 1972) and remained a positive structural feature throughout the Cretaceous (Lewis, 1977). San Miguel deposition was affected by the ridge in that the section thickens in the associated syncline north of the ridge.

Few large faults occur in the Maverick Basin. Because no thick shale sequences were deposited on the stable carbonate platform, Upper Cretaceous clastics of the Maverick Basin do not display large growth faults common in thick Gulf Coast Tertiary clastics occurring farther gulfward. The only major faults are those of the Charlotte Fault system trending northeastward in the eastern part of the basin and faults associated with the Pearsall Ridge and Chittim Anticline (fig. 3). The Charlotte Fault system occurs along strike and may be a southwestward extension of the Mexia-Talco Fault system of Central and northeast Texas. The Charlotte and Mexia-Talco systems both lie within the hinge zone of the Gulf Coast Basin and are composed of en echelon grabens (Murray, 1961). A large normal fault along the north side of the Pearsall Ridge is downthrown to the north, accentuating the adjacent syncline (fig. 3). Several other normal faults cut the Chittim Anticline perpendicular to its axis.

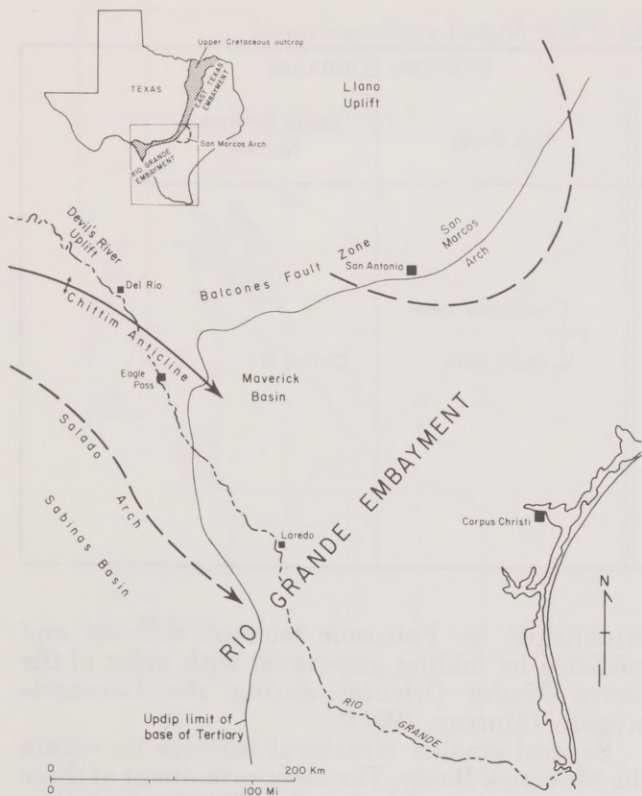


Figure 2. Structural framework of the Rio Grande Embayment. Modified from Spencer (1965).

Numerous basaltic volcanic plugs, erroneously described as "serpentine plugs," occur within the northern part of the Maverick Basin, especially in Zavala County. The plugs are at the southern end of an arcuate belt of plugs that extends approximately 250 mi (400 km) from Milam County southwestward to Dimmit County (fig. 4). Most of the volcanic activity took place during deposition of the Austin Group and the lower part of the Taylor Group. The distribution of the plugs suggests that the intrusions followed faults through the Precambrian and Paleozoic rocks of the Ouachita complex, moved up along fracture zones related to the Balcones Fault Zone, and finally penetrated the Austin and Taylor deposits (Simmons, 1967).

Differential compaction of sediments around the volcanic plugs produced complex structures involving local domes and tensional graben systems in overlying strata. Some San Miguel depositional sequences thin over plugs, depending on the rate of differential compaction and the degree of bathymetric expression of the plug.

Upper Cretaceous Stratigraphy

The thickest Upper Cretaceous deposits within the Gulf Coast Basin occur in the Rio Grande Embayment (Murray, 1957). A generalized dip

section through the Maverick Basin (fig. 5) shows most of the Upper Cretaceous stratigraphic units. Carbonate sedimentation dominated during the Cretaceous until the end of Austin deposition. Terrigenous clastic sedimentation began to prevail with deposition of the Taylor Group. While shallow-water carbonates of the Anacacho Formation accumulated updip around volcanic islands (Luttrell, 1977), shelf muds of the Upson Formation were deposited downdip. The three youngest Cretaceous formations in the basin, the San Miguel, Olmos, and Escondido, are dominantly clastics derived from Late Cretaceous tectonic uplifts to the west and northwest. The Austin, Anacacho/Upson, San Miguel, Olmos, and Escondido stratigraphic sequence prevails throughout most of the Maverick Basin subsurface. In the northernmost parts of the basin, however, the Escondido Formation (Navarro Group) directly overlies the Anacacho Formation (lower Taylor Group). An uplift at the end of Taylor deposition caused erosion of Olmos and San Miguel strata along the northern margin of the basin (Spencer, 1965).

SAN MIGUEL DEPOSITION

Cross sections and net-sandstone maps indicate that there were two Maverick subbasins in Texas during San Miguel deposition. These subbasins were primarily depositional features rather than prominent structural features and accumulated two distinct series of sand deposits supplied from two different sources. Stratigraphic strike section Y-Y' (fig. 6 and pl. V) best defines the two subbasins, although some of the mapped sandstone units are absent along the line of cross section. Sandstone units A through I were deposited in the western subbasin occupying much of Maverick, Zavala, and Dimmit Counties. Sandstone bodies labeled P were deposited in the eastern subbasin centered in Frio County (fig. 7 and table 1). Strike section Z-Z' (fig. 8 and pl. VI) crosses the eastern subbasin closer to its depocenter and indicates that sand supplied to the two subbasins overlapped through time.

Sediment Sources

Sediments were delivered to the western subbasin from the northwest (fig. 7) and probably originated from tectonic activity in either northern Mexico or New Mexico. Sediments were introduced to the eastern subbasin from the north and were probably derived from New Mexico.

Differences in sandstone mineralogy would help identify different source areas for eastern and western subbasins, but no cores or cuttings were available for sandstone units in the eastern subbasin. It is possible, however, that the fluvial systems feeding the two principal Maverick

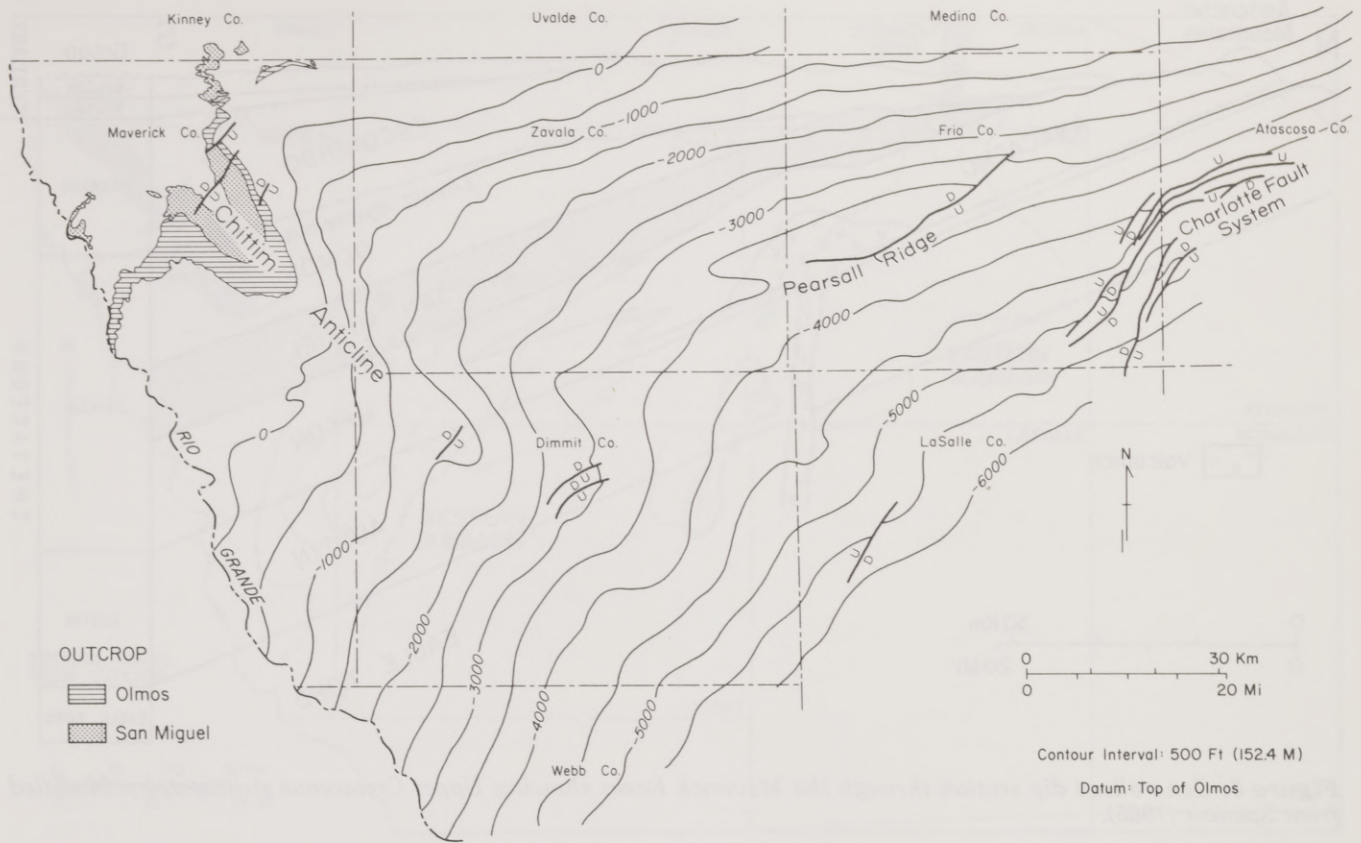


Figure 3. Structural configuration on top of the Olmos Formation. The Olmos directly overlies the San Miguel, and its regional structure closely resembles that of the San Miguel. Courtesy of Geomap Company.

subbasins originated in the same region or at least drained comparable terrain with similar rock types and climates, so that mineralogy and other sediment characteristics of the two may be similar. Also, both areas may have received volcanic debris either eroded from local volcanic plugs or contributed directly by volcanic activity in the northern part of the Maverick Basin.

Depositional Systems and Origin of Sandstone Geometry—General Comments

San Miguel sandstone units are deltaic facies reworked to varying degrees by contemporaneous marine processes and by physical and biological processes during subsequent transgression. The thickest parts of the sandstone units are strike aligned, but most net-sandstone patterns also indicate updip feeder systems.

Delta morphology is influenced by many factors but is primarily the product of an interplay between fluvial sediment input and reworking of sediments by wave or tidal processes or both (Coleman and Wright, 1975; Galloway, 1975). During their prograding stages, San Miguel depositional systems could have been broadly classed as

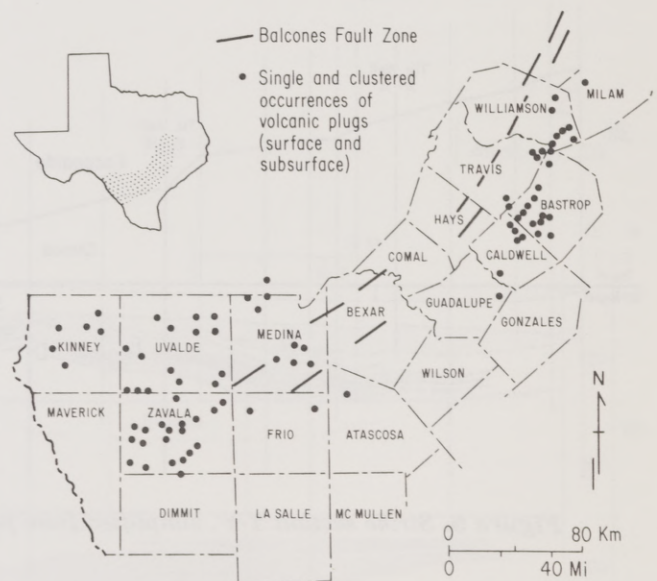


Figure 4. Location of Cretaceous volcanic plugs, Central and South Texas. Modified from Luttrell (1977).

high-destructive, wave-dominated deltas, which were described by Fisher and others (1969) as deltas in which “principal accumulation is as a series of coastal barriers flanking the river mouth, giving a cusped to arcuate trend of the main sand

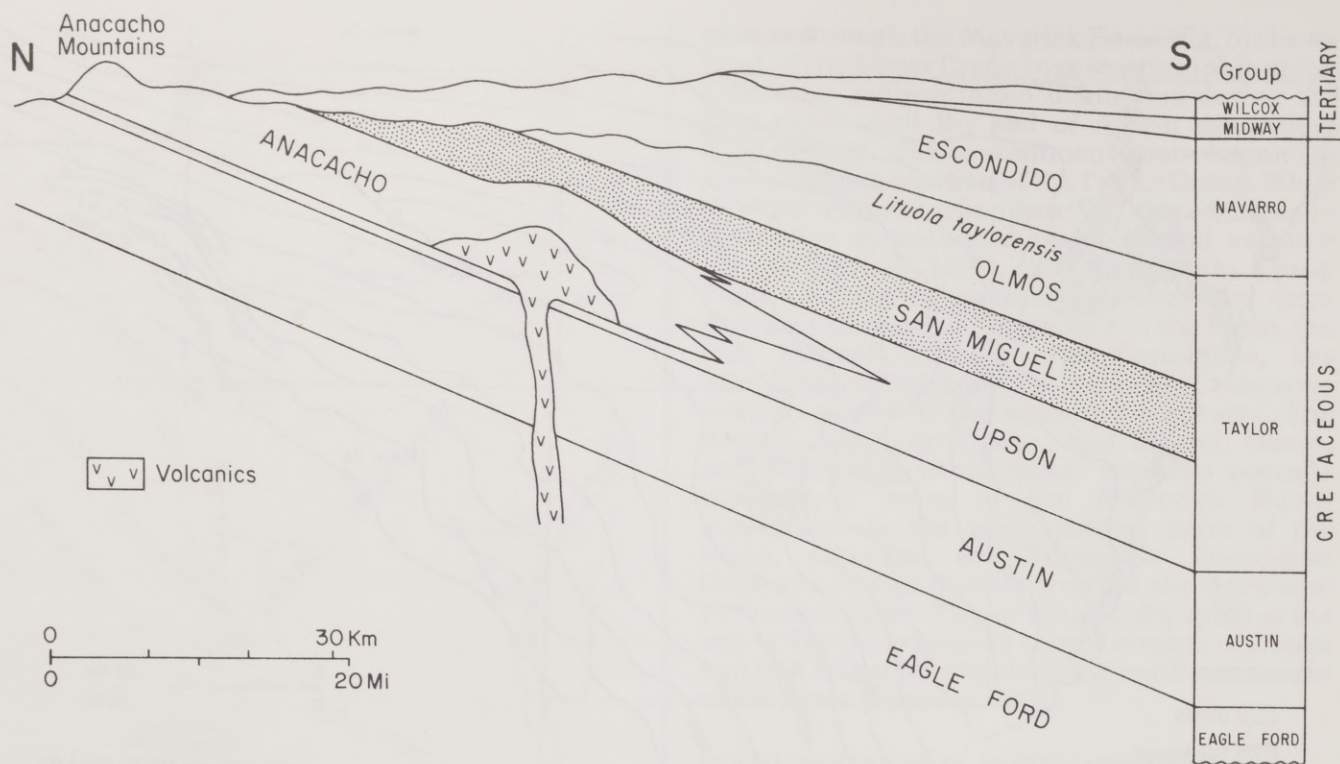


Figure 5. Generalized dip section through the Maverick Basin showing Upper Cretaceous stratigraphy. Modified from Spencer (1965).

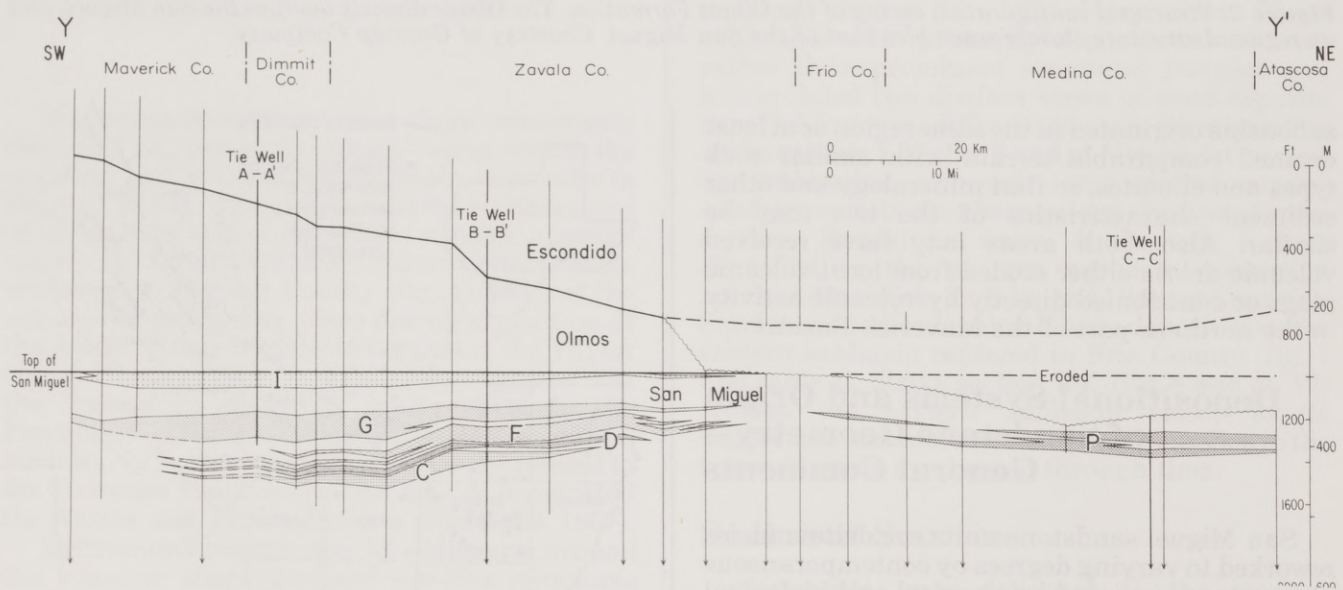


Figure 6. Strike section Y-Y', simplified from plate V. Line of cross section is shown in figure 1.

units." In these systems, wave energy dominates over rate of sediment input and tidal energy. Consequently, most of the sediments discharged into the marine environment are reworked along strike by wave processes, so that the main sand bodies are strike oriented (fig. 9).

On Galloway's (1975) delta-classification triangle (fig. 10), most of the San Miguel systems

plot in the lower left third and near the triangle border connecting the wave energy flux and sediment input apexes. The San Miguel deposits show no evidence of strong tidal influence; tidal range was probably microtidal, as it is along the present Texas Gulf Coast.

The preserved morphology of the San Miguel sandstone bodies depended on three primary

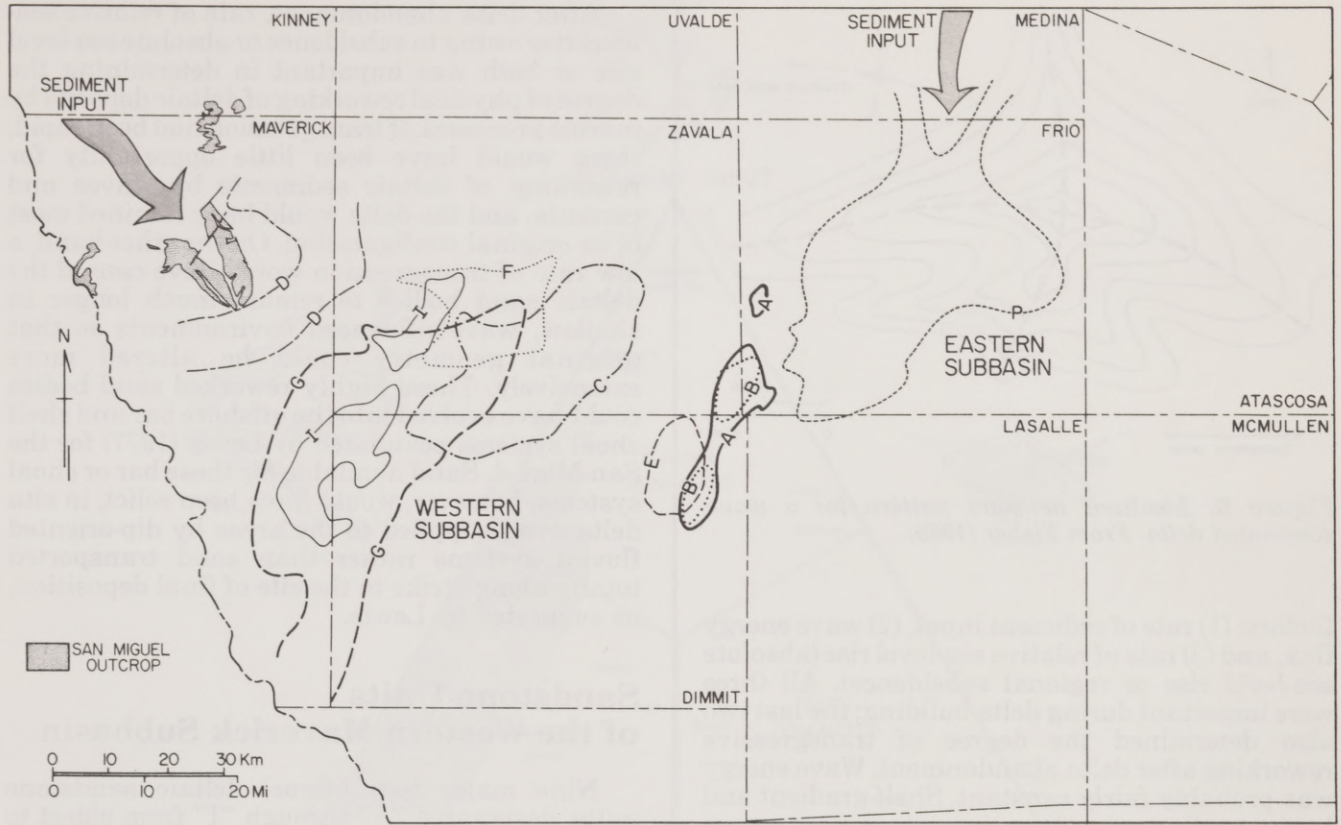


Figure 7. Depocenters of San Miguel sandstone units and directions of sediment input. Depocenters are defined by the 70-ft (21-m) net-sandstone contour.

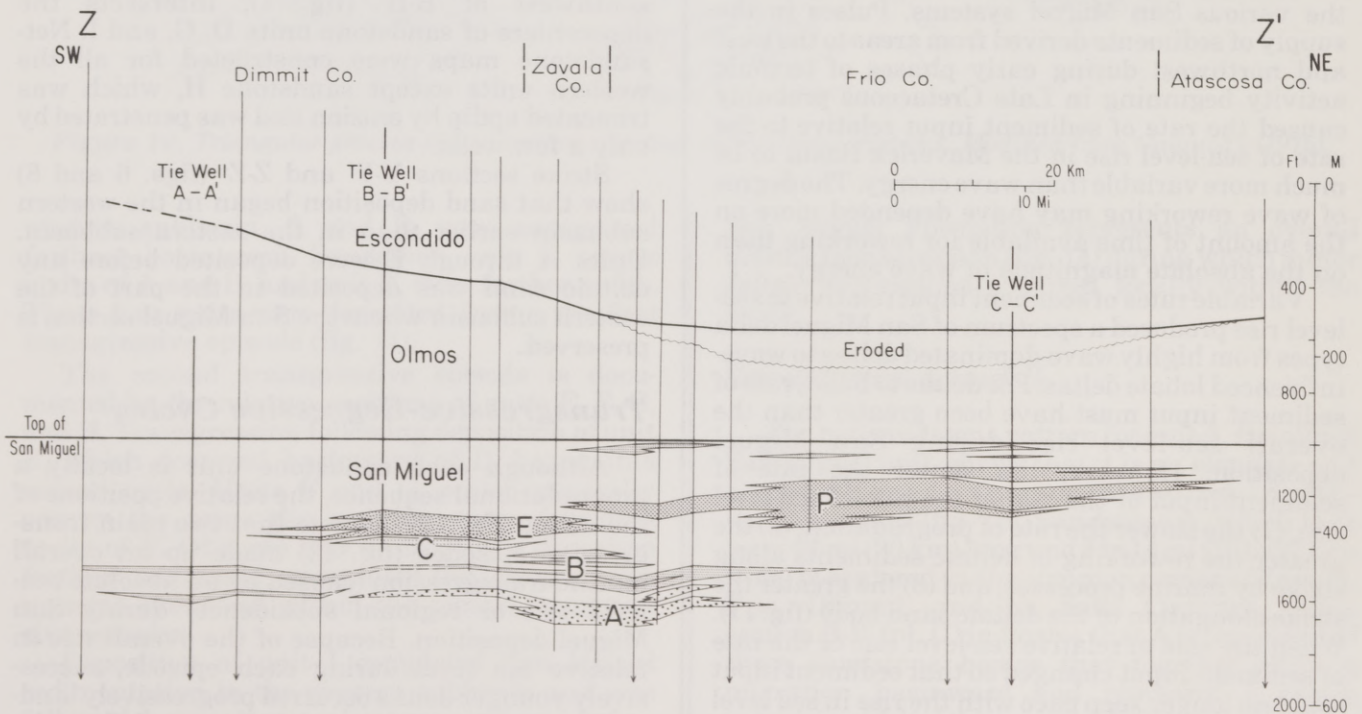


Figure 8. Strike section Z-Z', simplified from plate VI. Line of cross section is shown in figure 1.

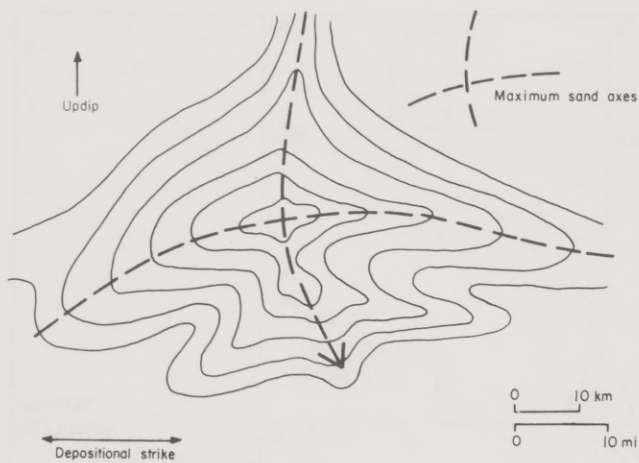


Figure 9. Idealized net-sand pattern for a wave-dominated delta. From Fisher (1969).

factors: (1) rate of sediment input, (2) wave energy flux, and (3) rate of relative sea-level rise (absolute sea-level rise or regional subsidence). All three were important during delta building; the last two also determined the degree of transgressive reworking after delta abandonment. Wave energy was probably fairly constant. Shelf gradient and basin configuration, two important parameters that determine wave energy, did not change significantly during San Miguel deposition. Shelf width, another possible influence upon wave energy, varied with the distance that each delta built toward the shelf edge, but most likely did not result in significant differences in wave energy for the various San Miguel systems. Pulses in the supply of sediments derived from areas to the west and northwest during early phases of tectonic activity beginning in Late Cretaceous probably caused the rate of sediment input relative to the rate of sea-level rise in the Maverick Basin to be much more variable than wave energy. The degree of wave reworking may have depended more on the amount of time available for reworking than on the absolute magnitude of wave energy.

Variable rates of sediment input relative to sea-level rise produced a spectrum of San Miguel delta types from highly wave-dominated deltas to wave-influenced lobate deltas. For deltas to build, rate of sediment input must have been greater than the overall sea-level rise during San Miguel deposition. However, the slower the rate of sediment input or the higher the rate of sea-level rise, (1) the slower the rate of progradation, (2) the greater the reworking of deltaic sediments along strike by marine processes, and (3) the greater the strike-elongation of the deltaic sand body (fig. 11). When the rate of relative sea-level rise or the rate of sediment input changed so that sediment input could no longer keep pace with the rise in sea level and reworking by marine processes, then progradation ceased and the delta was abandoned.

After delta abandonment, rate of relative sea-level rise owing to subsidence or absolute sea-level rise or both was important in determining the degree of physical reworking of deltaic deposits by marine processes. If transgression had been rapid, there would have been little opportunity for reworking of deltaic sediments by waves and currents, and the delta would have retained most of its original configuration. On the other hand, a low rate of transgression would have caused the deltaic sand bodies to remain much longer in shallow, wave-influenced environments so that original geometry could be altered more extensively. These highly reworked sand bodies could have evolved into the offshore bar and shelf shoal systems postulated by Lewis (1977) for the San Miguel. Sand available for these bar or shoal systems, however, would have been relict, in situ delta sand supplied to the areas by dip-oriented fluvial systems rather than sand transported totally along strike to the site of final deposition, as suggested by Lewis.

Sandstone Units of the Western Maverick Subbasin

Nine major San Miguel deltaic sandstone units, designated "A" through "I" from oldest to youngest, were delineated in the western subbasin of the Maverick Basin. Dip section B-B' (fig. 12 and pl. II) follows the central dip axis of the western subbasin (figs. 1 and 7) and intersects all nine units, including the main depocenters of most. Dip section A-A' (pl. I), parallel to but southwest of B-B' (fig. 1), intersects the depocenters of sandstone units D, G, and I. Net-sandstone maps were constructed for all the western units except sandstone H, which was truncated updip by erosion and was penetrated by only a few wells.

Strike sections Y-Y' and Z-Z' (figs. 6 and 8) show that sand deposition began in the western subbasin earlier than in the eastern subbasin. Units A through E were deposited before any deltaic sand was deposited in the part of the eastern subbasin where the San Miguel section is preserved.

Transgressive-Regressive Cycles

Although each sandstone unit is locally a progradational sequence, the relative positions of the deltas (fig. 12) indicate that two main transgressive episodes (fig. 13) made up an overall marine transgression (caused by an absolute sea-level rise or regional subsidence) during San Miguel deposition. Because of the overall rise in relative sea level during each episode, successively younger deltas occurred progressively landward, resulting in coastal onlap, as defined by Vail and others (1977). The oldest units in the

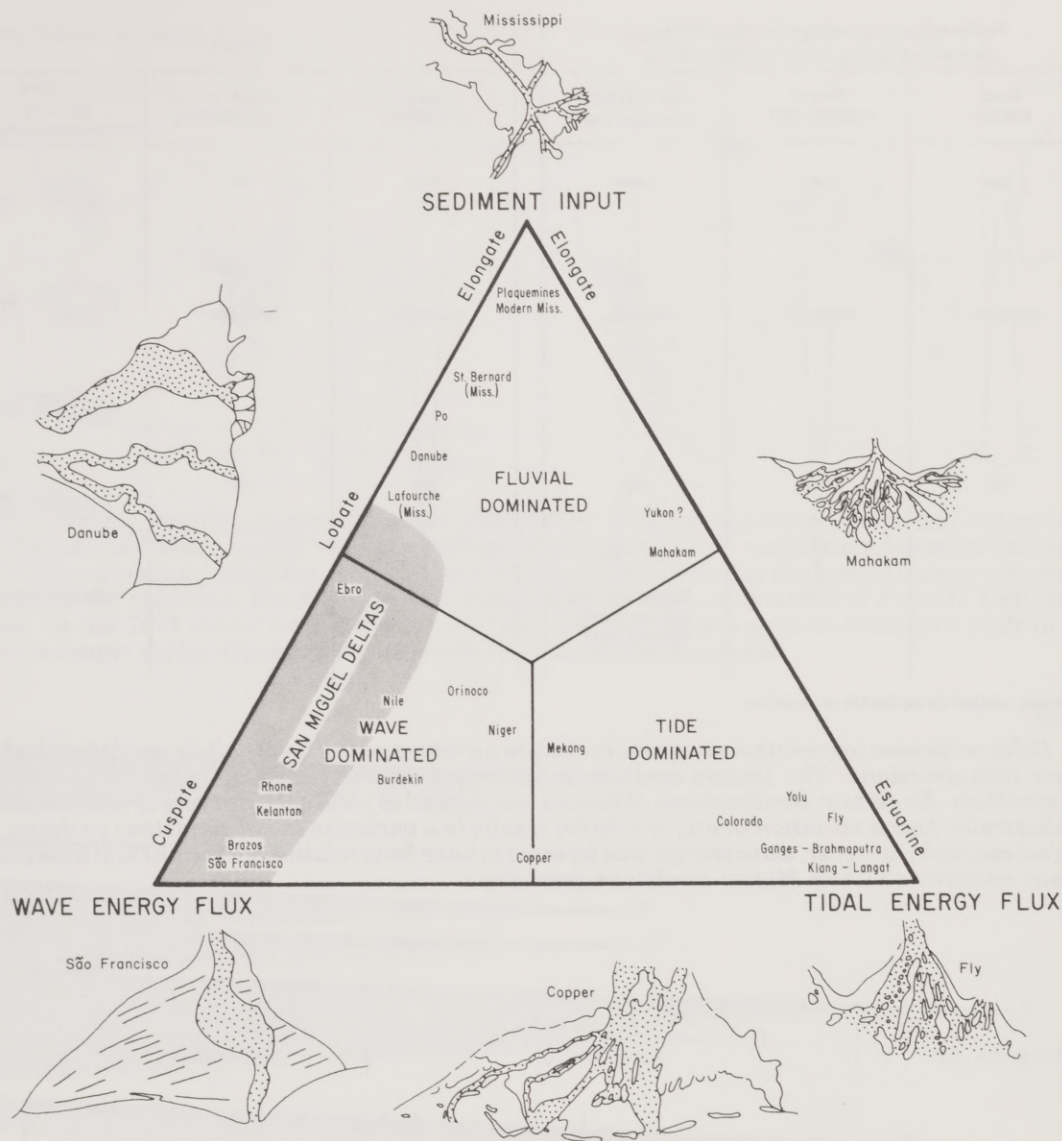


Figure 10. Triangular process classification of deltaic depositional systems. Modified from Galloway (1975).

western subbasin, A and B, were superposed farthest basinward. Sandstone unit C occurs updip of A and B, and unit D, even farther updip. These four units were deposited during the first transgressive episode (fig. 14).

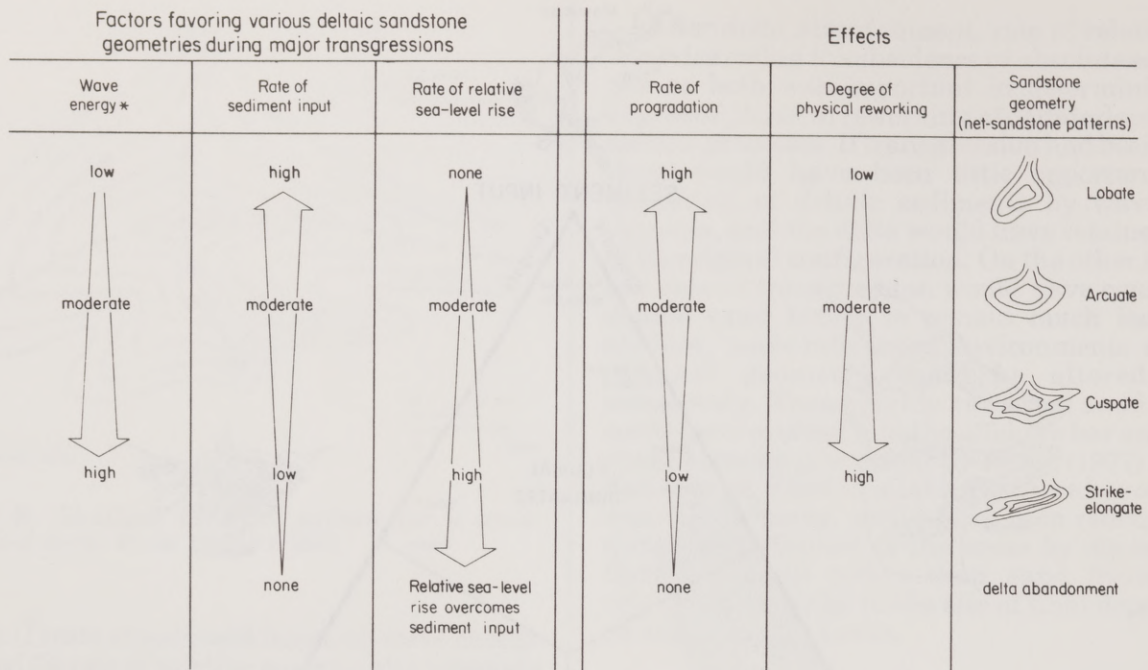
The second transgressive episode is documented by the relative positions of units E, F, G, and H. Transgression following deposition of unit E, which occurred basinward of D, began this second cycle. Units F and G, which generally occupy the same dip position, were deposited updip of E. Of these four units, H was deposited farthest updip and represented the last minor regression preserved within the second transgressive complex.

Deposition of unit I completed San Miguel sedimentation in the western subbasin and was followed by another major transgression before progradation of Olmos delta systems. Thus, the

San Miguel Formation represents an overall marine transgression (fig. 14) during which minor deltaic regressions occurred locally within the basin.

Sandstones A and B

The net-sandstone pattern for unit A, the oldest San Miguel unit, shows that it is an elongate and strike-aligned system trending north-northeastward (fig. 15). Sandstone A, which is at least 43 mi (70 km) long and 8 to 14 mi (13 to 22 km) wide, is centered in the common corner of Zavala, Frio, Dimmit, and La Salle Counties. Cross section B-B' (pl. II) indicates that A is composed of three sandstone bodies that together show a migration basinward and represent a minor regressive (deltaic) sequence. At the northern end of sandstone unit A is vague evidence of an updip



*Relatively constant during San Miguel deposition.

Figure 11. Delta responses to variations in primary factors affecting geometry of deltaic sandstone bodies deposited during major transgressions. The factors and parameters they affect, including sandstone geometry, define a continuous spectrum. No certain combinations of factors are implied to yield specific types of net-sandstone patterns. The figure illustrates how a variation in any one factor results in a variation in net-sandstone patterns. Note that in the San Miguel example, however, wave energy was inferred to have been relatively constant and thus did not account for significant variations in San Miguel sandstone geometry.

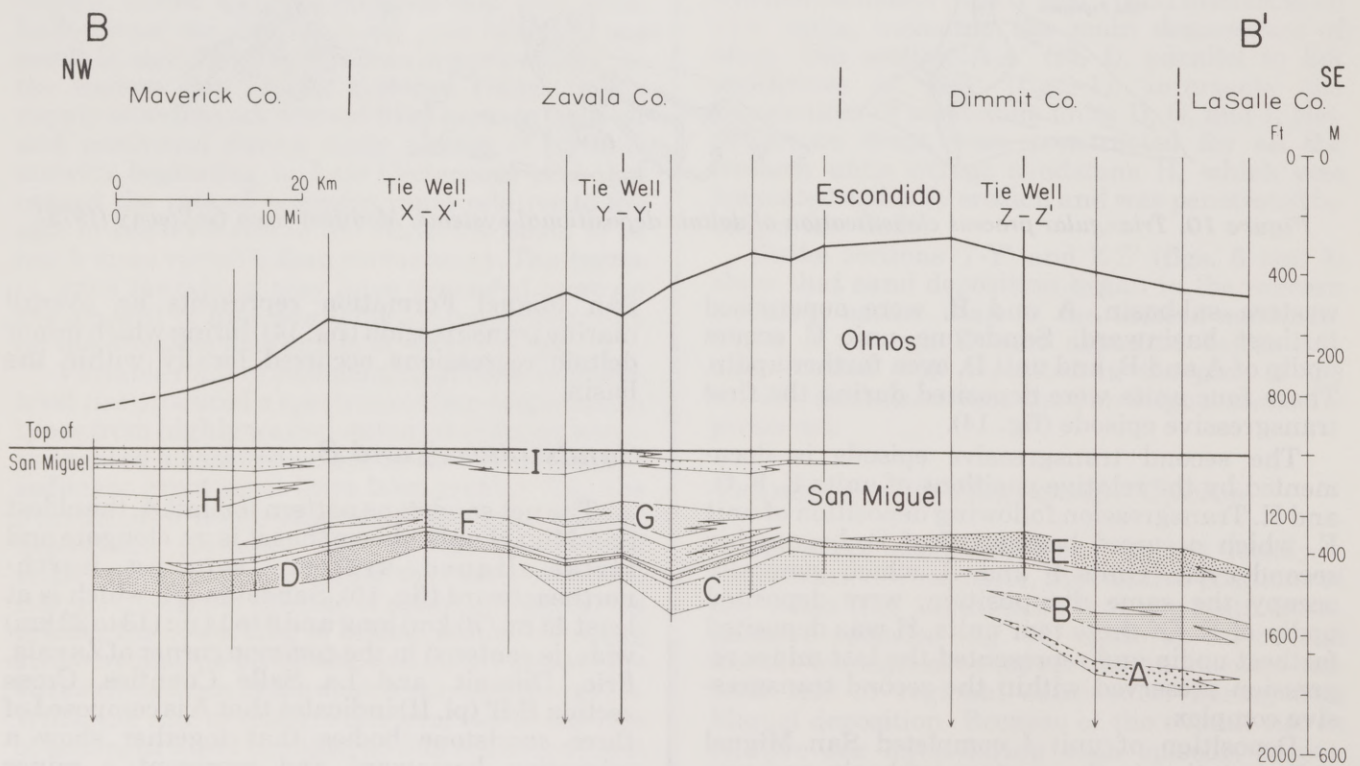


Figure 12. Dip section B-B', simplified from plate II. Line of cross section is shown in figure 1.

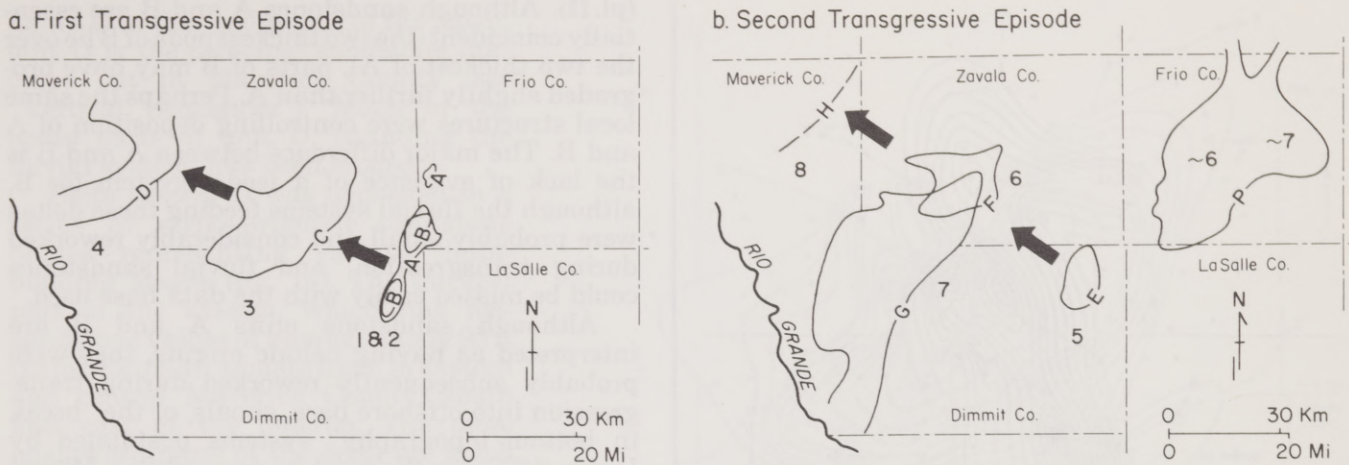


Figure 13. Two transgressive episodes of the San Miguel defined by the relative positions and order of deposition (1 through 8) of sandstone units. Locally regressive deltaic sandstones A, B, C, and D were deposited during the first net transgressive episode (a) and sandstones E, F, G, and H were deposited during the second transgressive episode (b) in the western Maverick subbasin. The two lobes of P are approximate time equivalents of F and G. Unit configurations are indicated by the 70-ft (21-m) net-sandstone contour. Arrows indicate general landward shift in positions of progressively younger deltas deposited during each net transgressive episode.

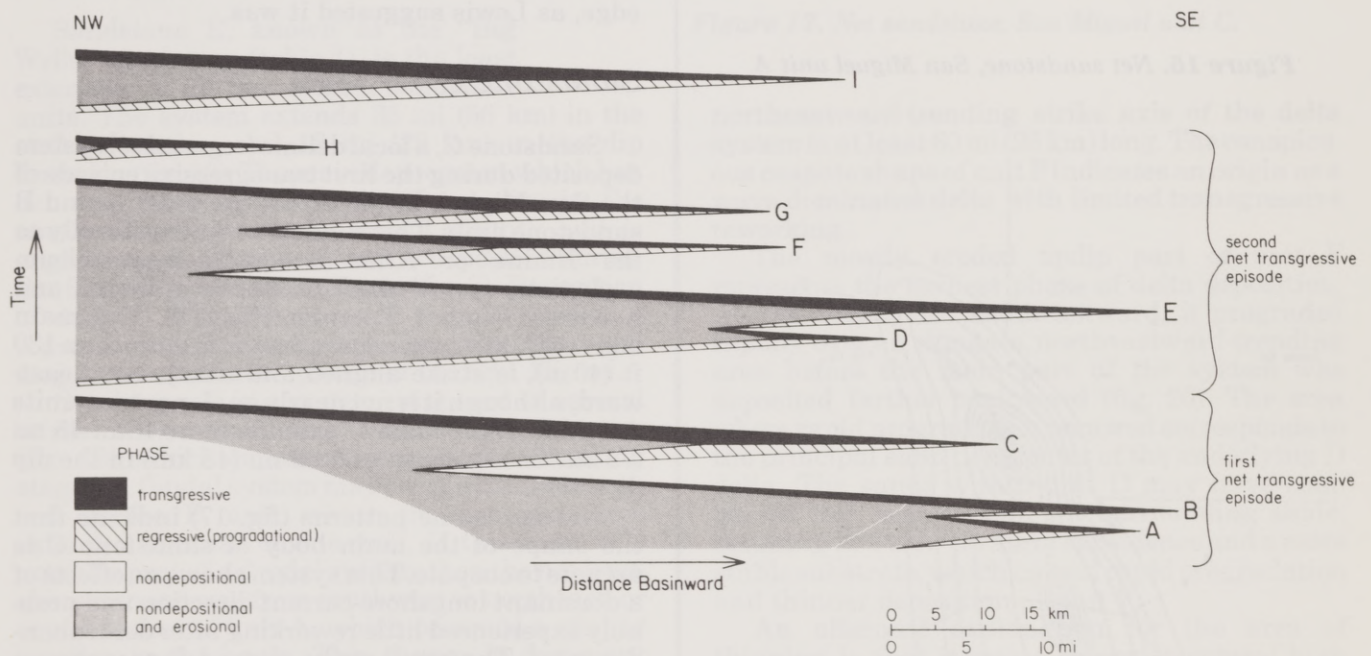


Figure 14. Transgressive-regressive cycles shown by a schematic dip section through the axis of the western Maverick subbasin. Based on the schematic convention of Frazier (1974).

feeder system trending westward. Because most of the unit extends to the south of this feeder system, net longshore currents must have been from northeast to southwest. Thickness of sandstone is not uniform along the strike axis of A. The sandstone is concentrated in three main "pods," or depocenters, the thickest of which is almost 130 ft (40 m).

Sandstone B (fig. 16) is elongate and strike aligned and, consequently, is similar to A. However, unit B trends slightly more to the northeast

than A. Unit B is generally superposed on A but covers a greater area and extends farther southwestward, almost to the Webb county line. The strike pinch-outs of B are difficult to define because of limited well control, but the unit is longer than the 54 mi (86 km) estimated between 10-ft (3.05-m) contours (0-ft contours are not shown for any of the net-sandstone maps constructed in this study). Another similarity between A and B is that the two principal sandstone bodies of B, like those of A, show evidence of a slight regression

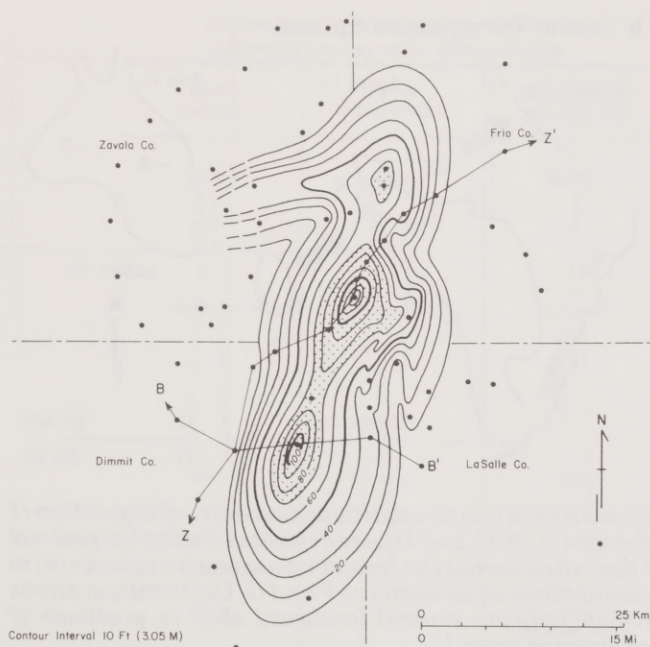


Figure 15. Net sandstone, San Miguel unit A.

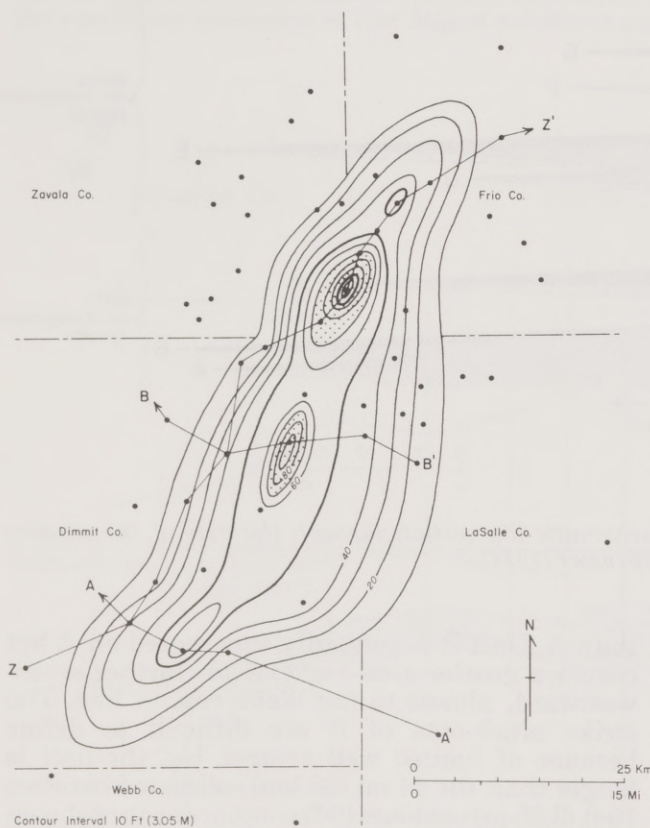


Figure 16. Net sandstone, San Miguel unit B.

(pl. II). Although sandstones A and B are essentially coincident (the two thickest pods of B lie over the two thickest of A), parts of B may have prograded slightly farther than A. Perhaps the same local structures were controlling deposition of A and B. The major difference between A and B is the lack of evidence of a feeder system for B, although the fluvial systems feeding these deltas were probably small and considerably reworked during transgression, and fluvial sandstones could be missed easily with the data base used.

Although sandstone units A and B are interpreted as having deltaic origins, they were probably subsequently reworked during transgression into offshore bars, shoals, or the "break in bottom topography" systems postulated by Lewis (1977) for the most basinward San Miguel sandstones. Correlations (pl. II) show that these units pinch out updip onto what may have been a sharply defined basin margin at the time of deltaic deposition. With transgression, however, the old basin margin became a sharp break in bottom topography where the deltaic sand was reworked, although this break was probably not the shelf edge, as Lewis suggested it was.

Sandstone C

Sandstone C, a local deltaic (regressive) system deposited during the first transgressive episode of the San Miguel, lies updip of the older A and B sandstone units. This sandstone, known locally as the "Elaine" or "Atlas" sandstone by petroleum geologists, covers much of southern Zavala and northern Dimmit Counties (fig. 17). The main body of C, in which net sandstone is more than 130 ft (40 m), is strike aligned and trends northeastward, although it is not nearly as elongate as units A and B. Sandstone C extends more than 45 mi (72 km) along strike and 30 mi (48 km) in the dip direction.

Net-sandstone patterns (fig. 17) indicate that the shape of the main body of sandstone C is arcuate to cusped. This system shows no effects of a dominant longshore-current direction and probably experienced little reworking after delta abandonment. The small strike-aligned depocenter on the downdip side of unit C resulted from the last building episode of the C delta, during which sand was reworked along strike. On the updip side, net-sandstone patterns indicate the position of a fluvial system, although most of this system has been eroded.

Sandstone D

Sandstone D, the unit deposited farthest updip during the first San Miguel transgressive episode, extends over much of the northern half of Maverick and western Zavala Counties (fig. 18). Known as the "basal San Miguel" sandstone

(table 1) in this updip part of the basin, unit D is the principal sandstone that crops out in Maverick County (see "Vertical Sequences"). Much of the updip parts of unit D, including the fluvial system, has been eroded.

Delta system D was deposited in a series of strike-oriented sandstone bodies representing various delta-building stages (fig. 18). The thickest part of the system, which has net sandstone values of approximately 95 ft (29 m), forms an arcuate trend in eastern and central Maverick County, south and east of the outcrop. The more basinward parts of the delta are much thinner. The thinner parts of the D system probably resulted from rapid progradation over the sand depocenter of unit C where subsidence was less significant than in surrounding shale.

Sandstone E

Sandstone E, known as the "Big Wells" sandstone (table 1), is the least extensive of all San Miguel sandstone units. The system extends 35 mi (56 km) in the strike direction and 18 mi (29 km) in the dip direction (fig. 19). The main depocenter, which has net sandstone up to 90 ft (27 m), lies in the northeastern corner of Dimmit County and is slightly updip of units A and B deposited during the first transgressive episode (fig. 7). Deposition of delta E farther basinward than D marked a regression, which was then followed by the second major transgressive episode of the San Miguel.

Sandstone E is a system composed of several northeastward-trending, strike-aligned bodies (fig. 19), which represent several delta-building stages. A fluvial system may occur at the southern end of the E unit, where the contours were extended because of one well. If this feature is actually part of a fluvial system, then the net longshore current was from southwest to northeast, or opposite that of unit A, which occupied a similar location in the basin. This change in dominant longshore-current direction is reasonable because the Maverick Basin shoreline may have been situated analogous to the present "coastal bend" part of the South Texas coastline, where opposing longshore currents converge. Changes in shoreline configuration need not have been very great to cause periodic reversals in the dominant longshore-current direction.

Sandstone F

The main depocenter of sandstone F, which lies updip of unit E, is in the southwest quarter of Zavala County (fig. 20), where almost 90 ft (27 m) of net sandstone was deposited. The main,

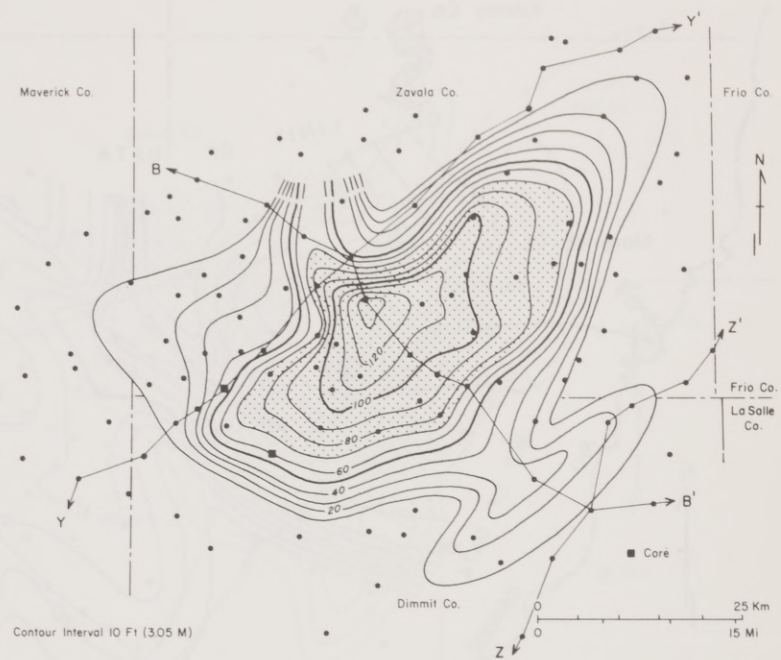


Figure 17. Net sandstone, San Miguel unit C.

northeastward-trending strike axis of the delta system is at least 60 mi (96 km) long. The conspicuous cusped shape of unit F indicates an origin as a wave-dominated delta with limited transgressive reworking.

The mostly eroded updip part of unit F represents the earliest phase of delta deposition. As the delta built southeastward, it prograded rapidly over an elongate, northeastward-trending area before the main part of the system was deposited farther basinward (fig. 20). The area where rapid progradation occurred corresponds to the principal sand depocenter of the underlying D delta. The sands within unit D may have compacted less readily than the surrounding shale, resulting in a slower rate of subsidence and a more stable substrate, which caused rapid progradation and thinner deposition of unit F.

An alternate explanation for the area of thinning is that it was a minor structural high that affected sedimentation. Such a structural feature would have been formed after deposition of delta D, however, because D is thickest in that area. There is no present structural evidence of an elongate high, although such a feature probably would have been masked by the younger Chittim Anticline. Erosion as a cause of thinning is unlikely because none of the sedimentary cycles that thin in the area show signs of truncation.

Sandstone G

Sandstone G, known variously by petroleum geologists as the "Torch," the "King" (Lewis, 1962), the "second San Miguel," or the

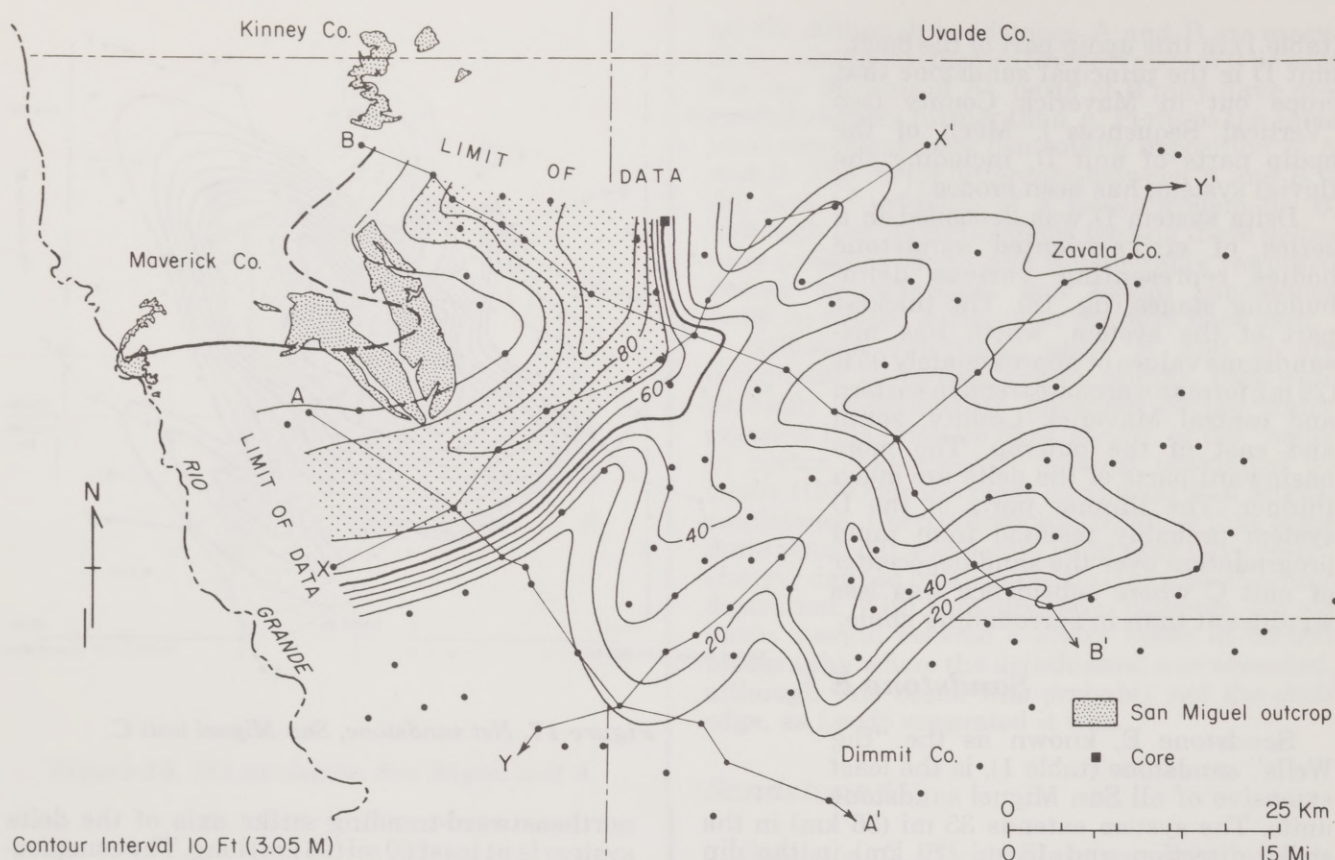


Figure 18. Net sandstone, San Miguel unit D.

“Fitzsimmons” sandstone (table 1), is a large, northeastward-trending, strike-oriented system covering western Zavala, western Dimmit, and southern Maverick Counties (fig. 21). Sandstone G extends at least 60 mi (96 km) along strike in Texas and into Mexico past the limits of this study. The main depocenter, which has net-sandstone values up to almost 140 ft (43 m), lies in southwestern Zavala and northwestern Dimmit Counties.

Sandstone G, a small regressive delta deposited during the second major San Miguel transgressive episode, occupies almost the same dip position as unit F (fig. 13b). Although the thickest part of G lies southwest of the depocenter of unit F, sandstone G overlaps much of the F system and thins in the same area that F does (fig. 20).

Sandstone G is a deltaic system which was reworked along strike probably during both the delta building and the transgression following delta abandonment. The position of a feeder system at the northern end of the sandstone unit indicates that sand was transported to the southwest by strong longshore currents.

Sandstone I

Sandstone I, known informally as the “first San Miguel” sandstone (table 1), is the youngest of

the San Miguel sandstone units in the western subbasin of the Maverick Basin. This elongate, northeastward-trending, strike-oriented system occupies generally the same area as unit G (figs. 21 and 22). The outline formed by the 10-ft (3.05-m) net-sandstone contour shows that system I is at least 60 mi (96 km) long and 22 mi (35 km) wide. The main sandstone body, which has maximum net-sandstone values slightly greater than 80 ft (24 m), extends almost to the Rio Grande; a few thin sandstones possibly extend into Mexico.

A highly eroded older phase of system I lies updip, analogous to that of unit F (fig. 20). Although net-sandstone patterns in that updip part of sandstone I were contoured with a dominant dip alignment, data are too few to be certain of the patterns. It is possible that the updip part may have been reworked along strike like the downdip younger part of the system. After deposition of the updip part, delta I prograded rapidly over the same stable northeastward-trending area where thinning of unit F occurred in eastern Maverick and western Zavala Counties.

Because longshore transport was toward the southwest, system I prograded primarily in that direction. As with unit G, reworking by waves and the strong longshore currents significantly affected the final sandstone-body shape.

Sandstone Units of the Eastern Maverick Subbasin

San Miguel deltaic sand deposition began later in the eastern subbasin (at least where San Miguel deposits are preserved) than in the western subbasin of the Maverick Basin. According to regional correlations, the largest eastern sandstone bodies (grouped as P) are interpreted to be stratigraphically equivalent to units F and G of the western subbasin (fig. 13b and pl. V). The thickest sandstone body in unit P is known by some geologists as the "Olmos B" sandstone (table 1). Detailed correlations, however, show that unit P interfingers with San Miguel deposits of the western subbasin and is definitely older than the Olmos. In addition, subsurface correlations carried from the Olmos section in Atascosa County described by Glover (1955) show that the P sandstone bodies are older than the Olmos B defined in that eastern part of the Maverick Basin.

Unit P (fig. 23) is a composite of two main delta lobes (pls. III, V, and VI), which prograded farther into the Maverick Basin than did their western counterparts (fig. 13b). The P deltas were probably more highly constructive and more nearly lobate than were the western deltas. Although the systems were wave influenced, the rate of sediment input, which was from the north, may have been greater than that for the western subbasin, which received sediments from the northwest. Another possible reason the deltas of the P unit prograded farther than did the western deltas was that the eastern subbasin was closer to the San Marcos Arch, where subsidence was much slower and relative sea level more stable.

The two main delta lobes of unit P, which occupy most of Frio County (fig. 23), were combined for net-sandstone mapping because it is difficult to pick a boundary between the two where the sandstones closely overlap. Correlations show, however, that the older and thicker of the two lobes composes most of the western part of unit P. This older P lobe shows the thickest single upward-coarsening sandstone sequence of any San Miguel unit (pl. VI, Parker #1-R Oppenheimer). The second lobe was developed in the eastern side of the area covered by unit P.

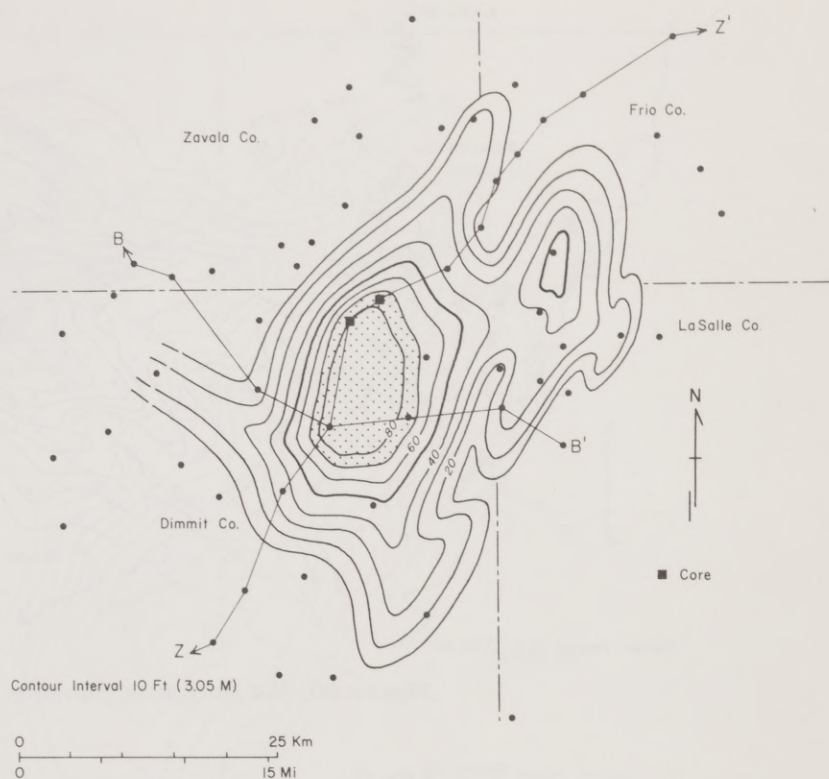


Figure 19. Net sandstone, San Miguel unit E.

Vertical Sequences

Cores available for study came from the C, D, E, G, and I sandstone units of the San Miguel. Unfortunately, only a few cores, which were taken from only the main depocenters or the nearby flanks of the units, were available for each unit. Thus, core distribution did not allow observation of lateral changes within the systems. Electric logs did, however, document lateral changes within each system, but they indicated great similarities in vertical sequences of the various sandstone units, especially in the main depocenters.

Textures

Both cores and electric logs indicate that the sandstone bodies are dominated by upward-coarsening cycles, such as shown in figure 24. Figure 25 illustrates the distribution of types of log patterns in sandstone G. Individual vertical sequences in the depocenter of unit G predominantly show more than one upward-coarsening cycle (log pattern A). Updip and downdip, however, the sequences generally show single upward-coarsening cycles (log pattern B). These upward-coarsening cycles, multiple or single, either have a sharp upper boundary or show a finer zone at the

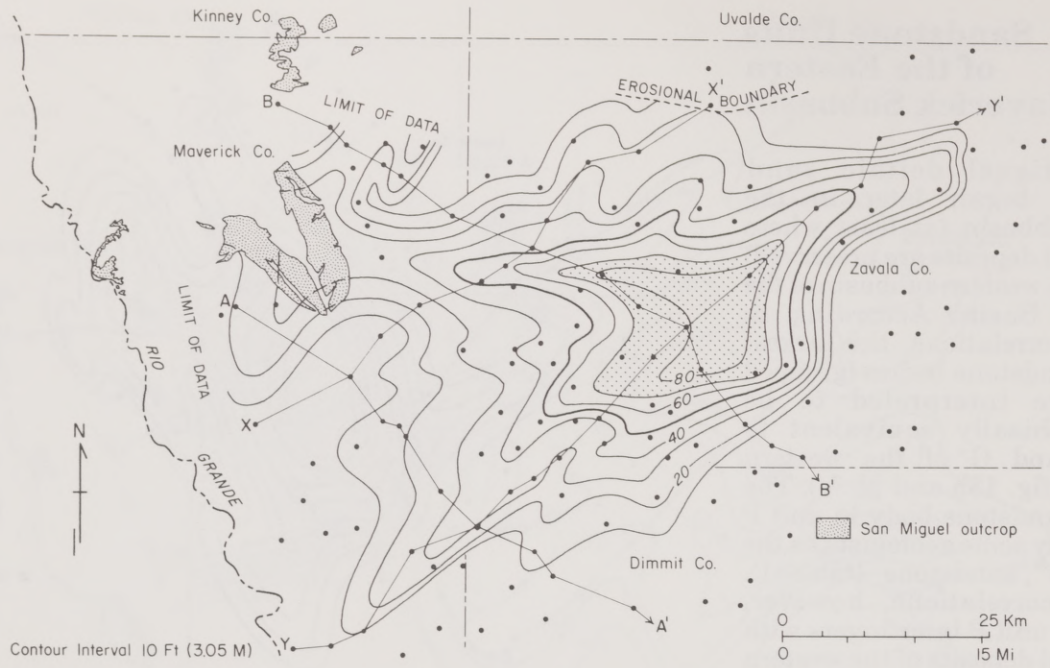


Figure 20. Net sandstone, San Miguel unit F.

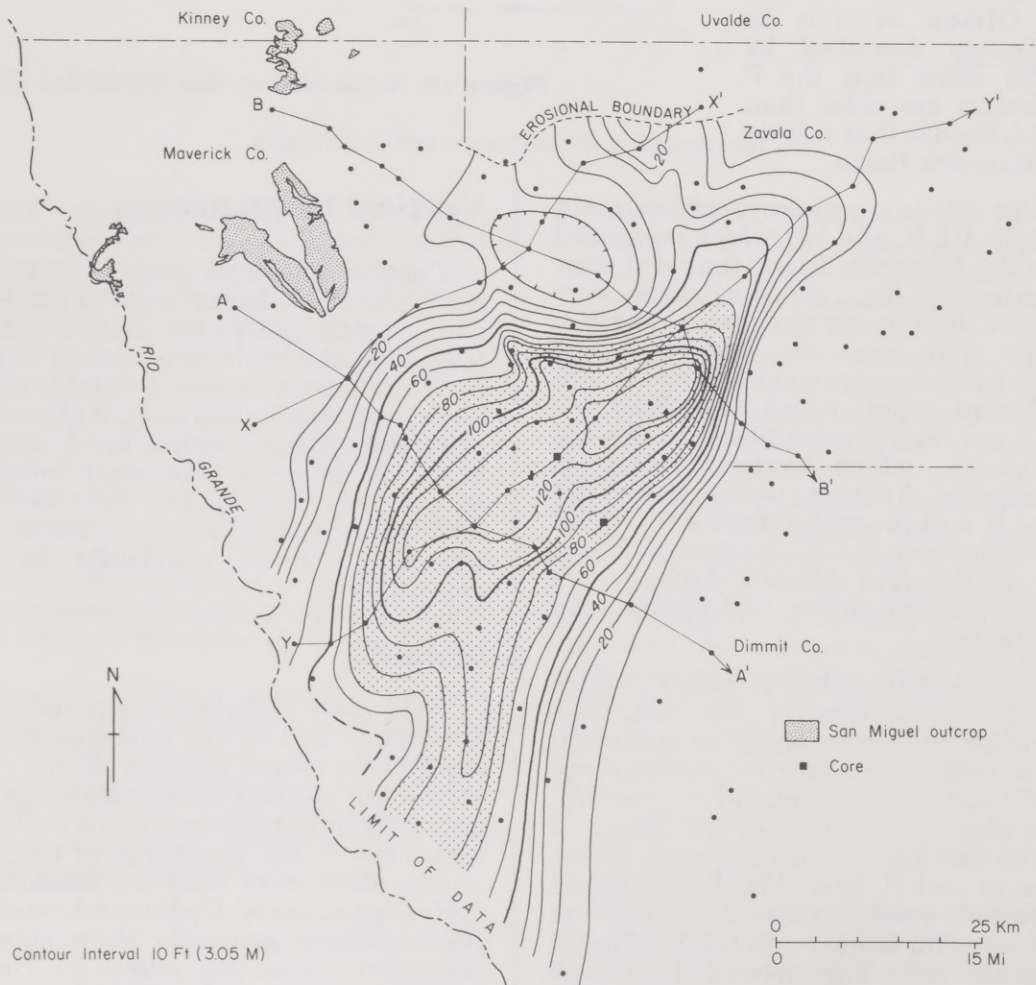


Figure 21. Net sandstone, San Miguel unit G.

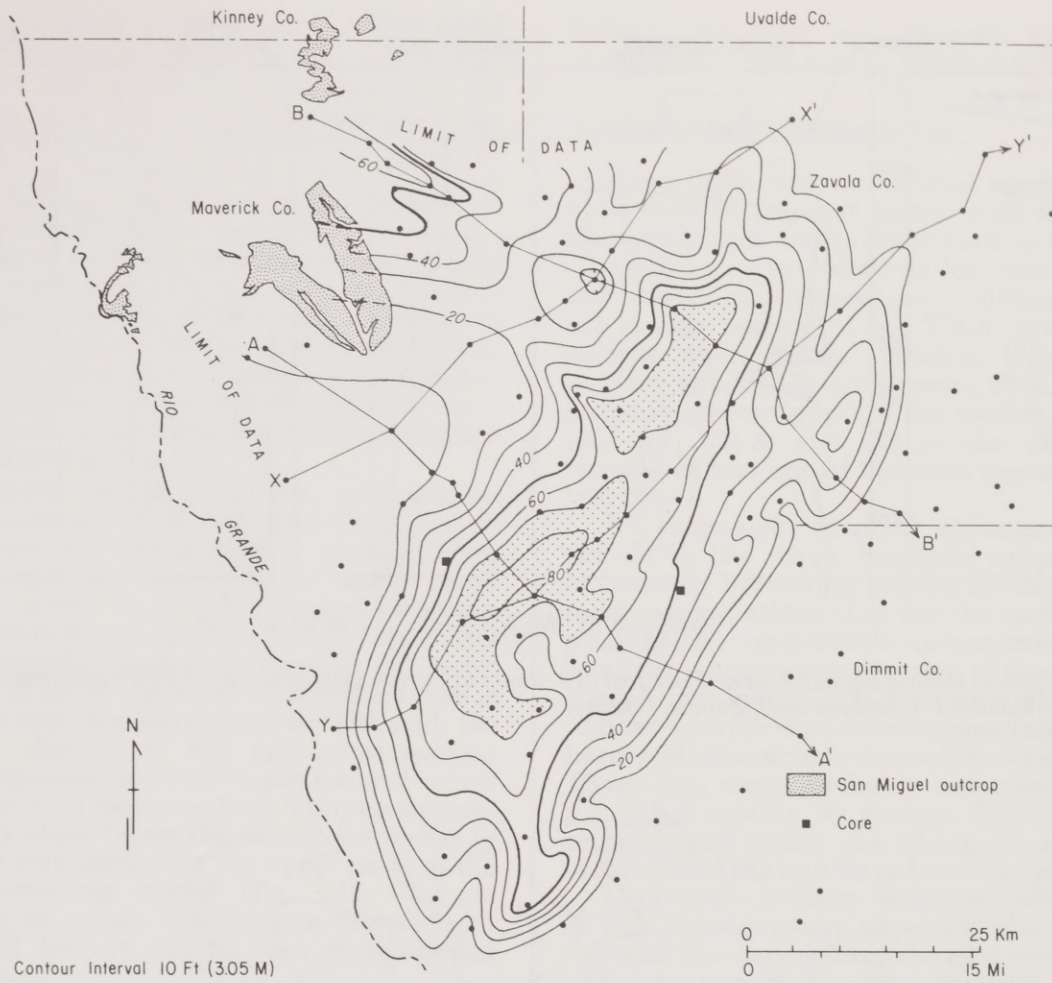


Figure 22. Net sandstone, San Miguel unit I.

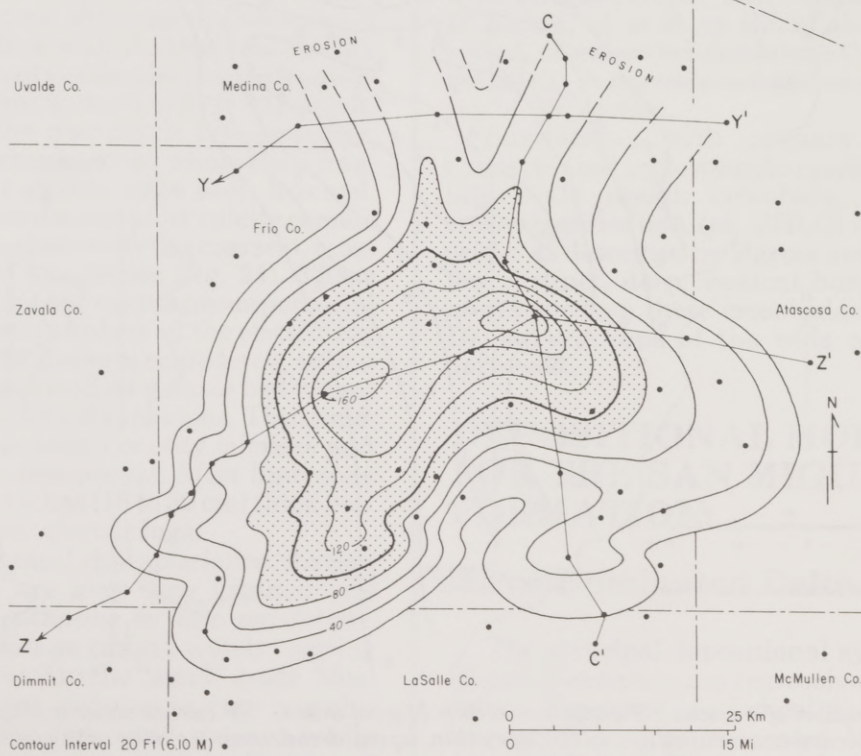


Figure 23. Net sandstone, San Miguel unit P.

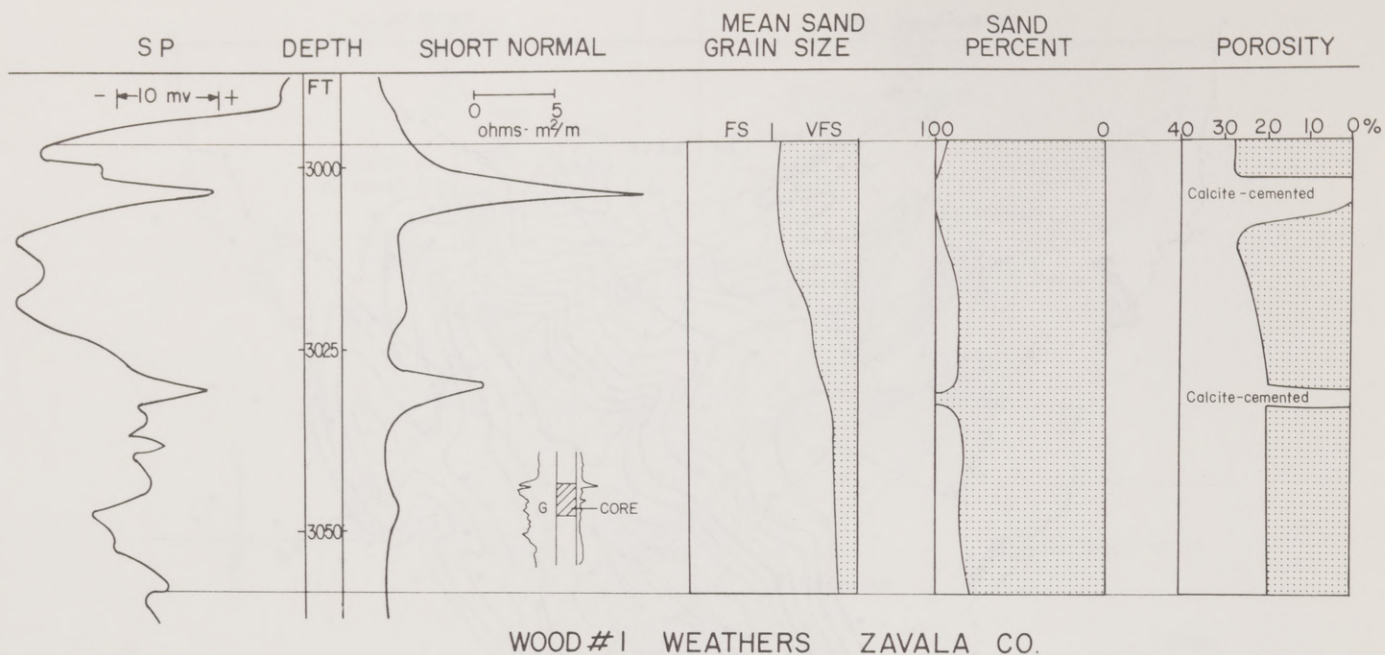


Figure 24. Typical electric log patterns and vertical distribution of grain sizes and porosity in a core from San Miguel unit G in the Wood # 1 Weathers well, Zavala County.

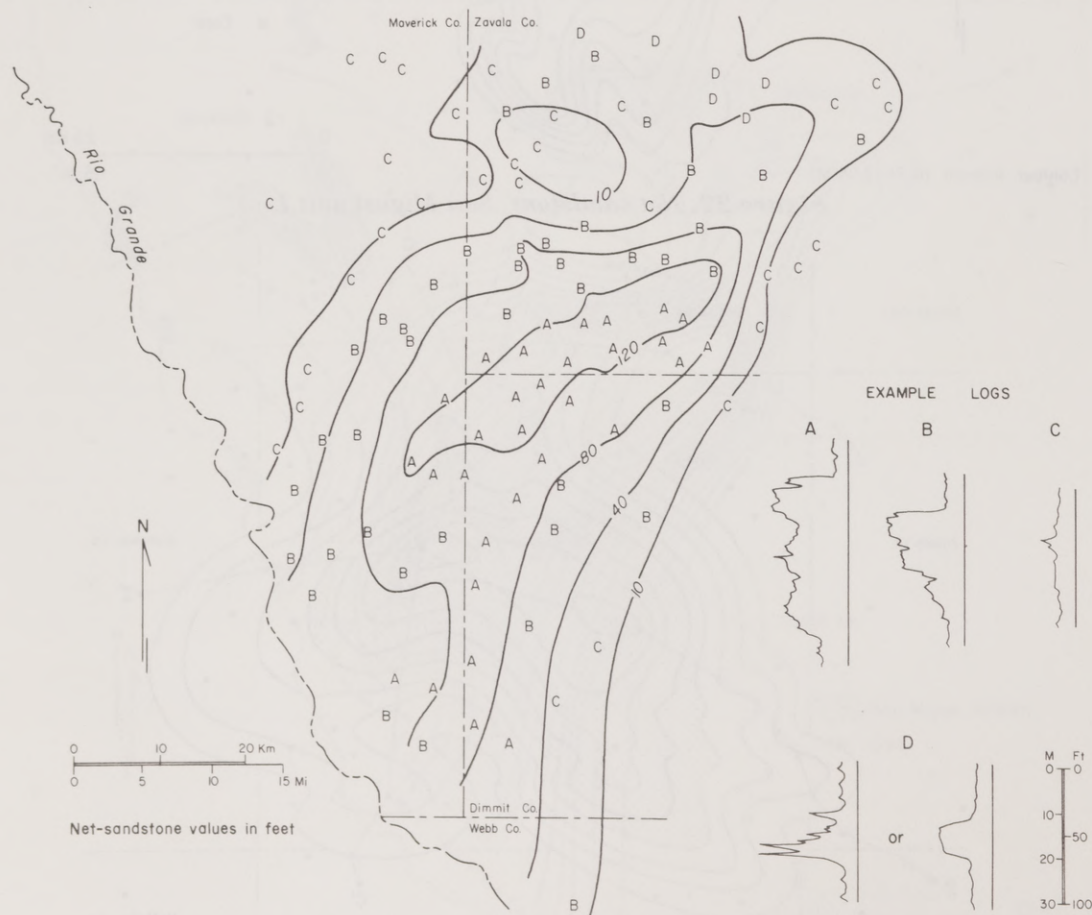


Figure 25. Distribution of various SP patterns in San Miguel unit G. SP curves show multiple upward-coarsening cycles (A), single upward-coarsening cycles (B), very thin, upward-coarsening cycles with symmetrical peaks (C), and upward-fining or blocky patterns (D).

top that is slightly gradational into the shale above. On the fringes of the system, sandstones show either thin upward-coarsening sequences (log pattern C) or thin symmetrical peaks on the logs. This distribution of vertical sequences is expected if the delta prograded in more than one phase; the thickest "stack" of cycles should be in the depocenter. The other San Miguel sandstone units, however, generally do not show multiplicity of cycles but rather exhibit single upward-coarsening cycles in the depocenters, as well as in the peripheral parts of the sandstone bodies. Upward-fining or blocky log patterns (log patterns D), which suggest channel deposits, are common in the area where net-sandstone contours indicate a fluvial system (fig. 25).

Core study shows that the predominant upward-coarsening cycles are reflected primarily by a decrease upward in amount of clay rather than a marked increase in mean "sand" grain size. The mean "sand" grain size generally coarsens from coarse silt at the bases of the cycles to very fine or fine sand at the tops (fig. 24). Mean grain size in all of the Wood #1 Weathers core is within the very fine sand fraction, although the base (not shown) of the upward-coarsening sequence probably has a mean grain size of coarse silt. Clay content decreases from high percentages in the silty shale below the sandstone bodies to essentially zero percent in the upper parts of the upward-coarsening cycles (fig. 24). Clay is distributed in wispy laminations, lenses, and burrow-wall linings rather than disseminated throughout.

Porosity, determined from thin section estimates and core analyses, shows an overall upward increase corresponding with the decrease in clay content (fig. 24). Porosity generally ranges from approximately 10 percent upward to 25 to 30 percent. Although most of the porosity is intergranular, highest porosities occur in zones where shell fragments and feldspar grains have been leached. Original porosity was destroyed by calcite cementation in some zones, commonly the coarsest, most well-sorted zones of the cycles (fig. 24). These cemented zones exhibit low spontaneous potential (SP) and high resistivity values on the electric log (fig. 24). If only the SP curve is considered, such a zone may be misinterpreted as a shale bed rather than as a clean, well-sorted sandstone. Thin limestone beds, which are sandy or silty micrites and biomicrites, are also non-porous. Most limestone beds are only 6 to 12 inches (15 to 30 cm) thick and are not recognizable on electric logs.

To summarize textural characteristics, the San Miguel sandstones are very fine grained and range from coarse siltstone to fine sandstone. Although clay percentage ranges widely, sorting is good to very good within the "sand" mode. Most of the sand grains are angular to very angular because silt and very fine sand are not easily rounded. Many of the grains (quartz slivers and

feldspar crystals) are elongate and oriented parallel or subparallel to bedding planes.

Sedimentary Structures

Cores from the San Miguel sandstone units show that, throughout, burrows are the predominant structures. In the lower parts of the upward-coarsening cycles, bioturbation was so intense that individual burrows are indistinct. Burrows are mostly horizontal (pl. VII-A) and generally become more distinct upward. Where vertical burrows (pl. VII-B) are present, they occupy the coarsest grained parts of the section. *Ophiomorpha* (pl. VII-A and -B) is the most readily recognized and one of the most common types of burrow.

No large-scale primary structures were observed in the cores. Sections not completely churned by burrowing display horizontal and irregular laminations that are the most abundant primary structures. Small-scale cross-laminations, however, are common in some of the cores. Thin zones (6 to 12 inches, 15 to 30 cm) of horizontal laminations with few or no burrows punctuate the thick, burrowed sequences in some of the cores (pl. VII-C). These thin zones probably represent sediments deposited rapidly by storms. The bases of the unburrowed zones are sharp, in some cases scoured, and the tops have burrowed contacts.

Large-scale primary structures were observed only in outcrop where upper shoreface facies are exposed. The only outcrop showing well-preserved structures is part of sandstone D (pl. VIII-A), in which friable, clayey, burrowed siltstone beds (6 to 18 inches, 15 to 45 cm thick) alternate with well-sorted, crossbedded sandstone (1 to 2.5 ft, 30 to 96 cm thick). A massive sandstone unit occurs at the top of the section.

Sandstones with primary structures are characterized by low-angle crossbeds (pl. VIII-B), large-scale trough crossbeds, and hummocky cross-stratification (pl. VIII-C) of possible storm origin as described by Harms and others (1975). A few distinct, deep, vertical burrows (*Ophiomorpha*) penetrate these crossbedded units (pl. VIII-D), but the tops of the beds are more densely burrowed.

DEPOSITIONAL MODELS FOR THE SAN MIGUEL FORMATION

Wave-Dominated Delta Model

The principal depositional systems of the San Miguel Formation are regressive wave-dominated deltas deposited periodically during a major transgression and separated by marine shales deposited during the transgressive phases.

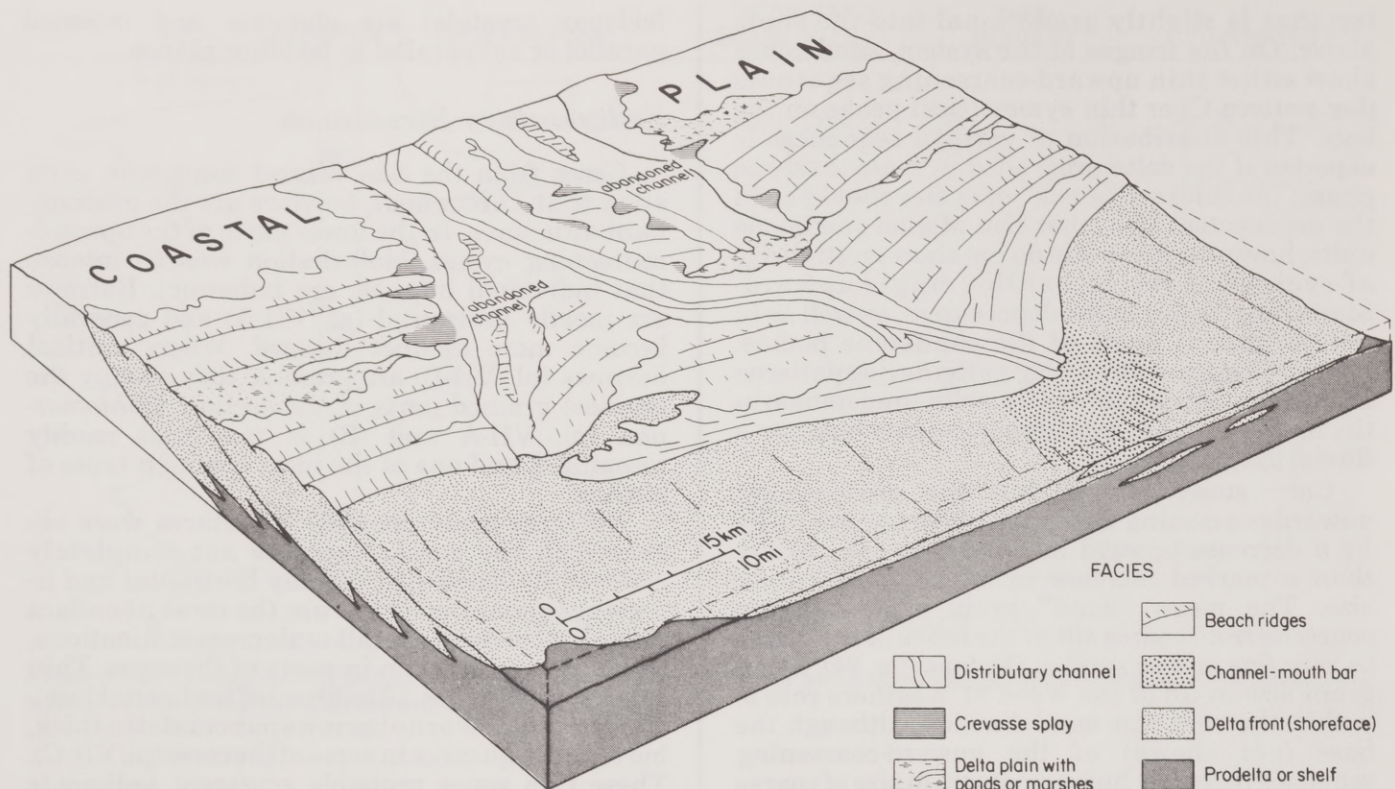


Figure 26. Three-dimensional model of a wave-dominated delta system. In cooperation with A. J. Scott.

Although the various San Miguel deltas differ in overall sandstone framework geometry, the three-dimensional model (fig. 26) illustrates sand-body geometry and facies of several "lobes" or subdeltas of a wave-dominated system. This model can be applied generally to all San Miguel delta systems. Sediments were debouched into the marine environment through one or two active distributaries. The sand was immediately redistributed to the sides of the distributary mouth by waves and worked into a series of strandplain, barrier, or spit deposits. Because of this reworking by waves and longshore currents, the principal sand bodies of wave-dominated systems are strike oriented.

Contrary to this deltaic model, Lewis (1977) considers the San Miguel sandstone units (western subbasin only) to be systems totally strike fed from the southwest but does not suggest a source for the sand. In his sedimentary model, he shows three main areas of sand deposition, two of which were 25 and 45 mi (40 and 72 km) offshore. If those depositional systems were totally strike fed, the sand-transporting currents could not have been normal longshore (nearshore) currents, as suggested by Lewis, but rather some heretofore unknown type of outer shelf current. In no known modern example do strike-directed shelf currents transporting sand over long distances (tens to hundreds of miles) deposit sand bodies in upward-coarsening sequences more than 120 ft (37 m)

thick, as are found in the San Miguel (western subbasin). Upward-coarsening cycles shown by eastern subbasin sandstones are even thicker.

Facies

The dominant deltaic sand facies in a wave-dominated delta is the shoreface facies of strandplain or barrier origin (fig. 26). Associated eolian facies (not shown in figure 26) and beach facies may compose a significant part of modern strandplain sequences but are the first to be removed by either subaerial erosion or transgressive reworking. Therefore, these facies may be absent in ancient wave-dominated deltaic sequences.

Fluvial facies are minor in the San Miguel Formation. Few electric logs show characteristic channel patterns in the updip parts of San Miguel sandstones. Although there are exceptions, wave-dominated deltaic systems, according to Fisher (1969), are fed typically by relatively small- to moderate-size meandering fluvial systems. Those fluvial systems that supplied the San Miguel deltas, particularly those of the western subbasin, were probably small and contributed sediments at slow rates. Unfortunately, most of the San Miguel fluvial systems, except the parts farthest downdip, have been eroded.

Delta-plain facies are poorly developed in the San Miguel wave-dominated deltas. Lignites or coals have not been interpreted from electric log

patterns, and none of the cores studied penetrated recognizable delta-plain deposits. However, on the electric log, delta-plain shales may not be distinguishable from marine shales. Instead of vast tidal flats or marshes, the subaerial parts of the wave-dominated deltas consisted primarily of beach ridges that were reworked during subsequent transgressions. Fisher (1969) stated that abundant organic deposits characteristic of the more highly constructive, rapidly subsiding, river-dominated systems like those of the Mississippi are lacking in wave-dominated deltas. However, factors other than delta type also determine abundance of organic deposits, most importantly climate. Lack of organic deposits could suggest an arid climate for the San Miguel, but the overlying Olmos contains abundant coals. Most or all San Miguel delta-plain organic deposits, as well as crevasse-splay deposits and the beach and eolian facies mentioned above, may have been removed during subsequent transgression.

Rivers feeding wave-dominated deltas generally have higher sand-to-mud ratios than do high-constructive elongate and lobate deltas (Fisher, 1969). Therefore, the thickness of the pro-delta mud facies basinward of the delta front is not as great as in other deltaic settings.

In emphasis, the principal sand facies of a wave-dominated delta is the shoreface. Because most of the sand discharged from the distributary-channel mouth is reworked along strike, channel-mouth bar deposits are minor. Environments represented in the San Miguel cores are primarily the lower shoreface and upper offshore. In the well-exposed outcrop of the upper part of sandstone D, physical and biogenic structures suggest an upper shoreface environment. Vertical changes in the physical structures and the types and abundance of biogenic structures in the San Miguel sandstone sequences fit well the trend outlined by Howard (1972) in his studies of Upper Cretaceous nearshore deposits exposed in the Book Cliffs and the Wasatch Plateau of Utah and Recent environments along the Georgia coast. According to Howard's sequence, the highly bioturbated lower parts of the San Miguel sequences represent the low-energy environment of the upper offshore. Higher in the upward-coarsening sequences, horizontal beds and abundant, distinct burrows are characteristic of the lower shoreface. Horizontal *Ophiomorpha*, abundant in the San Miguel cores, are restricted to this lower shoreface facies (Howard, 1972). San Miguel sandstones exposed in outcrop were deposited in a higher energy environment than those observed in cores, as indicated by the outcrop abundance of large-scale primary structures and the few, deep, vertical *Ophiomorpha*. Like the Book Cliffs example, low-angled crossbeds, interpreted as truncated, wedge-shaped sets (Howard, 1972), dominate this fairly high-energy upper shoreface environment.

Trough crossbeds and the hummocky crossbeds mentioned earlier also are present, although Harms and others (1975) interpret a lower shoreface environment for the hummocky stratification.

Although the trace fossil *Ophiomorpha* is characteristic of nearshore, shallow marine environments (Weimer and Hoyt, 1964), its presence alone is not diagnostic. For example, *Ophiomorpha* is found in deposits interpreted as turbidites of a deep-sea fan (Crimes, 1977) and bathyal grain-flow deposits (Kern and Warne, 1974) and in abandoned distributary channels and a variety of bay facies (A. J. Scott, personal communication, 1979). Nevertheless, the vertical changes in the abundance and orientation of the *Ophiomorpha* in the San Miguel cores favor the shoreface interpretation.

Incomplete Strandplain-Barrier Sequences

A complete strandplain or barrier sequence has a vertical succession of offshore, lower shoreface, upper shoreface, beach, and dune facies (fig. 27a). As mentioned above, however, the upper part of such a sequence is subject to erosion. The San Miguel upward-coarsening units are truncated sequences; only shoreface, most commonly lower shoreface, deposits are preserved. The primary mechanism of destruction was reworking by marine processes during the transgressions that followed progradation of each San Miguel delta. Most of the upper parts of the original shoreface sequences, which contained large-scale primary structures, were removed (fig. 27b). Any primary structures remaining in the upper part of the truncated sequences were destroyed by intense bioturbation as water depth increased and the sand bodies were submerged within a quiet shelf environment (fig. 27c).

The degree of transgressive reworking depended heavily on the rate of transgression; slower rates resulted in greater reworking. Whether or not all the beach and upper shoreface could have been destroyed also depended on the original thickness of those facies. Although San Miguel depositional systems are considered to have been wave-dominated, this does not mean that wave energy was necessarily high in the absolute sense, but that it was high relative to the rate of sediment input. If neither wave energy nor rate of sediment input were very high, then most of the original strandplain or barrier sequence might have been bioturbated, as along some modern low-energy coasts (Howard and Reineck, 1972a and b), and only a small amount of reworking was required to destroy the thin upper shoreface section containing large-scale crossbeds. Perhaps removal of only 10 to 20 ft (3 to 6 m) of the strandplain sequences occurred.

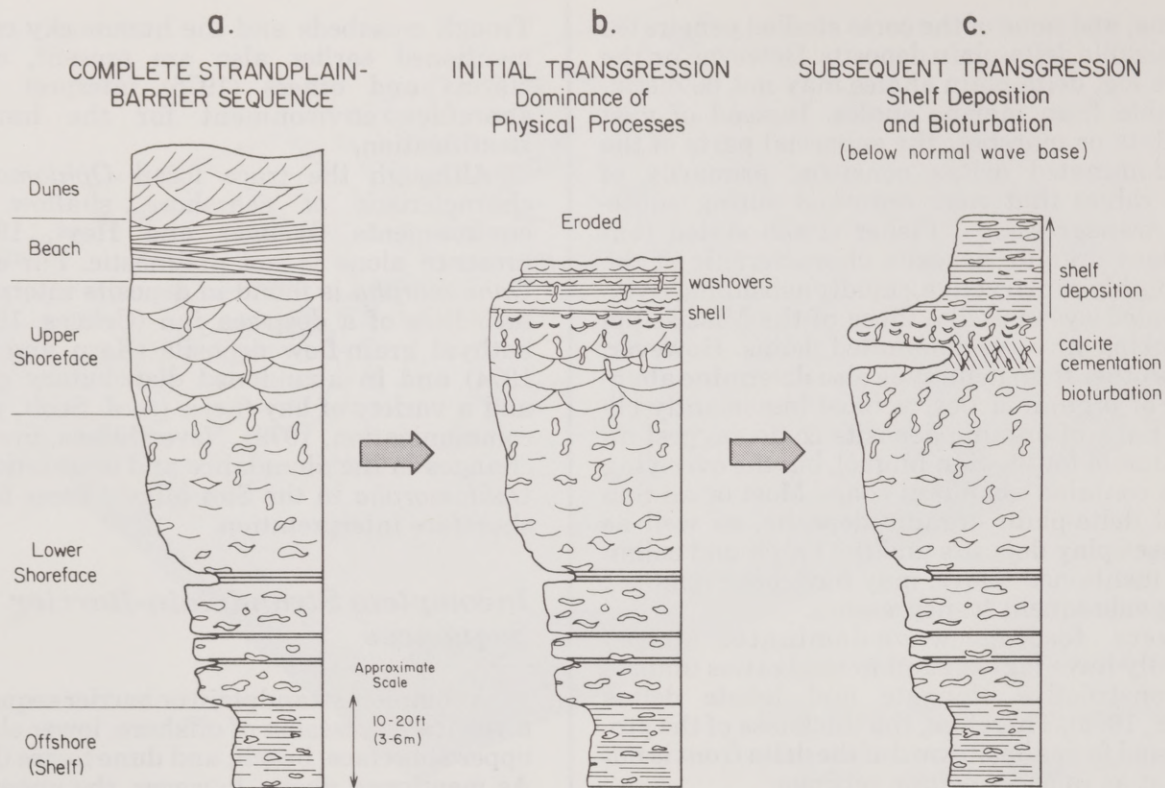


Figure 27. Evolution of incomplete strandplain-barrier sequences of the San Miguel Formation. Upper part of the original complete sequence (a) was eroded and reworked by physical processes during initial transgression immediately following delta abandonment (b). During subsequent transgression after the deposits had been submerged below normal wave base, primary structures remaining at the tops of truncated sequences were destroyed by bioturbation (c). Profiles of the columns represent SP curves expected from the sequences.

Net-Sandstone Patterns

The idealized net-sandstone patterns exhibited by wave-dominated deltas (fig. 9) have a cusped shape resulting from the wave reworking of sand from the distributary mouth into strike-aligned bodies. Basic shape variations, however, should be expected. On the basis of net-sandstone patterns, the San Miguel sandstone units display a wide spectrum of wave-dominated delta types (fig. 28) that are arranged according to the degree of reworking by marine processes. The spectrum does not necessarily show an order of increasing wave energy nor decreasing sediment input, but rather it simply reveals an order of increasing dominance by and/or asymmetry of marine processes regardless of the actual magnitudes of the factors affecting delta type.

Four of the San Miguel units have been used to illustrate delta shapes within the spectrum. The end member showing the least amount of wave reworking is illustrated by sandstone P, which is a composite of two delta lobes. Sandstone P should perhaps be described as wave influenced rather than wave dominated. As wave reworking increases, the delta front assumes a more arcuate shape, as exemplified by the largest body of sandstone C. Unit F most nearly resembles the

classic cusped delta, where almost all of the sand debouched from the distributary is reworked along strike. Although delta shape is largely determined by the degree of reworking, another consideration is the number of distributaries, which also exerts an important control on the overall shape of the delta system; this may account for some of the differences between units C and F. Sandstone G serves as the end member that shows the most extreme marine reworking by waves and resulting longshore currents. Progradation into the basin was slow as the delta built primarily along strike in the direction of the dominant longshore current. The other five San Miguel deltas not shown in figure 28 can be classified between deltas F and G near the "highly reworked" end of the delta spectrum.

It is difficult to judge the degree to which marine reworking of the deltas during subsequent transgression affected original net-sandstone patterns. Again, the result depended on the rate of transgression. Generally, the effect of transgressive reworking is to spread the upper parts of the shoreface sand into thin transgressive bodies, but the main net-sandstone trends are preserved. One other primary control on degree of reworking is bottom topography. For example, units A and B are located at an abrupt change in the slope of the

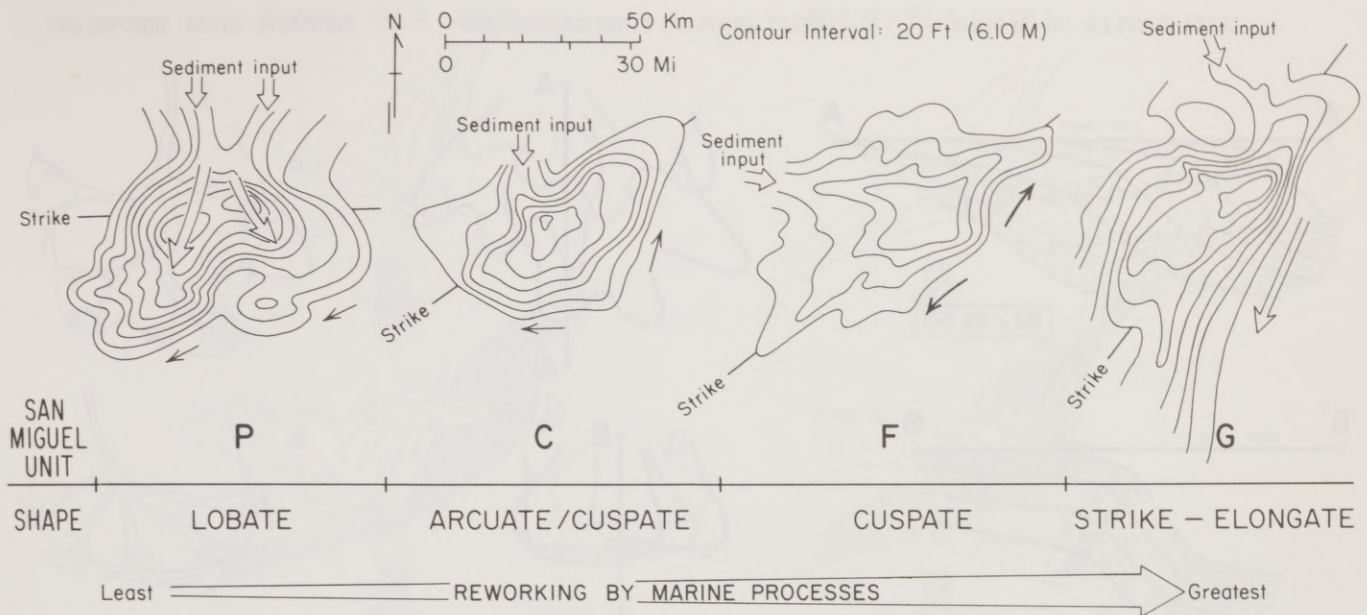


Figure 28. Spectrum of San Miguel deltas. Net-sandstone patterns show a range from the lobate unit P to the strike-elongate unit G, resulting from differences in the degree of reworking by marine processes. Relative magnitude and direction of sand transport are indicated by the weight and direction of the arrows.

shelf. Instead of being spread along both strike and dip by transgressive reworking, these sand bodies may have been reworked only along strike against the bathymetric break, which prevented the sand from being carried updip. On the other hand, much of the extremely strike-elongate shapes of the A and B sandstone bodies may have been attained during delta construction. These systems were built where bottom slope was steeper and wave energy consequently higher than farther updip on the more nearly level part of the shelf where the other San Miguel systems were deposited.

Deltaic Deposition During a Major Transgression

The San Miguel deltas were deposited in periodic regressions during two long-term, net transgressive episodes of an overall marine transgression. Deltaic systems formed during periods of net transgressions, net regressions, or times of stable relative sea level show definite differences in both morphology of the individual systems and their relationships to the other delta systems deposited during the same relative sea-level trend. Curtis (1970) illustrated models for deltaic sedimentation in a Miocene basin in Louisiana in which rates of deposition and rates of subsidence (or for equal effects, absolute sea-level rise) varied (fig. 29). Curtis considered three scenarios based on the ratio of the rate of deposition to the rate of subsidence where (1) the rate of deposition exceeds the rate of subsidence or absolute sea-level rise ($R_d/R_s > 1$), (2) the rates are

equal ($R_d/R_s=1$), and (3) the rate of deposition is less than the rate of subsidence ($R_d/R_s < 1$). Deposition of the regressive San Miguel deltas during the two net transgressive episodes, which were caused by regional subsidence, absolute sea-level rise, or both, generally fits the third model (fig. 29c).

The ratio of the two rates can be used to predict delta morphology. Deltas deposited during a long-term net transgressive episode are expected to exhibit moderate to extreme modification by marine processes and a dominance of strike-aligned destructive coastal and nearshore marine sand bodies (fig. 29c). Another result of a relative rise in sea level may be the stacking of sands of different phases or subdeltas of a particular delta system. The model in figure 26 shows the result of abandonment of distributary channels and changes in the sites of progradation. When a distributary changes course, the abandoned area is transgressed, and sand reworked along strike from the new distributary mouth, perhaps primarily in the process of spit accretion, is deposited atop the barrier, spit, or strandplain deposits of the older delta "lobe." Thus, facies are stacked, and relatively thick sand deposits may accumulate (fig. 30). If relative sea level had been stable, the series of subdeltas in phases I, II, and III in figure 30 would have prograded much farther into the basin to produce an extensive sheet sand instead of thick, strike-aligned sand deposits.

As shown in figure 29c, successive delta systems deposited during a relative rise in sea level occur farther and farther updip. If the supply of sediments abruptly ceases, as caused by a major

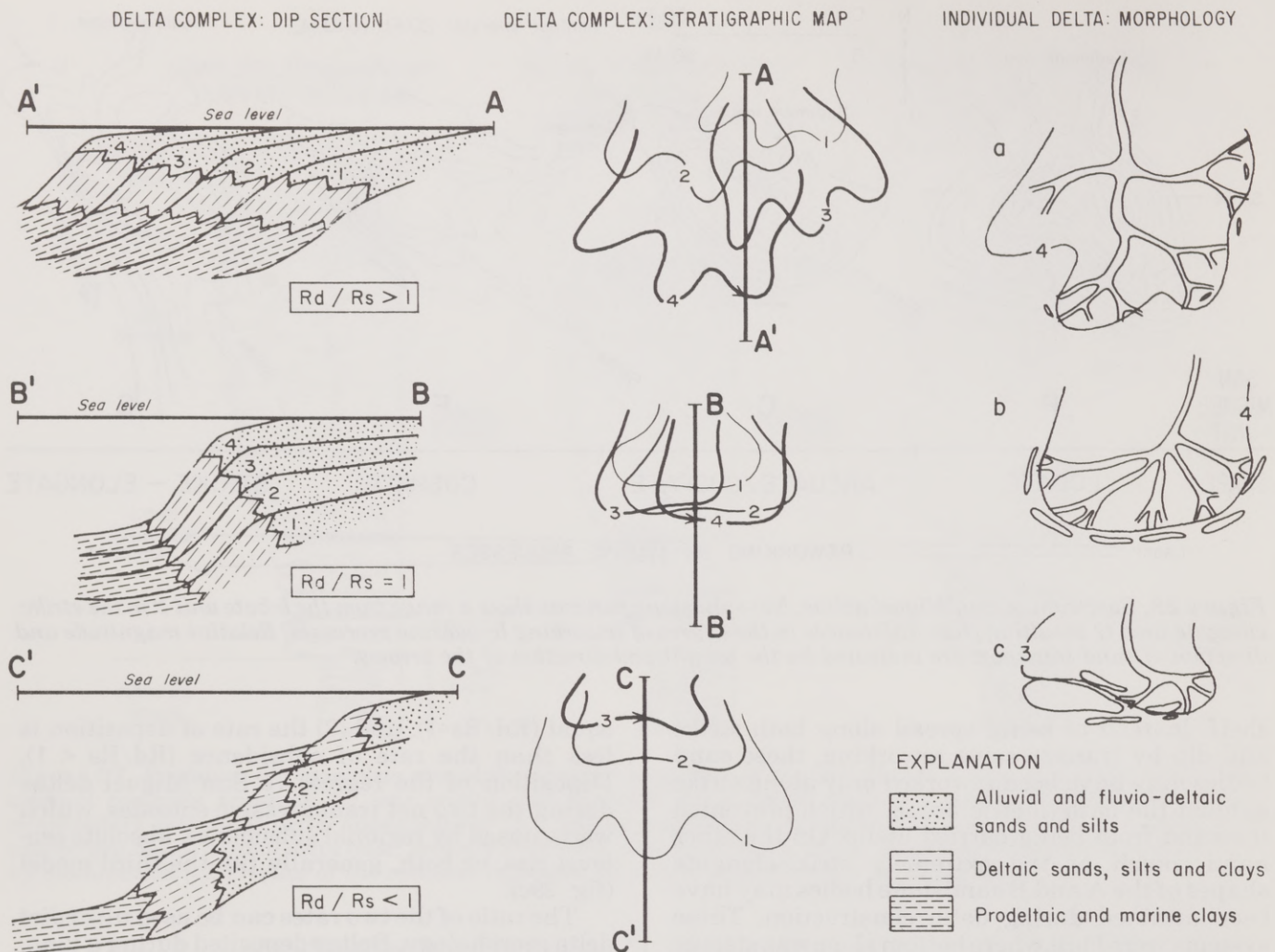


Figure 29. Model of deltaic sedimentation in a basin in which rates of deposition and rates of subsidence varied. The model, based on Miocene deltas of Louisiana, shows differences in morphology and spatial relationships of delta systems deposited under different rates of deposition and rates of subsidence: (a) rate of deposition was greater than rate of subsidence ($Rd/Rs > 1$), (b) rates were equal ($Rd/Rs = 1$), and (c) rate of deposition was less than rate of subsidence ($Rd/Rs < 1$). In the center column, shorelines of various deltas are numbered chronologically with that of the oldest lobe indicated at "1". Modified from Curtis (1970).

avulsion of the fluvial system upstream, the delta system is abandoned and transgressed (fig. 31, phase IV). The upper part of the abandoned delta deposits will be physically reworked into sandy bars and shoals on the shallow shelf (fig. 31, phase V). When sediment input is renewed, another delta system will be constructed farther updip. Thus, rather than producing a continuous landward migration of facies, a relative rise in sea level will result in isolated regressive delta systems positioned successively updip.

Although deposition of the San Miguel units occurred during an overall relative sea-level rise, the major depositional systems of the San Miguel are regressive. However, thin transgressive sandstones, composed of sediment reworked from the delta deposits, in addition to some shelf mud, onlap the delta deposits and are shown on many of the electric logs as finer zones above the upward-coarsening sequences.

Modern and Ancient Depositional Analogs

Modern wave-dominated deltas are generally recognized by cusped shapes and the dominance of strike-aligned sand systems, but, like the San Miguel deltas, they show a considerable range in delta morphology. Examples of these modern deltas, some of which Galloway (1975) plotted on his delta-classification triangle (fig. 10), are the São Francisco (Brazil), Brazos (Texas), Kelantan (Malaysia), Rhone (France), Nile (Egypt), Danube (Romania), Grijalva (Mexico), and Senegal (West Africa).

No identical modern analog of the San Miguel deltas exists; the modern deltas, however, do show many similarities in general morphology and sand distribution to some of the San Miguel deltas. Also, like the model of the San Miguel deltas

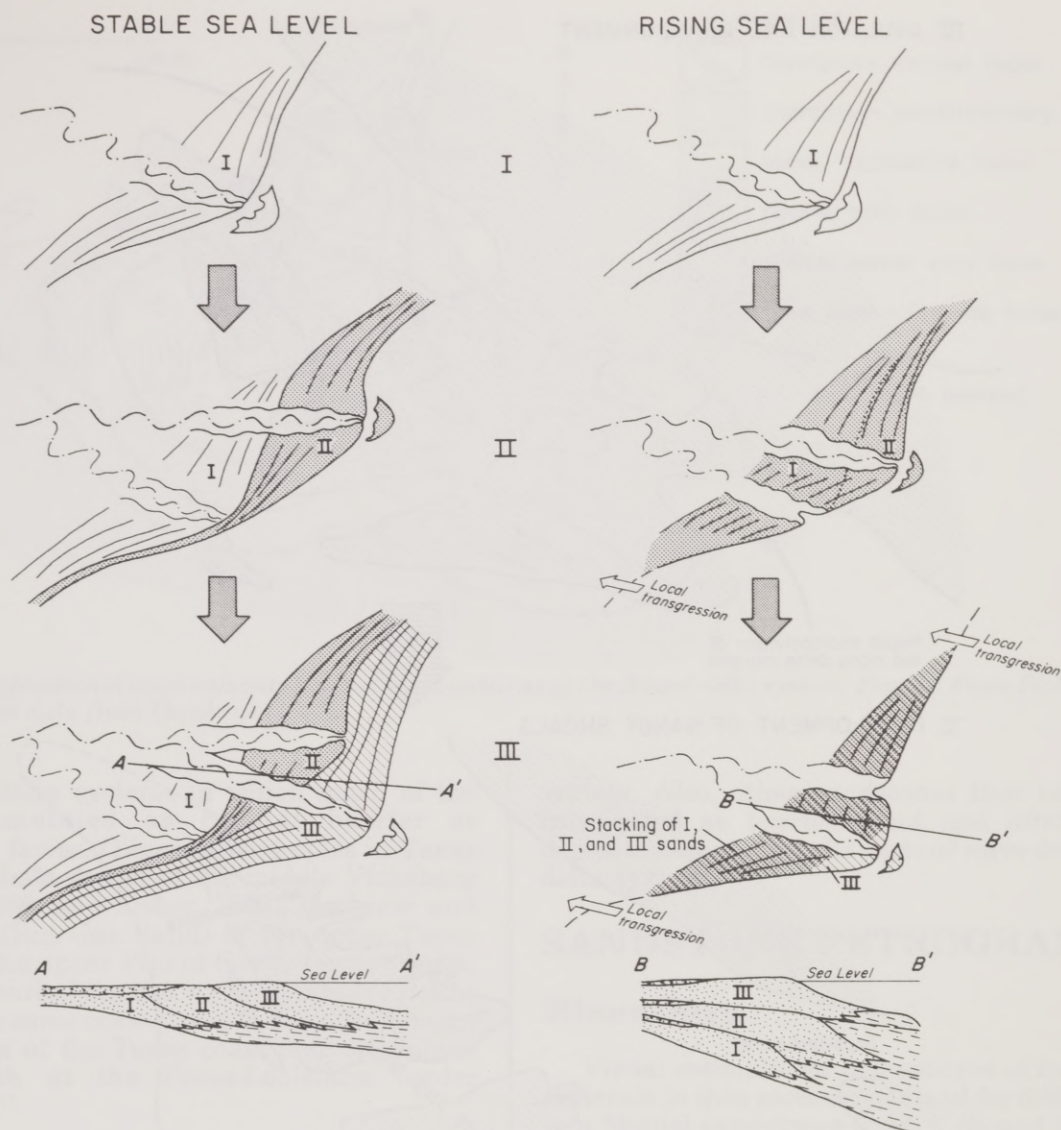


Figure 30. Effects of rising and stable relative sea level on delta formation. Rising sea level produced superposed sands of subdeltas (phases I, II, and III; cross section B-B'). If sea level had been stable, the delta system would have prograded farther into the basin to produce a sheet sand (cross section A-A'). In cooperation with A. J. Scott.

presented in the section entitled "Wave-Dominated Delta Model," the dominant facies in these modern examples are coastal barriers and strandplains.

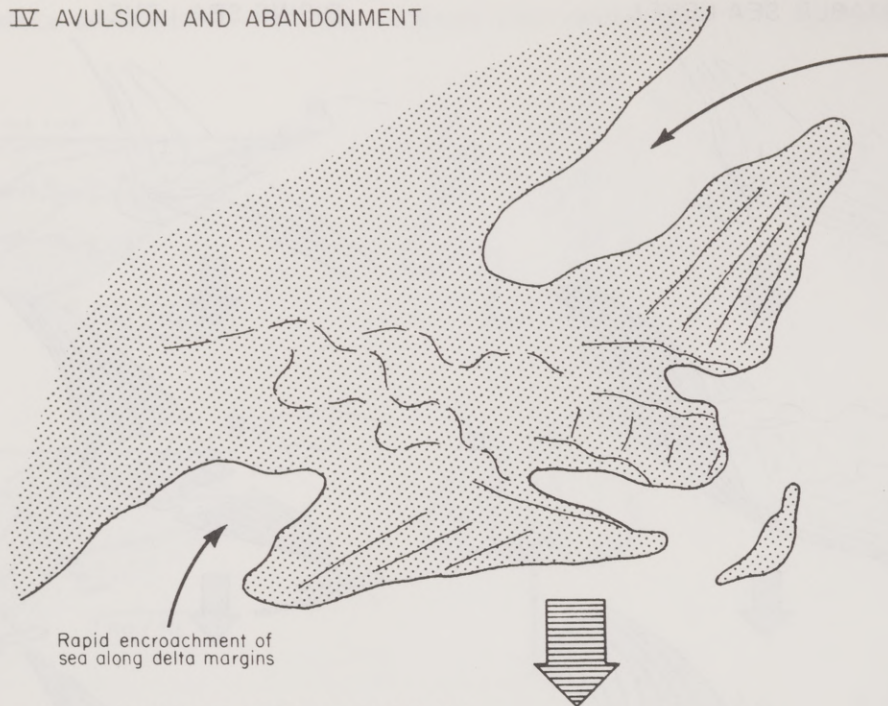
The Rhone delta, a modern wave-dominated system, has been studied by Kruit (1955) and Oomkens (1967, 1970). Two meandering distributaries, the Grand and Petit Rhone, have built the two lobes of the delta (fig. 32). Moderately high wave energy is sufficient to rework fluvial sediments into a series of coastal barriers, which compose the principal part of the delta. Net-sand patterns (fig. 32) are similar to those of some of the San Miguel delta systems, for example, sandstone E (fig. 19).

The shape of the São Francisco delta (fig. 33), built by one distributary, is strikingly similar to that of San Miguel delta F, as indicated by unit F

net-sandstone patterns (fig. 20). The São Francisco delta is subject to extremely high energy waves, and the fluvially formed sand bodies, such as channel-mouth bars, dominant in other types of deltas have been replaced by barrier and strandplain sands (Coleman and Wright, 1975). Unlike the San Miguel deltas, São Francisco delta deposits are rarely burrowed (Coleman and Wright, 1975). São Francisco deposits probably are being formed under much higher energy conditions than were the San Miguel systems and have not undergone transgression during which intense biological reworking may take place.

The Nile River delta (fig. 34) resembles the San Miguel delta C (fig. 17). Although the Nile is cusped in shape at the mouths of the Rosetta and the Danietta distributaries, the overall delta

IV AVULSION AND ABANDONMENT



V DEVELOPMENT OF SANDY SHOALS

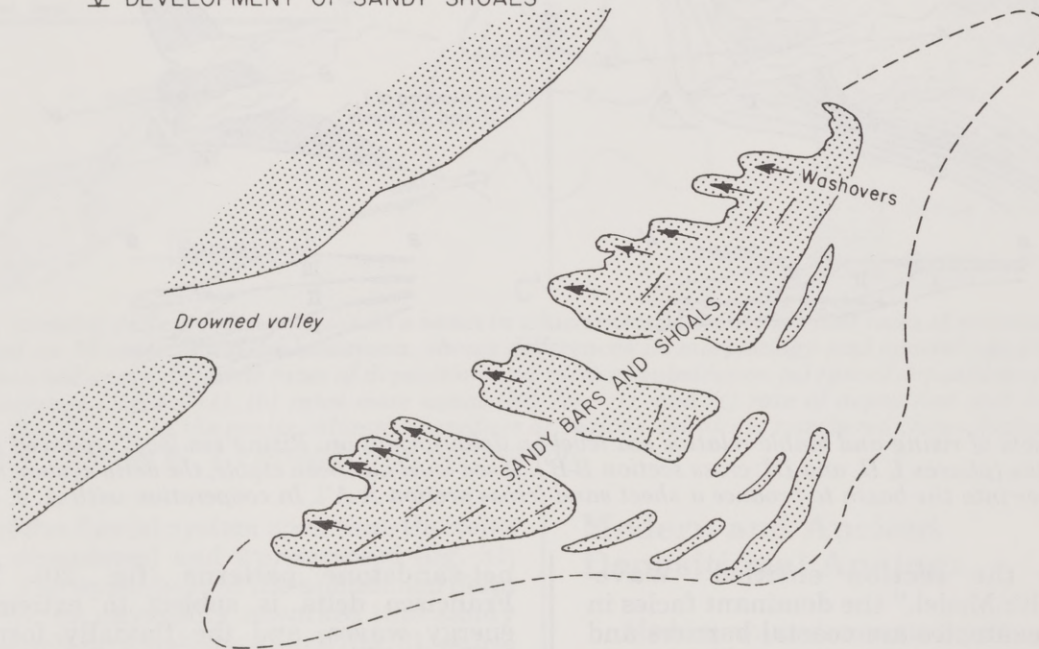


Figure 31. Delta abandonment, transgression, and development of sandy bars and shoals. In cooperation with A. J. Scott.

shape is arcuate like the main body of the San Miguel delta C. Mediterranean waves and a prevailing longshore current from west to east have redistributed the channel-mouth bar sand of the Nile into a series of flanking coastal-barrier and strandplain deposits (Fisher and others, 1969).

The markedly strike-elongate San Miguel systems, such as unit G, resemble the Senegal delta, West Africa, which is dominated by waves and strong, unidirectional longshore currents. High wave energy of the Atlantic, combined with

strong longshore currents, redistributes sand into long linear bodies parallel to the coastline (Coleman and Wright, 1975). The distributary patterns and the high mud load of the Senegal River, however, might be different from those of the rivers that fed the San Miguel deltas.

Like modern wave-dominated delta systems, ancient examples of wave-dominated delta systems are common. Several of these systems have been delineated in the Gulf Coast Tertiary. Fisher (1969) interpreted part of the upper Wilcox (Eocene) of the Texas Gulf Coast to be wave-

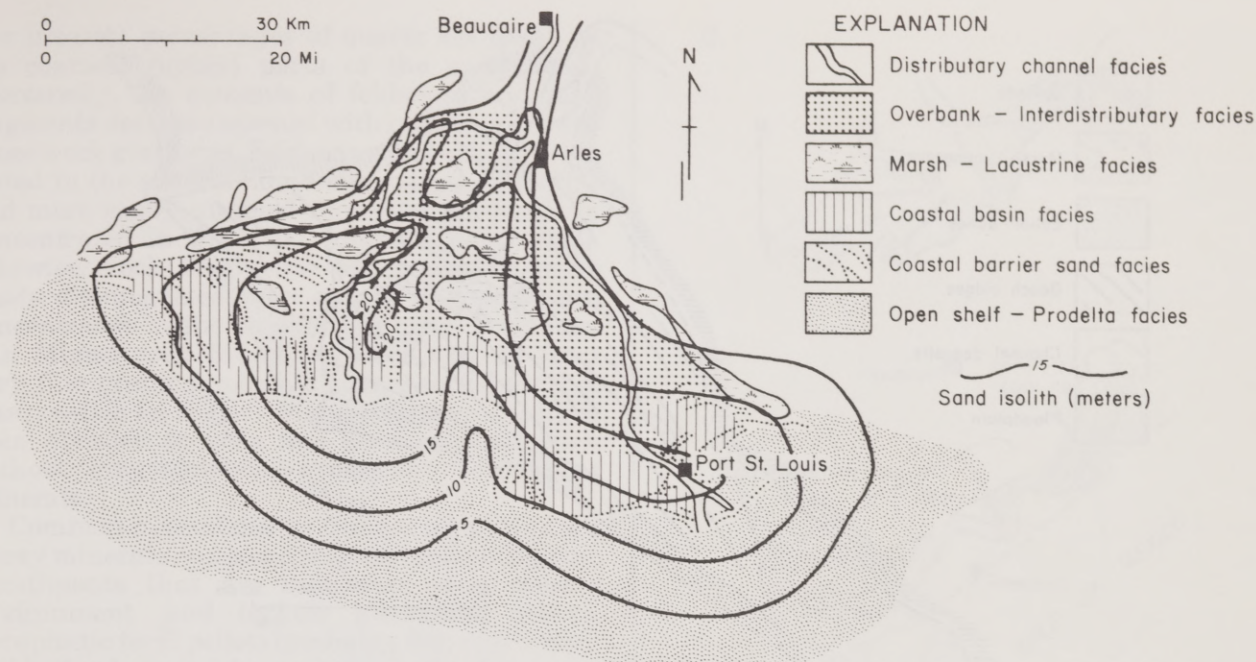


Figure 32. Depositional environments and net-sand patterns of the Rhone delta system, France. From Fisher (1969). Sand thickness data from Oomkens (1967).

dominated delta systems in which much of the sand accumulated as coastal barrier or strandplain facies. Oligocene examples in Texas (fig. 35) include deltas of the middle Vicksburg (Gregory, 1966; and Fisher, 1969), the lower and upper Frio (Big Gas Sand) of the upper Texas coast, and the upper Frio of South Texas (Smith, 1975). Two early Miocene wave-dominated deltas occupied the same coastal positions as the modern Brazos delta of the Texas coast and the Sabine River mouth at the Texas-Louisiana border (Smith, 1975).

The Upper Cretaceous of the Western Interior contains a variety of clastic sequences including fluvial, deltaic, barrier, and nearshore and offshore marine depositional systems. Most of the deltas have not been classified, but at least two of the sandstone formations have characteristics of wave-dominated deltas. Isbell and others (1976) interpreted the deltaic part of the Teapot Sandstone Member of the Mesaverde Formation, Powder River Basin, Wyoming, to be a strandplain/high-destructive delta complex dominated by wave action and longshore currents. Sediment characteristics and burrows in cores are similar to those of the San Miguel deltas. The Upper Cretaceous Castlegate Sandstone of Utah and Colorado is another example of a high-destructive (marine-dominated) delta system (Smith, 1975). Rows of beach ridges and the strike-elongate delta-front sands (Van de Graaff, 1972) suggest that deltaic deposition was dominated by wave energy. Perhaps with further study, other deltas of the Upper Cretaceous of the Western Interior will prove to be the wave-dominated

variety. Also, other sandstones that have been interpreted as barrier-island and offshore bar deposits may actually be parts of wave-dominated delta systems.

SANDSTONE PETROGRAPHY

Mineralogy

Visual estimates of percentages of framework minerals in thin sections (stained for feldspars) of San Miguel sandstones C, D, E, G, and I indicate that these rocks are dominantly arkoses (pl. IX-A), according to Folk's (1968) sandstone classification. The few thin limestones present are very sandy micrites and biomicrites. In the sandstones, various types of quartz compose 50 to 75 percent of the primary framework grains, but most quartz exhibits straight to slightly undulose extinction. Feldspars, including orthoclase, microcline, perthite, albite, and calcic plagioclase, account for 20 to 45 percent of the framework minerals. Rock fragments, primarily chert and volcanic rock fragments, compose the remaining 5 to 15 percent of the primary framework grains.

Calcic plagioclase, most of which is not twinned, is more abundant than albite and potassium feldspar. This abundance of calcic plagioclase, which is normally extremely subordinate to other feldspar types, is suggestive of a volcanic source. Upper Cretaceous volcanoes in the area may have contributed significantly to San Miguel sediments.

Cores from sandstones C and G show some mineralogical trends common among sandstones.

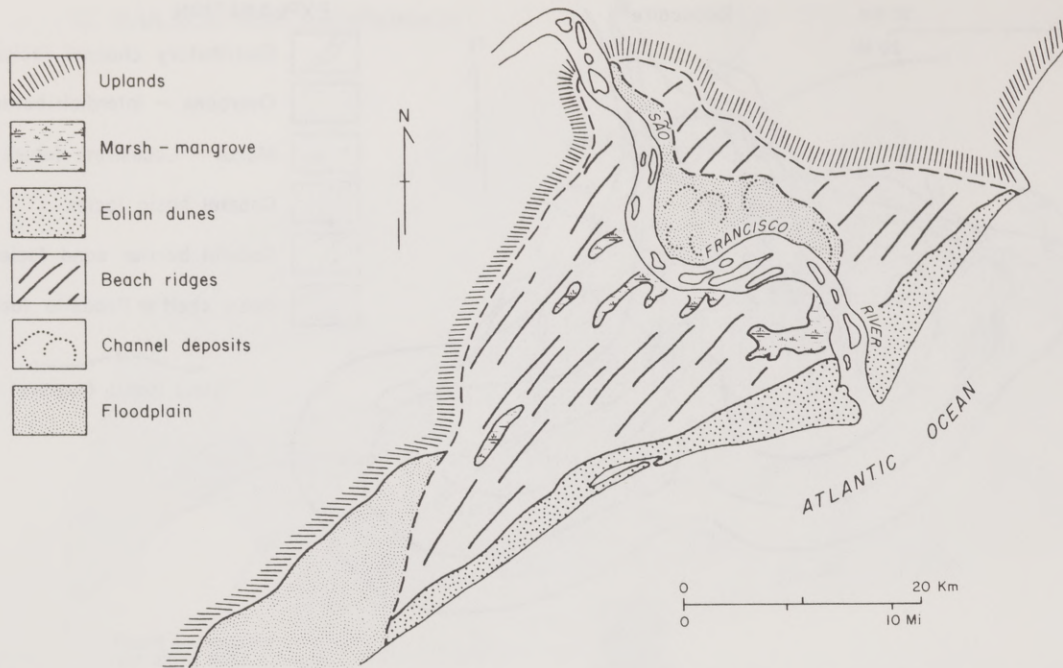


Figure 33. Depositional environments of the São Francisco delta, Brazil. From Coleman and Wright (1975).

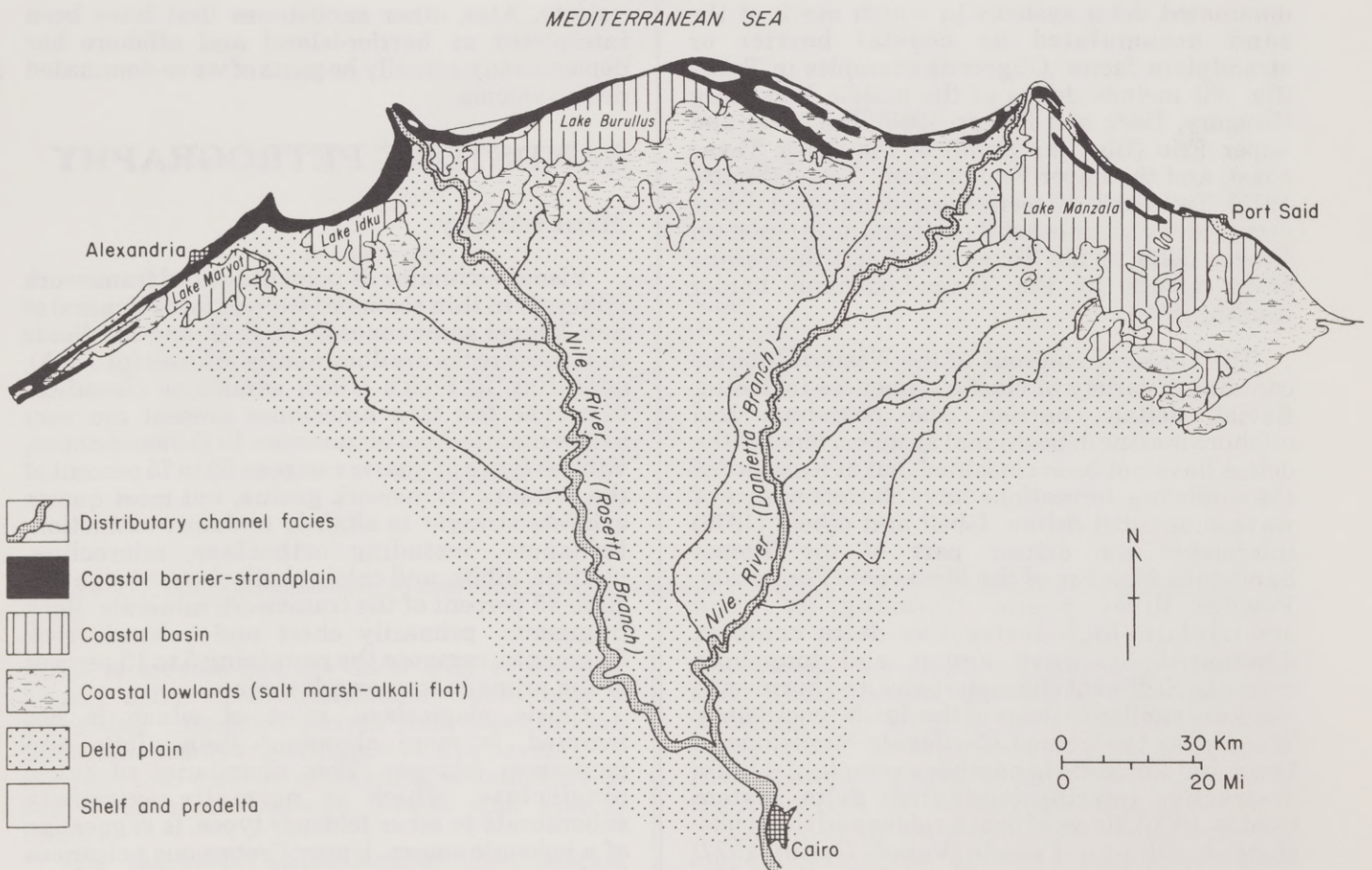


Figure 34. Depositional environments of the Nile delta system, Egypt. From Fisher and others (1969).

The greatest percentages of quartz are found in the coarsest (upper) parts of the sandstones. Conversely, the amounts of feldspars and rock fragments decrease upward with increasing mean framework grain size. Feldspars tend to be concentrated in the silt fraction because they are softer and more easily abraded than quartz; quartz is concentrated in the sand fraction (Folk, 1968). Likewise, rock fragments are generally more easily disintegrated than quartz and, thus, are concentrated in the smaller grain-size fractions. San Miguel rock fragments were derived from very fine grained volcanic source rocks; thus, it was possible for the San Miguel fragments to have been abraded to very fine sand and silt sizes without being completely broken into constituent minerals.

Common miscellaneous framework grains are heavy minerals and some biogenic and authigenic constituents that are indicators of a marine environment and include glauconite pellets, phosphatic fecal pellets (probably fish coprolites), and both whole and fragmented shells of an open-marine fauna. Glauconite is present in all cores, but its percentage varies considerably. Shell material in most cores, however, is concentrated in thin zones no more than a few feet thick. Pelecypods and gastropods are most abundant in these shelly beds. Scattered through some cores are a few scaphopods, echinoids, hydrozoans, and foraminifers.

Biotite is the most abundant heavy mineral and is common in most of the cores. Some biotite flakes appear to have hexagonal shapes typical of volcanic biotite. Other detrital heavy minerals include muscovite, zircon, hornblende, pyroxene, and opaques which are probably magnetite.

Diagenesis

The most common cements in the San Miguel sandstones are sparry and poikilotopic calcite and quartz overgrowths. Other diagenetic minerals are kaolinite, feldspar (rare overgrowths), illite (clay rims), pyrite, and hematite. Quartz overgrowths are present throughout most of the available cores, but they are not as important volumetrically as calcite cement. The cleanest and originally most porous and permeable zones in the sandstones now are commonly cemented tightly with calcite.

The diagenetic sequence in San Miguel sandstones fits the general sequence described by Loucks and others (1979) and modified by Loucks and others (1980) for Gulf Coast Tertiary sandstones (fig. 36). Most of the San Miguel diagenetic events, however, occurred at shallower depths than those of the Tertiary sandstones. In San Miguel sandstones, leaching of feldspars and their replacement by calcite was common (pl. IX-B), but the timing of this diagenetic event is

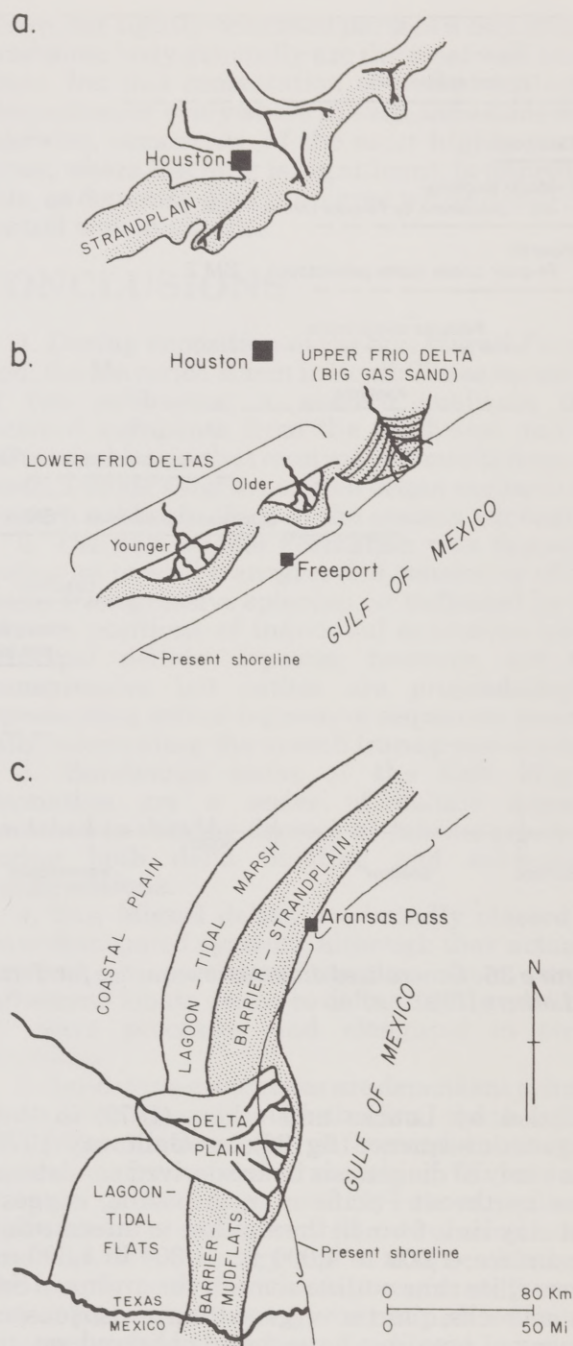


Figure 35. Oligocene wave-dominated delta systems of (a) the middle Vicksburg of the upper Texas coast, (b) the lower and upper Frio of the upper Texas coast, and (c) the upper Frio of South Texas. Modified from Smith (1975).

difficult to determine. Feldspar leaching may have been an early event, indicated as SM 1 in figure 36. Poikilotopic calcite (SM 2) was an early cement, as evidenced by the loosely packed grains (pl. IX-C). Development of clay rims was not

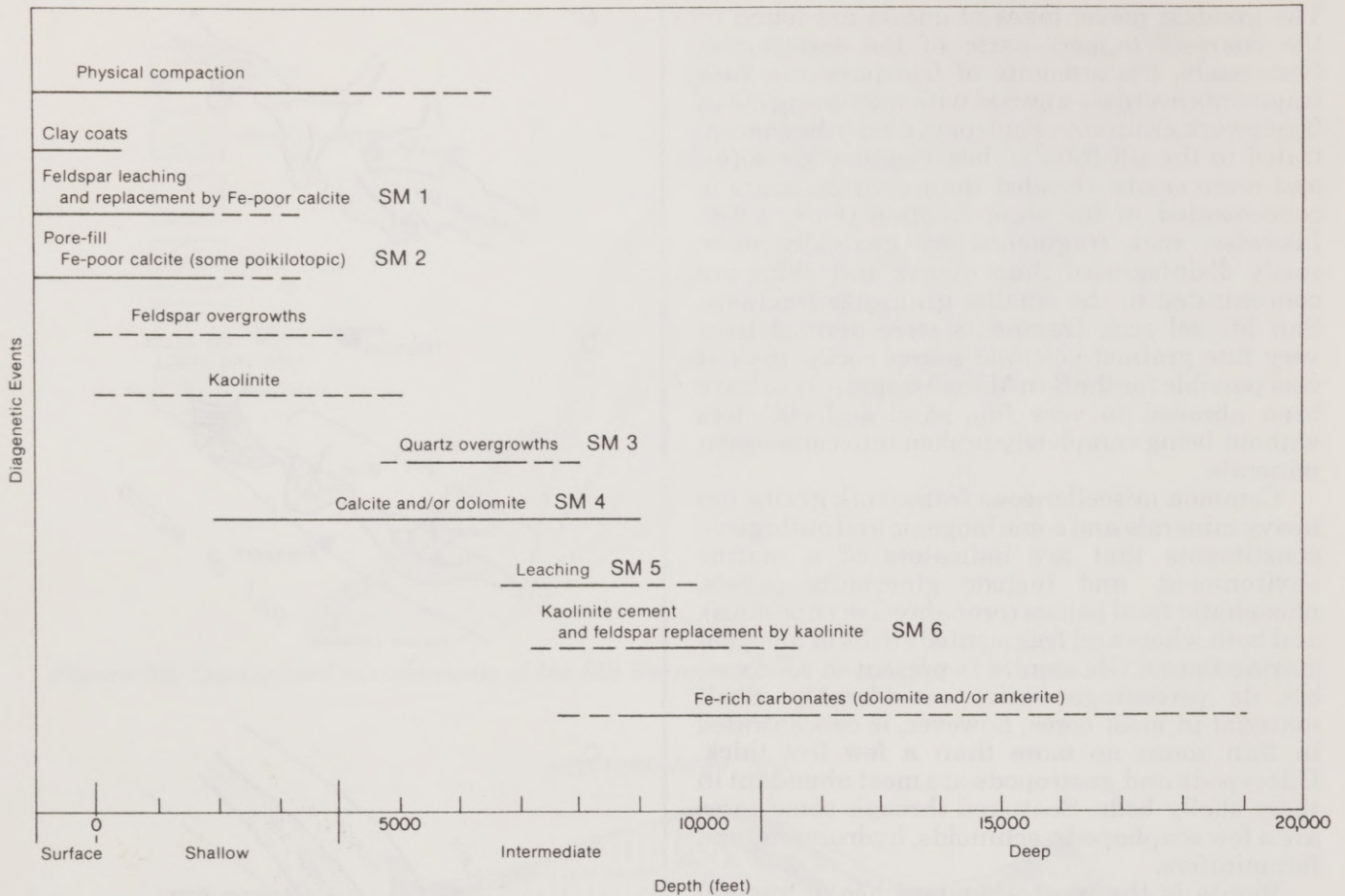


Figure 36. Generalized diagenetic sequence for Tertiary sandstones of the Texas Gulf Coast. Modified from Loucks and others (1980).

included by Loucks and others (1979) in their diagenetic sequence (fig. 36), but Galloway (1979), in a study of diagenesis in arc-derived sandstones from northeast Pacific margin basins, suggests that clay rims form in the shallow to intermediate subsurface (1,000 to 4,000 ft, or 300 to 1,300 m). Where illite rims outline some of the grains in San Miguel rocks, quartz overgrowths are also present. However, no rims have been observed on the outside of the overgrowths, a suggestion that formation of clay rims preceded that of the overgrowths. Formation of quartz overgrowths (SM 3) preceded the sparry calcite (SM 4) (pl. IX-D). Leaching of shell material (pl. IX-E) and calcite cement (SM 5) followed formation of the sparry calcite. The greatest porosity in the San Miguel sandstones generally is in zones of leached shells and in the zones of leached feldspars. Authigenic kaolinite (SM 6) occupies the central parts of some primary intergranular pore spaces as well as central parts of larger cavities (pl. IX-F), an indication that kaolinite was a very late cement in this diagenetic sequence.

SAN MIGUEL SANDSTONES AS PETROLEUM RESERVOIRS

History of Production

Early in the history of Gulf Coast oil exploration, interest in the San Miguel was aroused by outcrop evidence of the large Chittim Anticline. The first well to test the San Miguel was drilled in 1912 in Maverick County. This and subsequent test wells, however, showed that the shallow San Miguel sandstones contained mostly low-gravity oil. Commercial production was not established until the late 1940's when the Del Monte Field in Zavala County was discovered and developed (Lewis, 1977). Higher gravity oil was found when other deeper San Miguel sandstones were tested. In addition, improved recovery techniques allowed some of the shallow, low-gravity oil to be produced.

Fifty-four fields in the Maverick Basin have produced hydrocarbons from one or more of the

San Miguel sandstones. Total oil produced from the San Miguel as of January 1, 1980, is 71,053,209 barrels (Railroad Commission of Texas, 1979). As pointed out by Lewis (1977), most of the production has been from fields discovered since 1970. The San Miguel E sandstone is the biggest producer, yielding over half the total oil produced from the San Miguel Formation.

Trapping Mechanisms and Types of Fields

Lewis (1977) described two basic kinds of hydrocarbon traps in San Miguel sandstones: (1) structural traps formed over volcanic plugs and (2) stratigraphic traps formed by updip pinchouts of porous sandstones. Fields with structural traps are small, consisting of only a few wells, but they account for most of the San Miguel fields. Examples of fields with structural traps are the Elaine, Torch, Holdsworth, Indio, South Batesville, and Del Monte Fields. In the first phases of exploratory drilling, the plugs were found accidentally. Later, magnetic surveys were used to locate the plugs, which are magnetic anomalies (Simmons, 1967). Now seismic methods are the most important tools used to find these plugs.

Many fields that Lewis (1977) classified as stratigraphic-type fields actually involve both stratigraphic and structural traps. In many places, the elongate, strike-aligned San Miguel sandstone bodies are surrounded by shale, providing excellent stratigraphic traps. Many actual reservoirs, however, are restricted to the areas where these sandstone bodies lie across structural noses, so that there is closure in the strike directions in addition to updip sandstone pinchouts. The stratigraphic-type fields, such as Sacatosa in Maverick County, are fewer but much larger than the fields developed over volcanic plugs. Most San Miguel oil has been produced from these large fields, the greatest of which is Big Wells Field, which produces from sandstone E in Dimmit County.

Role of Diagenesis in Reservoir Development

Diagenesis is an important factor in determining reservoir quality of the San Miguel sandstones. Cementation destroyed porosity in some places, while in others, porosity was created by the leaching of feldspars and shell material or re-established by the leaching of earlier cement. Unfortunately, no predictable diagenetic patterns related to facies distribution have been recognized. Shoreface facies constitute most of the sandstone bodies, and lateral facies variations within the sandstones are not great. As reported

above, the tightly cemented parts of a San Miguel sandstone body generally are the most well sorted zones, but this cementation of well-sorted zones does not occur everywhere in each sandstone unit. Likewise, occurrence of the most highly porous zones, where leaching is significant, is unpredictable, as demonstrated in an area where dense core control was available.

CONCLUSIONS

1. During deposition of the San Miguel Formation, the Maverick Basin in South Texas consisted of two subbasins: a western subbasin that received sediments from the northwest and an eastern subbasin that received sediments from the north. Deltaic sand deposition began earlier in the western subbasin than in the eastern subbasin.

2. The San Miguel Formation was deposited during an overall transgression consisting of two major transgressive episodes, as indicated by the relative positions of individual sandstone units. Principal deltaic deposits, however, are not transgressive but rather are progradational, representing minor regressive sequences periodically interrupting the overall transgressive trend.

3. Sandstone units of the San Miguel Formation are a series of deltaic deposits reworked to varying degrees by marine processes during both delta building and subsequent transgressions.

4. San Miguel deltas are broadly classed as wave-dominated systems, although they actually compose a spectrum ranging from wave-influenced lobate deltas to deltas highly modified by wave processes and elongated in strike directions.

5. Sandstone geometries are dependent primarily on delta type, although the final shapes of the San Miguel units were influenced to varying degrees by transgressive reworking. Major determinants of delta type were (1) rate of sediment input, (2) wave energy, and (3) rate of relative sea-level rise. Wave energy and rate of sea-level rise also largely controlled the degree of transgressive reworking. Wave energy remained relatively constant, while the rates of sediment input and sea-level rise varied to produce the spectrum of sandstone geometries.

6. Dominant facies interpreted within the San Miguel sandstones are those of shoreface origin. Abundance of burrows throughout most cores and a general lack of large-scale primary structures characteristic of beach and upper shoreface deposits indicate that San Miguel sandstones are incomplete strandplain or barrier sequences. Tops of original, complete shoreface sequences were physically reworked during subsequent transgression. Biological reworking destroyed primary structures in the upper parts of the truncated sequences.

7. San Miguel strike-oriented sandstone bodies are excellent stratigraphic traps for hydrocarbons, although most of the known reservoirs are generally restricted to areas where both structural and stratigraphic trapping are involved.

8. Hydrocarbon reservoir quality in some zones is affected considerably by sandstone diagenesis, but the lateral distribution of diagenetic effects is unpredictable.

ACKNOWLEDGMENTS

This report presents the results of a study conducted both as a Bureau of Economic Geology research project and as a Master's thesis for the Department of Geological Sciences, The University of Texas at Austin. Many thanks go to my thesis supervisor, D. G. Bebout, and other thesis committee members, A. J. Scott and R. L. Folk. I also thank R. G. Loucks, W. E. Galloway, J. M. Boyles, M. B. Edwards, D. K. Hobday, and L. F. Brown, Jr., for many helpful suggestions and critical review of the manuscript.

REFERENCES

- Caffey, K. C., 1978, Depositional environments of the Olmos, San Miguel, and Upson Formations (Upper Cretaceous), Rio Escondido Basin, Coahuila, Mexico: The University of Texas at Austin, Master's thesis, 86 p.
- Coleman, J. M., and Wright, L. D., 1975, Modern river deltas: variability of processes and sand bodies, in Broussard, M. L., ed., Deltas: models for exploration: Houston Geological Society, p. 99-150.
- Crimes, T. P., 1977, Trace fossils of an Eocene deep-sea sand fan, northern Spain, in Crimes, T. P., and Harper, J. C., eds., Trace fossils 2: Geological Journal Special Issue No. 9, p. 71-90.
- Curtis, D. M., 1970, Miocene deltaic sedimentation, Louisiana Gulf Coast, in Morgan, J. P., ed., Deltaic sedimentation, modern and ancient: Society of Economic Paleontologists and Mineralogists Special Publication No. 15, p. 293-308.
- Dumble, E. T., 1892, Notes on the geology of the valley of the middle Rio Grande: Geological Society of America Bulletin, v. 3, p. 219-230.
- Fisher, W. L., 1969, Facies characterization of Gulf Coast Basin delta systems, with some Holocene analogues: Gulf Coast Association of Geological Societies Transactions, v. 19, p. 239-261.
- Fisher, W. L., Brown, L. F., Jr., Scott, A. J., and McGowen, J. H., 1969, Delta systems in the exploration for oil and gas: a research colloquium: The University of Texas at Austin, Bureau of Economic Geology, 210 p.
- Folk, R. L., 1968, Petrology of sedimentary rocks: Austin, Texas, Hemphill's, 170 p.
- Frazier, D. E., 1974, Depositional-episodes: their relationship to the Quaternary stratigraphic framework in the northwestern portion of the Gulf Basin: The University of Texas at Austin, Bureau of Economic Geology Geological Circular 74-1, 28 p.
- Galloway, W. E., 1975, Process framework for describing the morphologic and stratigraphic evolution of deltaic depositional systems, in Broussard, M. L., ed., Deltas: models for exploration: Houston Geological Society, p. 87-98.
- _____, 1979, Diagenetic control of reservoir quality in arc-derived sandstones: implications for petroleum exploration: Society of Economic Paleontologists and Mineralogists Special Publication No. 26, p. 251-262.
- Glover, J. E., 1955, Olmos sand facies of southwest Texas: Gulf Coast Association of Geological Societies Transactions, v. 5, p. 135-143.
- Gregory, J. L., 1966, A lower Oligocene delta in the subsurface of southeastern Texas, in Shirley, M. C., ed., Deltas in their geological framework: Houston Geological Society, p. 213-227.
- Harms, J. C., Southard, J. B., Spearing, D. R., and Walker, R. G., 1975, Depositional environments as interpreted from primary sedimentary structures and stratification sequences: Society of Economic Paleontologists and Mineralogists Short Course No. 2, 161 p.
- Howard, J. D., 1972, Trace fossils as criteria for recognizing shorelines in the stratigraphic record, in Rigby, J. K., and Hamblin, W. K., eds., Recognition of ancient sedimentary environments: Society of Economic Paleontologists and Mineralogists Special Publication No. 16, p. 215-225.
- Howard, J. D., and Reineck, H.-E., 1972a, Georgia coastal region, Sapelo Island, U. S. A.: sedimentology and biology. IV. physical and biogenic sedimentary structures of the nearshore shelf: Senckenbergiana Maritima, v. 4, p. 81-123.
- _____, 1972b, Georgia coastal region, Sapelo Island, U. S. A.: sedimentology and biology. VIII. conclusions: Senckenbergiana Maritima, v. 4, p. 217-222.
- Isbell, E. B., Spencer, C. W., and Seitz, T., 1976, Petroleum geology of the Well Draw Field, Converse County, Wyoming, in Landon, R. B., ed., Geology and energy resources of the Powder River: Wyoming Geological Association Guidebook, 28th Annual Field Conference, p. 165-174.
- Kern, J. P., and Warme, J. E., 1974, Trace fossils and bathymetry of the Upper Cretaceous Point Loma Formation, San Diego, California: Geological Society of America Bulletin, v. 85, p. 893-900.
- Kruit, C., 1955, Sediments of the Rhone delta: part I, grain size and microfauna: Geologie en Mijnbouw, v. 15, p. 357-514.

- Lewis, J. O., 1962, Torch Field, Zavala County, Texas: South Texas Geological Society Bulletin, v. 2, no. 5, p. 5-14.
- _____, 1977, Stratigraphy and entrapment of hydrocarbons in the San Miguel sands of southwest Texas: Gulf Coast Association of Geological Societies Transactions, v. 27, p. 90-98.
- Loucks, R. G., 1976, Pearsall Formation, Lower Cretaceous, South Texas: depositional facies and carbonate diagenesis and their relationship to porosity: The University of Texas at Austin, Ph.D. dissertation, 362 p.
- Loucks, R. G., Dodge, M. M., and Galloway, W. E., 1979, Sandstone consolidation analysis to delineate areas of high-quality reservoirs suitable for production of geopressured geothermal energy along the Texas Gulf Coast: The University of Texas at Austin, Bureau of Economic Geology, report for U. S. Department of Energy, Contract No. EG-77-5-05-5554.
- Loucks, R. G., Richmann, D. L., and Milliken, K. L., 1980, Factors controlling porosity and permeability in geopressured Frio sandstone reservoirs, General Crude Oil/Department of Energy Pleasant Bayou test wells, Brazoria County, Texas: Fourth Geopressured Geothermal Energy Conference Proceedings, Center for Energy Studies, The University of Texas at Austin, v. 1, p. 46-84.
- Luttrell, P. E., 1977, Carbonate facies distribution and diagenesis associated with volcanic cones—Anacacho Limestone (Upper Cretaceous), Elaine Field, Dimmit County, Texas, in Bebout, D. G., and Loucks, R. G., eds., Cretaceous carbonates of Texas and Mexico—applications to subsurface exploration: The University of Texas at Austin, Bureau of Economic Geology Report of Investigations 89, p. 260-285.
- Murray, G. E., 1957, Geologic occurrence of hydrocarbons in Gulf Coastal Province of the United States: Gulf Coast Association of Geological Societies Transactions, v. 7, p. 253-299.
- _____, 1961, Geology of the Atlantic and Gulf Coast Province of North America: New York, Harper Brothers, 629 p.
- Oomkens, E., 1967, Depositional sequences and sand distribution in a deltaic complex: Geologie en Mijnbouw, v. 46, p. 265-278.
- _____, 1970, Depositional sequences and sand distribution in the postglacial Rhone delta complex, in Morgan, J. P., ed., Deltaic sedimentation, modern and ancient: Society of Economic Paleontologists and Mineralogists Special Publication No. 15, p. 198-212.
- Railroad Commission of Texas, 1979, Annual report of the Oil and Gas Division: Railroad Commission of Texas, 587 p.
- Rose, P. R., 1972, Edwards Group, surface and subsurface Central Texas: The University of Texas at Austin, Bureau of Economic Geology Report of Investigations 74, 198 p.
- Sellards, E. H., Adkins, W. S., and Plummer, F. B., 1932, The geology of Texas, volume 1, stratigraphy: University of Texas, Austin, Bureau of Economic Geology, Bulletin 3232, 1007 p.
- Simmons, K. A., 1967, A primer on "serpentine plugs" in South Texas, in Ellis, W. G., ed., Contributions to the geology of South Texas: South Texas Geological Society, p. 125-132.
- Smith, A. E., Jr., 1975, Ancient deltas: comparison maps (appendix), in Broussard, M. L., ed., Deltas: models for exploration: Houston Geological Society, p. 529-555.
- Spencer, A. B., 1965, Upper Cretaceous asphalt deposits of the Rio Grande Embayment: Corpus Christi Geological Society Guidebook, 67 p.
- Stephenson, L. W., 1931, Taylor age of San Miguel Formation of Maverick County, Texas: American Association of Petroleum Geologists Bulletin, v. 15, p. 793-800.
- Vail, P. R., Mitchum, R. M., Jr., and Thompson, S., III, 1977, Seismic stratigraphy and global changes of sea level, part 3: relative changes of sea level from coastal onlap, in Payton, C. E., ed., Seismic stratigraphy—applications to hydrocarbon exploration: American Association of Petroleum Geologists Memoir 26, p. 63-97.
- Van de Graaff, F. R., 1972, Fluvial-deltaic facies of the Castlegate Sandstone (Cretaceous), east-central Utah: Journal of Sedimentary Petrology, v. 42, p. 558-571.
- Walper, J. L., 1977, Paleozoic tectonics of the southern margin of North America: Gulf Coast Association of Geological Societies Transactions, v. 27, p. 230-241.
- Weimer, R. J., and Hoyt, J. H., 1964, Burrows of *Callianassa major* Say, geologic indicators of littoral and shallow neritic environments: Journal of Paleontology, v. 38, p. 761-767.

APPENDIX

Wells plotted on figure 1.

Tobin grid	Name
7S-4E-7	International #1 Kincaid
7S-5E-6	Ford & Hamilton # 1 Nunley
7S-6E-3	Tenneco # 1 Ney
7S-6E-8	Glasscock # 1 Carle Mercantile
7S-7E-5	Pan Am # 1 Ward
7S-7E-7	Tenneco # 1 Wilson
7S-7E-9	Pan Am # 1 Muennink
7S-8E-3	Houston Oil and Minerals # 1 Neumann
7S-8E-6	Johnston # 1 Howard "A"
7S-9E-4	Cities Service # 1A Briscoe
7S-9E-5	Hughes & Hughes # 1 Cadenhead
7S-9E-8	Progress # 1 Haas
7S-10E-4	Hughes & Hughes # 1 Plachy
7S-10E-8	Moncrief # 1 Collins
8S-3W-9	General Crude # 1 Dunbar
8S-2E-5	Steeger, et al. # 1 Smyth
8S-2E-8	Wofford # 1 Bonnett
8S-4E-5	King & Heyne # 1 Kincaid
8S-4E-7	Wilcox # 6 Gilligan
8S-4E-8	Zink, et al. # 1 Vanham
8S-4E-9	Intex # 1 Vanham
8S-5E-2	Gorman # 6 Woodley
8S-5E-4	Humble # 1 Kincaid
8S-5E-7	Tenneco # 1 Machen
8S-5E-9	Rowe # 1 Kincaid
8S-6E-2	Galaxy # 1 Leoncita
8S-6E-5	Pagenkopf & Jamieson # 1 Blackaller
8S-6E-6	Tenneco & Pennzoil # 1 Goad
8S-7E-3	Humble # 1 Wilson
8S-7E-7	Tenneco & Pennzoil # 1 Wilbeck
8S-7E-8	Jergins # 1 Goad
8S-8E-3	Morrison # 1 Boggus
8S-8E-5	Michelson # 2 Jones
8S-8E-9	Lake # 1 Gracey & Wegenhoff
8S-9E-2	Pan Am # 1 Lilly
8S-9E-3	Douglas # 1 Watson
8S-9E-4	Pennzoil # 1 Akers
8S-9E-5	Tenneco & Pennzoil # 1 Edgar
8S-10E-1	Clark # 1 Jones
8S-10E-4	Wilson # 1 Kuykendall
8S-10E-6	Sabine # 1 Tomblin
8S-10E-7	Producers of Nevada, et al. # 1 Wright
8S-10E-9	Shell # 1-E Hardin
8S-11E-8	Beard & Turnbull # 1 Graf
8S-12E-1	Brown, et al. # 1 Katesmorak
8S-12E-8	Gorman # 1 Gorman Fee
8S-12E-9	Killam # 1 Schraeter
9S-3W-1	Harrison # B-7 Saner
9S-3W-2	Harrison # B-6 Saner
9S-3W-6	Southworth & Wood # 2 Chittim
9S-3W-7	Southworth & Wood # 3 Chittim
9S-2W-2	Monsanto # 1 Saner
9S-2W-3	Monsanto # 3 Saner
9S-2W-4	Southworth & Wood # 6 Fessman
9S-2W-5	Southworth & Wood # 5 Fessman
9S-2W-7	Southworth & Wood # 2 Wozencroft
9S-2W-9	Manor & Midwest # 1 Chittim
9S-1W-4	Norton & Grage # 32 Chaparrosa
9S-1W-5	Chaparrosa # 1 Johnson (Core - D)
9S-1W-6	Norton & Grage # 23 Chaparrosa
9S-1W-7	Norton & Grage # 17 Norton- Chaparrosa
9S-1W-8	Norton & Grage # 39 Chaparrosa
9S-1E-1	Getty # 1 Greele
9S-1E-3	Tenneco # 2 Matthews
9S-1E-4	Tenneco # 1 Matthews
9S-1E-7	Brown (Electrothermic) # 2 Matthews
9S-1E-8	Electrothermic & Dougherty # A-1 Matthews
9S-2E-5	Tipperary # 1 Atwood
9S-2E-6	Beer # 11 Pryor
9S-2E-7	Humble # 2 Pryor
9S-2E-8	Continental # 1 Pryor
9S-3E-6	Reece # 1 Brewster
9S-3E-8	Haas # 1 Bartlett
9S-4E-3	Wilcox # 1 Voight
9S-4E-6	Winn # 1 Kirchner
9S-4E-9	Brill # 1 Hope
9S-5E-1	Kirkwood # 1A Brown
9S-5E-2	Winn (Zavala) # 1 Murphy
9S-5E-3	Moncrief # 1 Sawyer
9S-5E-8	Jocelyn-Varn # 1 Schoolfield C
9S-6E-2	Moncrief # 2 Rheiner
9S-6E-4	Tenneco # 1 Mack
9S-6E-7	Morgan # 1 Halff & Oppenheimer
9S-7E-1	Tenneco # 1 Stoker
9S-7E-4	Forest # 1 Halff & Oppenheimer
9S-8E-1	Smith # 1 Benz
9S-8E-3	Pronto # 1 Gracey
9S-8E-8	Mabee # 1 Newsom
9S-8E-9	Pronto # 1 Halff & Oppenheimer
9S-9E-1	Humble # 2 Houston
9S-9E-4	Magnolia # 1 McKinley
9S-10E-8	Killam # 1 Favor
9S-11E-2	Placid # 1 Eisenhauer
9S-11E-8	Humble # 1 Matocha
9S-12E-6	Texas Crude # 1 Benz
9S-12E-8	Humble # 1 Moursand
9S-12E-9	Skelly # 1 Winkler
10S-4W-6	McCabe-Turner, et al. # 1 Kincaid
10S-4W-7	Texas Gas (Winn) # 1 Kincaid
10S-4W-8	Belco # 3 Kincaid
10S-3W-4	Lockhart # 1 Mangum
10S-2W-3	Continental # N Chittim Test
10S-2W-5	Continental # 606-1 Chittim
10S-2W-9	Continental # 209-1 Chittim
10S-1W-1	Norton & Grage # 14 Norton
10S-1W-2	Norton & Grage # 15 Norton
10S-1W-4	Shell # 2 Plumley
10S-1W-5	Cain # 1 Plumley
10S-1W-7	Shield & Steeger # 1 Stuart-Griffin
10S-1W-8	Texas # 1 Stuart
10S-1W-9	Continental # 608-1 Chittim
10S-1E-4	Norton & Grage # 2 Norton
10S-1E-5	Norton & Grage # 5 Norton
10S-1E-6	General Crude # 1 Guyler

10S-1E-9	Minton, et al. # 1-C Rosenberg, et al.	11S-3E-3	Charter # 1 Cross "S" Ranch
10S-2E-3	Little # 1 Scroggins	11S-3E-5	General Crude # 1 Donnelly
10S-2E-6	Burr & Crews # 1 H & F	11S-3E-7	Davis # 1 Weaver
10S-2E-9	Texas # 3 Northeastern Farming	11S-3E-8	Little, et al. # 1 Rutledge
10S-3E-1	Superior # 1 Raine	11S-3E-9	Moore # 1 Northeastern Farming
10S-3E-5	Winn # 2 Holdsworth	11S-4E-4	Tipperary # A-2 Buchanan
10S-3E-7	Walsh & Watts # 1 Holdsworth	11S-4E-5	Ladd # 29-1 Blalock
10S-3E-8	Hughes & Hughes # 1 Holdsworth "B"	11S-4E-6	Davis # 1 Chinn & Ashby
10S-4E-5	Harvey # 1 Whitecotton	11S-4E-7	Delray # 1-25 Baggett, et al. (Core - E)
10S-4E-6	Leona # 1 West	11S-4E-9	Brown # 1 Heitz
10S-4E-7	Retama # 1-44 Glasscock	11S-5E-1	Pan Am # 1 Buerger
10S-4E-8	Mobil # 1 Byrne	11S-5E-6	Sun # 1 Thompson
10S-4E-9	Ancon & Beamon # 2 Gates	11S-5E-8	Sun # 2 Garner
10S-5E-3	Northern & Phillips-Stringer # 1 Dunbar	11S-6E-3	Hughes & Hughes # 1 Whitwell
10S-5E-7	Humble # C-1 Marrs McLean	11S-6E-8	Harkins # 1 Dunn
10S-5E-8	Texas # 2 West	11S-7E-2	Kirkwood & Morgan # 1 Bell
10S-6E-1	Tenneco & Pennzoil # 1 Halff	11S-7E-5	Harkins # 1 Avant
10S-6E-4	Bounty # 1 Hausser	11S-8E-2	Pan Am # 1 Culpepper
10S-6E-5	Humble # 1 Park	11S-8E-3	Harkins # 1 Thompson
10S-6E-9	Anderson # 1 McCarthy	11S-9E-1	Harkins, et al. # 1 Shiner
10S-7E-3	Parker # 1-P Halff & Oppenheimer	11S-9E-5	Sunray DX # 1 Shiner, et al.
10S-7E-7	Flamingo (Pronto) # 1 Bennett	11S-9E-7	Skelly # 1A La Salle
10S-7E-9	Tipperary # 3 Massey	11S-10E-3	Texas Co. # 1B NCT-2 Kothmann
10S-8E-6	Hawkins # 1 Whitworth & Mills	11S-10E-4	Harkins # 1 Atchison
10S-8E-9	Danwoody # 1 White	11S-10E-9	Texas # 1 La Salle
10S-9E-5	Pan Am # 1 Oppenheimer-Lang	12S-3W-2	Tiger # 6 Halsell Fnd.
10S-9E-7	Southwestern # 2 McKinney	12S-3W-4	Exsun # 1-A Halsell
10S-9E-8	Flournoy # 1 Carnes	12S-3W-5	Exsun & Tideway # 2-A Halsell
10S-10E-1	Humble # 3 Nixon	12S-3W-6	RKG Engineering # 16-1 Halsell
10S-10E-3	Stanolind # 1 Garcia	12S-3W-8	Ontex # 1 Keisling
10S-11E-4	Gulf # 1 Reese	12S-2W-1	National Assoc. # A-1 Halsell
11S-4W-6	Shaw # 2 Wipff	12S-2W-2	Caddo # 111-1-C Halsell
11S-3W-1	Continental # M Chittim Test	12S-2W-5	Union # 29-1 Halsell (Core - I)
11S-3W-7	Continental # 74-1 Chittim	12S-2W-7	Texon Royalty # 1 Sullivan
11S-3W-8	Continental # 97-2 Chittim	12S-1W-1	Howeth, et al. # 1 Myers
11S-2W-1	Continental # 4-5 Chittim	12S-1W-2	Shamrock # 1-602 Halsell
11S-2W-4	Continental # 44-4 Chittim	12S-1W-4	Shamrock # 1-663 Halsell
11S-2W-5	Continental # 65-12 Chittim	12S-1W-5	Wellington # B-2 Sullivan
11S-2W-8	Continental # 71-9 Chittim	12S-1W-6	Shamrock # C-2 Eubanks
11S-1W-1	Petroleum # 1 Flanagan	12S-1W-7	Caddo # 1-1 Hamilton
11S-1W-2	Texas # 2 Stuart	12S-1W-8	BTA # 1 Stowe
11S-1W-5	Shamrock # 1 Van Cleve	12S-1W-9	Wilbanks # 16-1 Halsell
11S-1W-6	Arriba # 1 Zowarka	12S-1E-1	Steeger # 1 Davis
11S-1W-8	Steeger # 1 Chittim	12S-1E-3	Continental # 1 O'Meara
11S-1W-9	Continental # 570-1 Chittim	12S-1E-5	One Star # 1 Bray (Core - C, G, and I)
11S-1E-1	Winn # 1 Cross	12S-2E-2	Safari # 1 Crane
11S-1E-2	Michelson # A-4-1 Norton	12S-2E-5	BTA # 1 77D4 JU-P Cardin
11S-1E-3	Winn & H & J # 1 Maegen	12S-2E-7	Gulf # 1 Bowman
11S-1E-4	Dixon # 1 Benham	12S-3E-3	Houston Oil & Minerals # 1 Allee
11S-1E-5	Steeger # 1 Stewart	12S-3E-4	Texsun # 1 Reynolds & Wilson, Humble
11S-1E-6	Steeger # 1 Carr	12S-4E-1	Delray # 6-14 Rogers (Core - E)
11S-1E-7	Steeger # 1-1-14 Stewart	12S-4E-3	Steeger # 1 Groos Nat'l Bank
11S-1E-8	Ford # 1 Stewart, et al.	12S-4E-4	Deep Rock # 1 Barker
11S-1E-9	Wood # 1 Weathers (Core - C and G)	12S-4E-8	Superior # 2 Henry
11S-2E-1	Dixon # 1 Kirk	12S-5E-5	Texas # 1 Standifer
11S-2E-2	Buttes & Beamon # S-1-81 Cross	12S-5E-6	Continental # 1 Alder
11S-2E-4	Ford & Hamilton # 1 Neel	12S-5E-7	Shell # 1 Matthews
11S-2E-6	Winn & Musselman # 1 Compton	12S-5E-9	Cockrell & Continental # 1 Rogers
11S-2E-7	Winn & Texas Seaboard # 1 Jackson	12S-6E-1	South Texas # 1 Brownlow
11S-2E-8	McCardy # 1 Ward	12S-6E-2	Lovelady # 1 Smith
11S-2E-9	Little # 1 Fee	12S-6E-3	Lovelady # 1 Pena

12S-6E-4 Lovelady # 1 Fuller
 12S-6E-5 Hytech # 1 Gonzales
 12S-6E-8 South Texas # 1 Schulze
 12S-7E-3 Mobil # 1 McNabb
 12S-8E-1 Harkins # 1 Burns
 12S-8E-8 Harkins # 1 Am. Nat. Bank, Austin
 12S-9E-1 Tidewater (Auld, et al.) # 2 Wilson
 12S-11E-1 Pan Am # 1 Franklin
 12S-11E-5 Maguire & Del Mar # 1 Franklin
 12S-12E-2 Gilcrease & Viking # 1 Houston
 12S-12E-6 Colorado # 1 Roark
 12S-12E-9 Stanolind # 1 Henry
 13S-3W-5 Coastal States # 1 Schwartz
 13S-3W-6 Ozark # B-8 Cage
 13S-3W-8 McGoldrick, Smith, & Gill # 1 Hagen
 13S-2W-1 Whitener # 3-W Baker
 13S-2W-3 Continental # 54-1 Cage
 13S-2W-5 Continental # 90-1 Cage
 13S-1W-1 Lovelady # 1 McKnight
 13S-1W-3 Rio Grande # 1-29 Risinger
 13S-1W-4 Shamrock # 12 Fitzsimmons
 13S-1W-8 Sutton # C-1 Eubanks
 13S-1E-1 Galaxy # 1 McKnight
 13S-2E-1 Bowman, et al. # 1 Richardson
 13S-2E-2 Pan Am (Amoco) # 1 Frost National Bank
 13S-2E-5 MGF # 1 Barrow
 13S-2E-9 Hughes & Hughes # 1 Garner Est.
 13S-3E-1 Stringer # 1 King Tr. 2
 13S-3E-2 Pan Am (Kallina) # 1 Bowman
 13S-3E-7 Western # 1 Tumlinson
 13S-4E-3 Stringer, et al. # 1 Taylor, et al.
 13S-4E-6 Snyder # 1 Hendrichsen "A"
 13S-4E-8 Belco # 1 Coffield
 13S-8E-4 Brown # 1 Storey
 13S-9E-6 Mound # 1 Naylor & Jones
 13S-9E-7 Gulf # 1 Naylor & Jones
 13S-11E-3 Fasken # 1 Henry
 13S-11E-6 Humble # 1 Martin
 13S-11E-8 Fasken # 1 Dilworth
 14S-2W-5 Shamrock # 1-39 Cage

14S-2W-6 Shamrock # 1-62 Cage
 14S-2W-8 Shamrock # 1-96 Cage
 14S-2W-9 Shamrock # 1-66 Cage
 14S-1W-3 Shamrock # 8 Fitzsimmons
 14S-1W-6 Harkins # 1 George
 14S-1W-8 Gulf # 1 Fitzsimmons, et al.
 14S-1W-9 Shamrock # 8 Fitzsimmons
 14S-1E-3 Haynes & Y. T. # 1 Fitzsimmons
 14S-2E-6 Western, et al. (Tarina) # 1 Briscoe
 14S-2E-8 Coquina # B-1 Briscoe
 14S-3E-1 Western # 1 Dillon
 14S-4E-4 Superior # 2 Wortham
 14S-4E-5 Superior # 3 Wortham
 14S-5E-2 Lightning # 1 Silver Lakes
 14S-8E-1 Plymouth # 1 Archbishop of San Antonio
 14S-8E-4 Pan Am # C-1 Cooke
 14S-9E-1 Standard of Texas # 2 South Texas Syndicate
 14S-9E-3 Pan Am # 1 Foerster
 14S-10E-3 Sutton # 1 South Texas Syndicate
 15S-2E-6 Richardson # A-1 Gates Ranch
 15S-5E-9 Sutton # 1 Kone
 15S-6E-2 Lyman # 1 Petty
 15S-7E-3 Less # 1 Martin
 16S-1E-3 Nordan (Beer) # 1 Briscoe
 16S-4E-5 Rowe # 1 Garner
 17S-1E-6 Copano # A-1 Apache
 17S-1E-7 Copano (Sutton) # A-2 Rachal
 17S-2E-8 Copano # A-1 Palafox
 17S-3E-6 Ginther, Warren & Maguire # 1 Middleton

Additional core wells

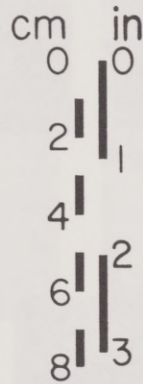
9S-1W-5 Chaparrosa # 3 Johnson (San Miguel D)
 12S-1E-5 Lone Star # 2 Bray (San Miguel C and I)
 12S-4E-1 Delray # 8-14 Rogers (San Miguel E)



A



B



C

Plate VII

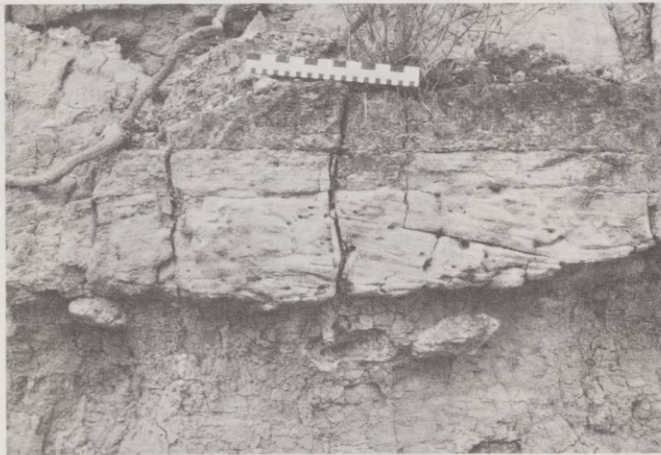
- A. Horizontal Ophiomorpha. These burrows, very similar to those of modern callianassid shrimp, have walls with smooth interiors and exteriors formed of a single layer of round mud pellets. Core slab from sandstone G, Wood # 1 Weathers, Zavala County.
- B. Vertical burrows, most of which are Ophiomorpha. Core slab from sandstone E, Delray # 6-14 Rogers, Dimmit County.
- C. Bed of horizontal laminations with few burrows. The base of the bed (at the break between the lower two core pieces) is a sharp contact. The upper contact is burrowed. Core slab from sandstone I, Lone Star # 1 Bray, Dimmit County.



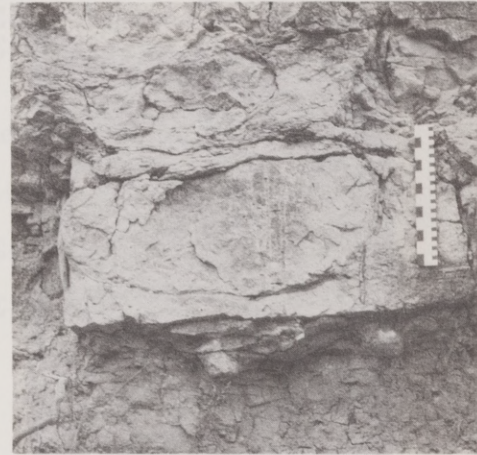
A



B



C



D

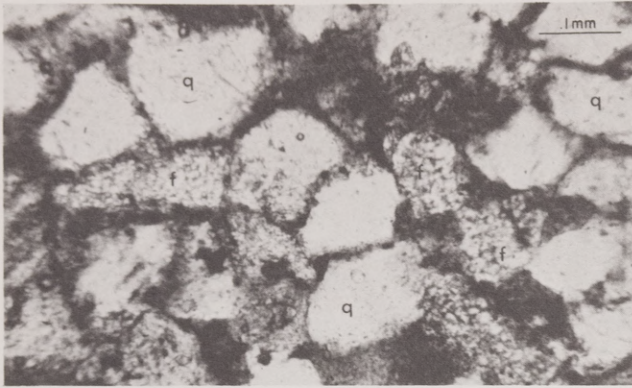
Plate VIII

A. The San Miguel sandstone D exposed in a roadcut along U. S. Highway 277 approximately 14 mi (22 km) north of Eagle Pass, Maverick County. In the lower part of the roadcut section, burrowed, clayey siltstone beds alternate with crossbedded sandstone units. At the top of the section is a massive sandstone unit.

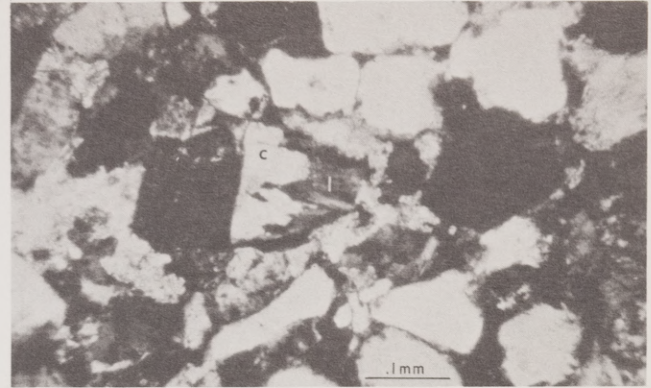
B. Low-angle crossbeds in sandstone units shown in plate VIII-A. Scale is 12 inches (30.5 cm).

C. Hummocky cross-stratification in sandstone units shown in plate VIII-A. Scale is 12 inches (30.5 cm).

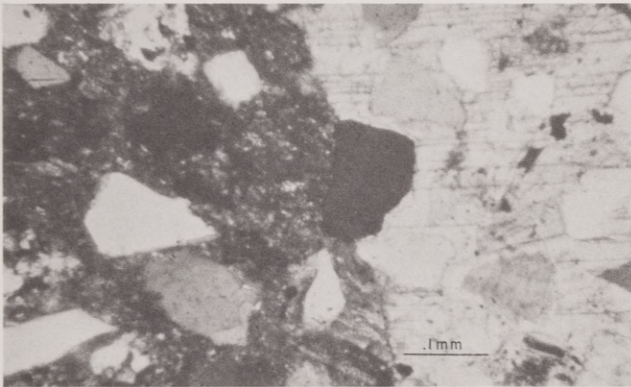
D. Deep, vertical Ophiomorpha penetrating one of the sandstone units shown in plate VIII-A. Scale is 12 inches (30.5 cm).



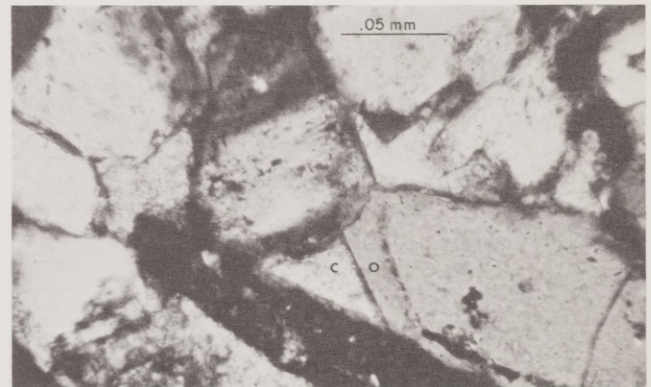
A



B



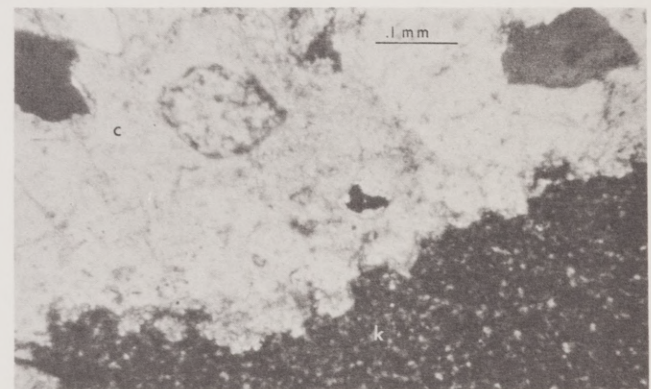
C



D



E



F

Plate IX

- A. Typical San Miguel sandstone with abundant feldspar. *f* = feldspar, *q* = quartz. Thin section from sandstone G, Wood # 1 Weathers, Zavala County.
- B. Leached feldspar grain partially replaced by calcite. *c* = calcite, *l* = leached porosity. Thin section from sandstone G, Wood # 1 Weathers, Zavala County. Crossed nicols.
- C. Poikilotopic calcite cement. Parts of two single calcite crystals, each cementing many sand grains, are shown under crossed nicols. Loose packing of grains indicates early cementation. Thin section from sandstone G, Wood # 1 Weathers, Zavala County.
- D. Quartz overgrowth (*o*) and sparry calcite cement (*c*). Formation of the quartz overgrowths preceded that of the sparry calcite. Thin section from sandstone C, Wood # 1 Weathers, Zavala County. Crossed nicols.
- E. Leached shell fragments (*l*). Thin section from sandstone D, Chaparrosa # 3 Johnson, Zavala County.
- F. Authigenic kaolinite (*k*) filling cavity rimmed with very coarse grained calcite, particularly poikilotopic calcite (*c*). Thin section from sandstone G, Wood # 1 Weathers, Zavala County. Crossed nicols.

PLATE I
 A'
 LA SALLE CO.

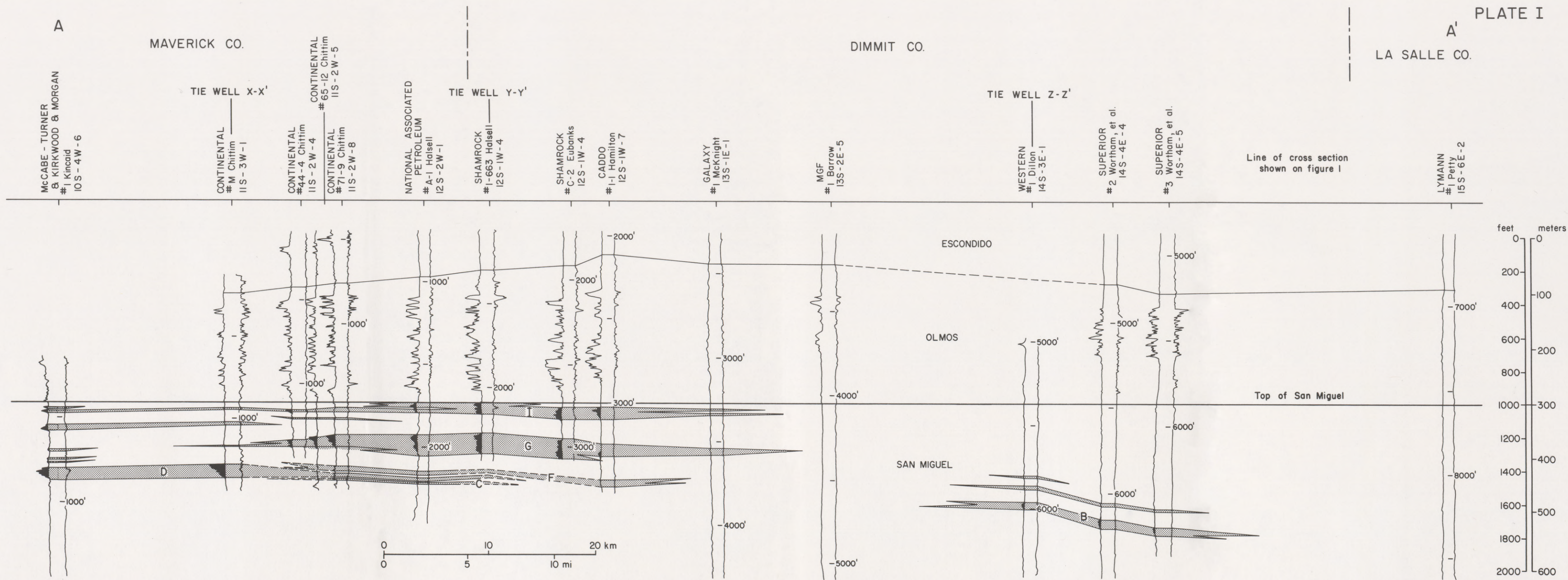


PLATE II
 B'
 LA SALLE CO.

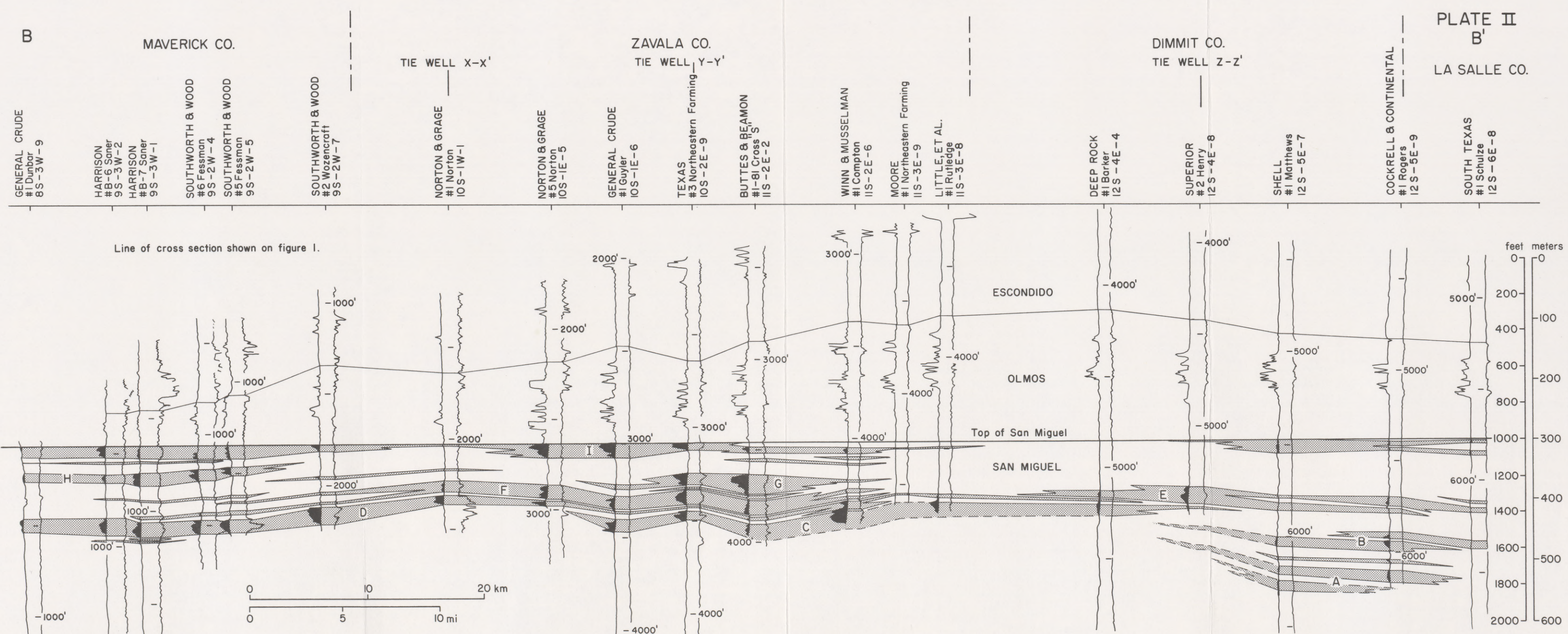


PLATE III

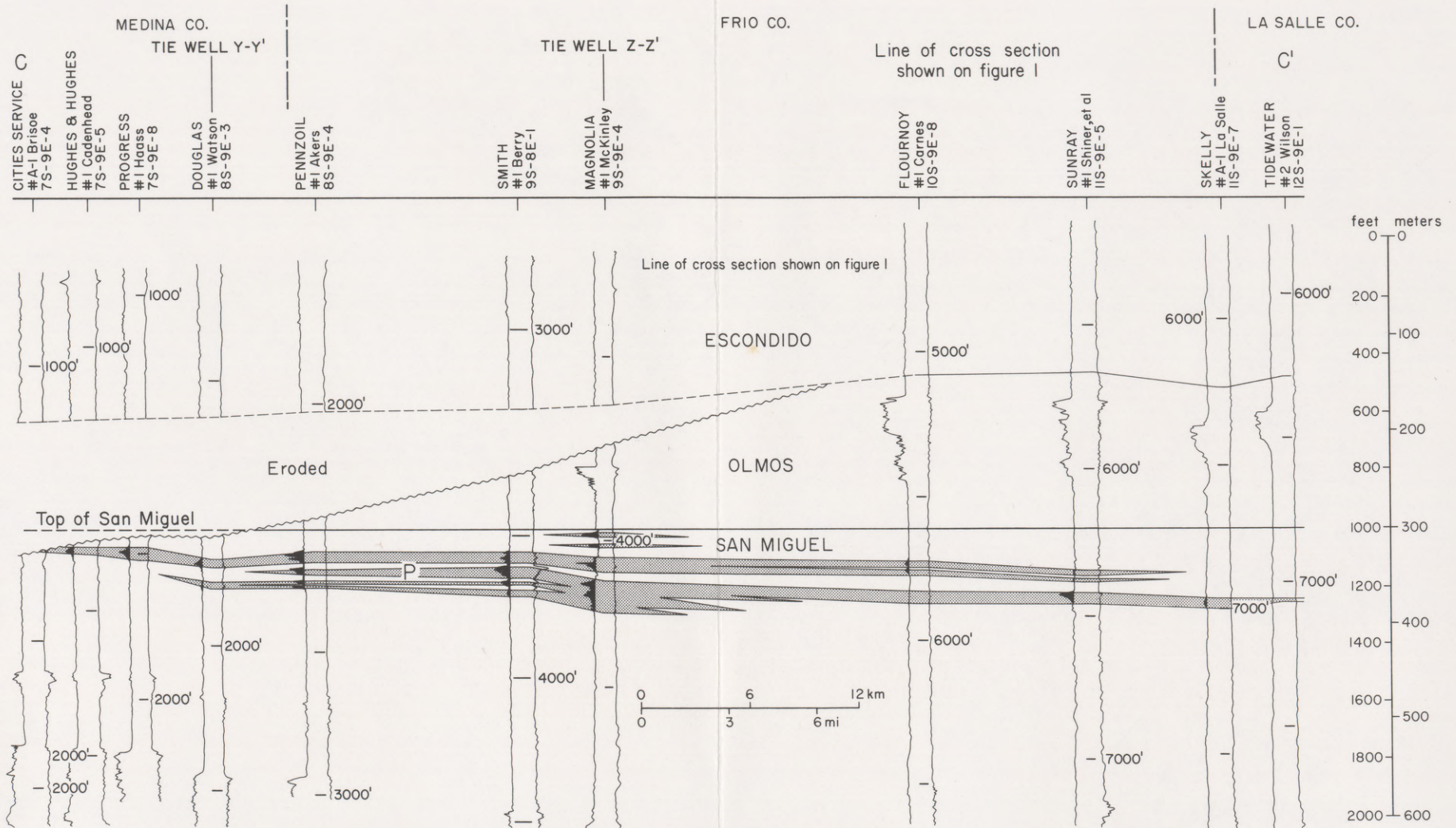
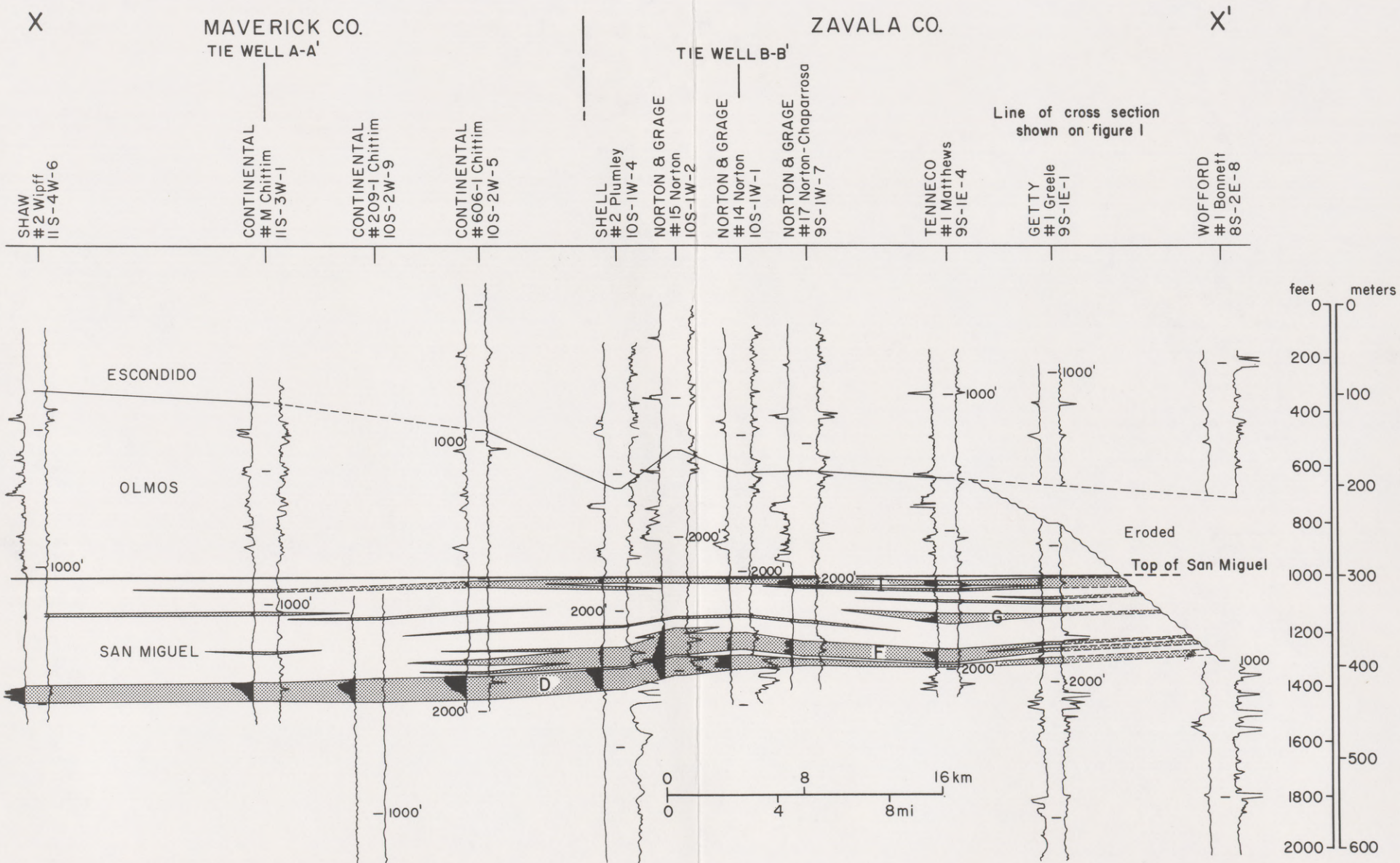
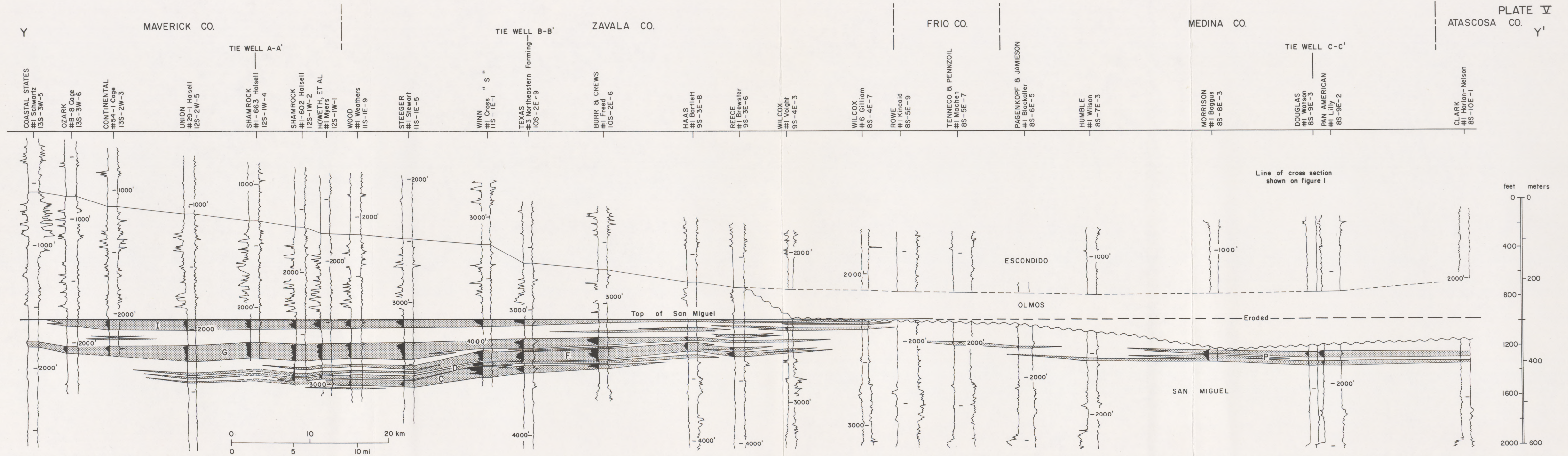
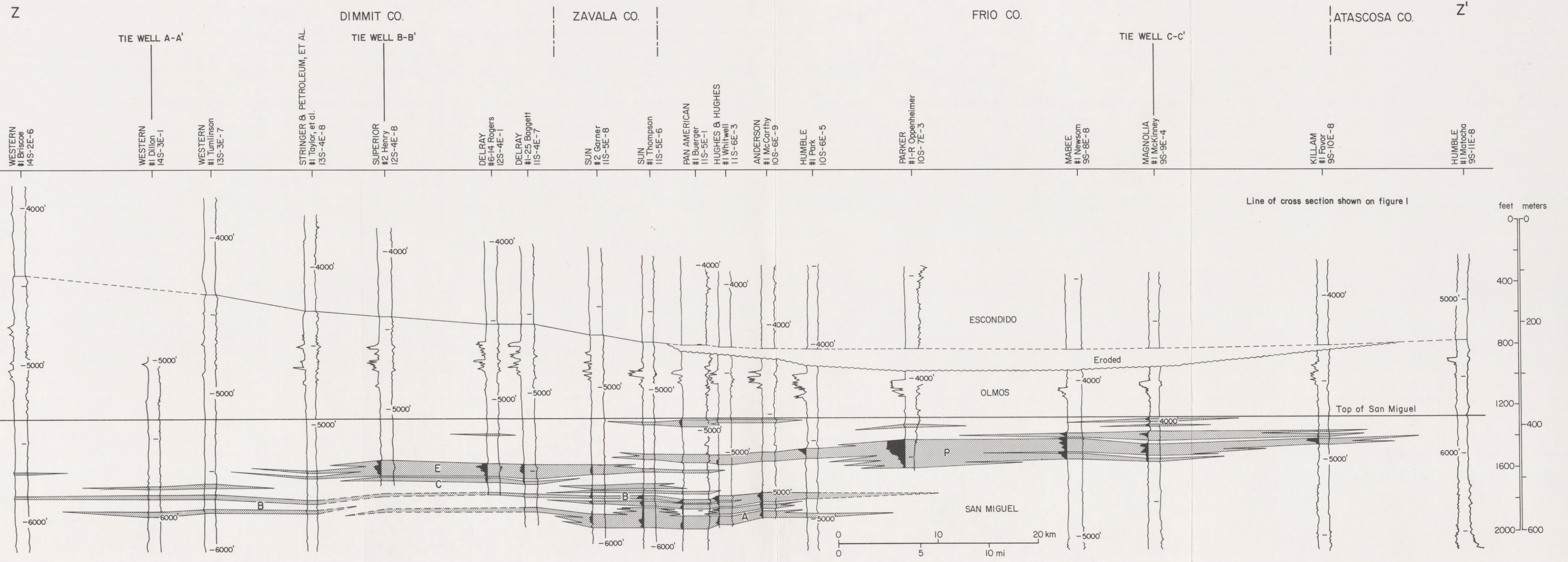


PLATE IV







6 plates
in
pocket

